Utilisation of trace element contents in benthic foraminifera for reconstructing sea water composition

Zur Erlangung des akademischen Grades eines

DOKTORS DER NATURWISSENSCHAFTEN

von der Fakultät für

Bauingenieur-, Geo- und Umweltwissenschaften

des Karlsruher Instituts für Technologie (KIT) – Universitätsbereich

genehmigte

DISSERTATION

von

Dipl.-Min. Dirk Munsel

aus Hammelburg

Tag der mündlichen Prüfung: 22.01.2014

Referent: Prof. Dr. Thomas Neumann

Korreferent: PD Dr. Jörg-Detlef Eckhardt

Karlsruhe 2013

Erklärung über die Erstellung der Dissertation

Hiermit erkläre ich, dass ich die vorliegende Dissertation selbstständig angefertigt, nur die angegebenen Quellen und Hilfsmittel verwendet und mich keiner unzulässigen Hilfe Dritter bedient habe. Insbesondere habe ich alle wörtlichen oder sinngemäßen Entlehnungen deutlich als solche gekennzeichnet sowie die Grundsätze des Karlsruher Instituts für Technologie (KIT) zur Sicherung guter wissenschaftlicher Praxis in ihrer aktuell gültigen Fassung beachtet.

Karlsruhe, November 2013

Kerstin und Julius gewidmet

Abstract

The incorporation of trace elements into carbonate tests of the shallow water benthic foraminifer *Ammonia tepida* was investigated under controlled laboratory conditions. Temperature, salinity, and pH of the culture solutions were kept constant throughout the duration of this experiment, while elemental concentrations were varied. Concentrations of Ni, Cu, and Mn, as well as of As, and V, were set in two experiments at 5-, 10-, and 20 times higher than levels found in natural North Sea water; for reference, a control experiment with pure filtered natural North Sea water was also analysed. The concentrations of all five elements from newly grown chambers were determined by means of both µ-synchrotron XRF and Laser Ablation Inductively Coupled Plasma Mass Spectroscopy (LA-ICP-MS). For Cu and Ni the results of both independent analytical techniques agreed within the analytical uncertainty, whereas for As and V only µ-synchrotron XRF data was reliable. In general, the concentration of the analysed elements in the tests increased in line with their concentration in the culture solutions. Potential toxic and/or chemical competition effects might have resulted in the decreased incorporation of Ni and Cu into the calcite of the specimens exposed to highest elemental concentrations. Manganese incorporation exhibited large variability in the experiment with the 20-fold increased element concentrations, potentially due to antagonistic effects with Cu and Ni. The speciation of As changed in the course of the experiment by oxidation probably due to bacterial activity in the culture media or by protection mechanism within the foraminifera. The partition coefficients of Cu, Ni, As, and V were calculated to be 0.14 ± 0.02, 1.0 ± 0.5, 5.0 ± 1.0 ($\times 10^{-2}$), and 12.0 ± 2.0 ($\times 10^{-3}$) respectively, whereas the partition coefficient of Mn was estimated to be least 2.4. These partition coefficients now open the way for reconstructing past concentrations for these elements in sea water and were applied in a first step to a species of benthic foraminifers (*Bulimina spp.*) in recent/sub-recent samples of a core from the Cariaco Trench. In a second step, these partition coefficients were then applied to fossilised benthic foraminifera (*Lenticulina spp.*) of the

Mullinax-1 core, which includes the Cretaceous-Palaeogene transition. In the Cariaco subset, the change of the distinct geochemical regimes was detectable in the analysed samples, whereas the samples of the Mullinax-1 subset do not appear to reflect a shift corresponding to the Cretaceous-Palaeogene transition.

Kurzfassung

Unter kontrollierten Umweltbedingungen wurde der Einbau von ausgewählten Spurenelementen in die karbonatischen Gehäuse benthischer Flachwasser-foraminiferen der Spezies *Ammonia tepida* im Labor durchgeführt. Hierzu wurden Temperatur, Salinität und pH-Wert konstant gehalten während die Konzentrationen bestimmter Spurenelemente variiert wurden. In zwei parallel ausgeführten Experimenten wurden einerseits die Elementkonzentrationen von Ni, Cu und Mn, andererseits die von As und V 5-, 10- und 20-fach gegenüber natürlichem Nordseewasser erhöht. Zusätzlich wurde ein Experiment ohne jegliche Konzentrationserhöhung für Referenzzwecke durchgeführt. Die Konzentrationen aller fünf Elemente wurden in neu gewachsenen Kammern mittels Mikrosynchrotron Röntgenfluoreszenzanalyse (µ-Synchrotron RFA) und Laserablationsmassen-spektrometrie mit induktiv gekoppeltem Plasma (LA-ICP-MS) ermittelt. Für Cu und Ni stimmten die Ergebnisse beider unabhängig gemessenen Techniken innerhalb der analytischen Toleranz überein, während für As und V lediglich die µ-Synchrotron RFA Ergebnisse verwendet werden konnten. Im Allgemeinen erhöhten sich die Elementkonzentrationen in den Foraminiferengehäusen proportional zu den Konzentrationen der Züchtungswässer. Etwaige toxische und/oder chemische Einbaukonkurrenzeffekte könnten für die niedrigeren Einbauraten von Ni und Cu in die kalzitischen Schalen der höchst konzentrierten Zuchtlösung verantwortlich sein. Der Einbau von Mn zeigte einen großen Schwankungsbereich in der 20-fach konzentrierten Zuchtlösung auf, welcher wahrscheinlich durch Antagonismuseffekte mit Cu und Ni erklärt werden kann. Die Speziation von As änderte sich im Verlauf des Experiments durch Oxidation, wahrscheinlich durch bakterielle Aktivität in der Zuchtlösung oder durch biologische Schutzmechanismen der Foraminiferen induziert. Die Verteilungskoeffizienten von Cu, Ni, As und V wurden berechnet und sind mit $0{,}14 \pm 0{,}02$, $1{,}0 \pm 0{,}5$, $5{,}0 \pm 1{,}0$ ($\times 10^{-2}$) bzw. $12{,}0 \pm 2{,}0$ ($\times 10^{-3}$) anzugeben. Der Verteilungskoeffizient von Mn wurde auf mindestens 2,4 geschätzt. Die

Verteilungskoeffizienten dieser Elemente eröffnen nun neue Perspektiven für die Rekonstruktion vergangener Meerwasserkonzentrationen. Sie wurden zunächst für eine Spezies benthischer Foraminiferen (*Bulimina spp.*) in einem rezenten/subrezenten Bohrkern des Cariaco Beckens angewandt. In einem zweiten Schritt wurden die Verteilungskoeffizienten dann für eine fossile Spezies benthischer Foraminiferen (*Lenticulina spp.*) aus dem Mullinax-1 Bohrkern, welcher den Kreide-Paläogen-Übergang enthält, angewandt. In den Proben des Cariaco Bohrkerns konnte der Wechsel des geochemischen Regimes nachgewiesen werden, während in den Proben des Mullinax-1 Bohrkerns die Katastrophe des Kreide-Paläogenübergangs nicht ablesbar war.

Acknowledgements

Thank you:

- Prof. Dr. D. Stüben for giving me the opportunity to create my own PhD project
- Prof. Dr. T. Neumann for supervision of my PhD
- PD Dr. J.-D. Eckhardt for the second review
- Prof. Dr. J. Bijma for the possibility to use his laboratory for free and instruction in all issues considering the culture experiments
- Dr. Z. Berner for invaluable help regarding all issues of this PhD thesis
- Dr. U. Kramar for support with the µ-synchrotron XRF measurements and his help with the data evaluation
- Dr. D. Dissard for sharing her experience during the culture experiments
- Dr. G. Nehrke, Dr. A. Benthien and Mrs. B. Müller for guidance and assistance in the AWI laboratory
- Dr. R. Simon, Dr. J. Göttlicher, and Dr. R. Steininger for support with the µ-synchrotron measurements at ANKA
- Dr. K. Appel for help with the µ-synchrotron measurements at HASYLAB
- Dr. G.-J. Reichart for his help regarding the LA-ICP-MS measurements
- Mrs. C. Haug for support with the preparation of the stock solutions for the culture experiments and all other laboratory issues at KIT
- Mrs. P. Khelashvili for assistance and support with the cleaning process of the foraminifera from the cores
- Mrs. C. Mößner for her efforts with the HR-ICP-MS measurements of the culture solutions and the measurements of the foraminifera from the cores
- Mrs. G. Preuß for help with the IRMS measurements
- Mrs. B. Oetzel for support with the XRF and CSA/CWA measurements of the sediment samples
- Mr. P. Illner for continuous literature support and endless discussions

- Mrs. L. Fay for polishing up my English

Furthermore, I thank:

- Prof. Dr. R. Röttger for discussions and special literature about benthic foraminifera
- Prof. Dr. S. Goldstein and Dr. H. Filippson for answering my questions concerning special issues on foraminifera
- Dr. S. Abramovich for introducing me into the picking of Cretaceous foraminifera
- Prof. Dr. D. Lea, PD Dr. O. Friedrich and Dr. W. Sunda for special literature

My greatest thank you goes to my wife for supporting and encouraging me the whole time to finally get this thesis done!

This work was partly supported by the German Research Foundation (DFG) under Grant No. STU 169-34/2, Grant No. BI 432/4-2 ("PaleoSalt"), and Grant No. BI 432/6-2 ("BioCalc"), as well as by the European Science Foundation (ESF) under the EUROCORES Programmes EuroCLIMATE and EuroMinScI, respectively, through Contract No. ERAS-CT-2003-980409 of the European Commission, DG Research, FP6.

Preliminary note

Parts of this study have been published before. The following two peer-reviewed publications contain material of this thesis:

- Kramar, U., Munsel, D., Berner, Z., Bijma, J. and Nehrke, G.: Determination of trace element incorporation into tests of in vitro grown foraminifera by micro-SYXRF – a basis for the development of paleoproxies, in: X-ray optics and microanalysis, edited by: Denecke, M.A. and Walker, C.T., American Institute of Physics Conference Proceedings, 1221, New York, 154-159, 2010.
- Munsel, D., Kramar, U., Dissard, D., Nehrke, G., Berner, Z., Bijma, J., Reichart, G.-J. and Neumann, T.: Heavy metal incorporation in foraminiferal calcite: Results from multi-element enrichment culture experiments with *Ammonia tepida*, Biogeosciences, 7, 2339-2350, 2010.

Table of contents

List of abbreviations and symbols

BP	before present
CSA	carbon-sulphur analyser
CWA	carbon-water-analyser
D	partition coefficient
DSDP	Deep sea drilling project
ED-XRF	energy dispersive X-ray fluorescence
EXAFS	extended X-ray absorption fine structure
FIAS	flow injection analysis system
HR-ICP-MS	high resolution inductively coupled plasma mass spectroscopy
IR-MS	isotope ratio mass spectrometry
ka	kilo anno
LA-ICP-MS	laser ablation inductively coupled plasma mass spectroscopy
mbsf	metres below sea floor
micro-XRF	
NSW	North Sea water
ODP	Ocean drilling program
p.a.	pro analysis
PCA	principle component analysis
ROW	reverse osmosis water
SEM	scanning electron microscope
spp.	species (plural)
TE	trace element
WD-XRF	wavelength dispersive X-ray fluorescence
XAFS	X-ray absorption fine structure
XANES	X-ray absorption near-edge structure
µ-synchrotron XRF	µ-synchrotron X-ray fluorescence spectroscopy

1 Introduction

A Chinese proverb says: “Consider the past and you shall know the future”. This combined with James Hutton’s theory of uniformitarianism make palaeo reconstructions play a significant role in climatic and oceanographic studies, as reconstructed data from the past may be used for modelling the future.

Environmental reconstructions of past climate and oceanic conditions require tools that give scientists insights into past conditions and processes. Tools that may be used for that are called proxies – measurable environmental descriptors that reflect a certain physical or chemical parameter.

Ideally a proxy depends on one physico-chemical parameter and is of acceptable precision and reliability when applied to various conditions (e.g. redox sensitive environment). Geochemical data obtained from foraminiferal calcite are widely used as proxies in palaeo-climatology and oceanography (e.g. Boyle, 1981; Wefer et al., 1999; Lea, 2004) as they enable a high temporal resolution by investigating a fairly simple and stable chemical system ($CaCO_3$).

Sea water as an elementary parameter of the climatic system is a conservative and stable system regarding the composition of its major components (Millero, 1996) as these have shown to be relatively constant over longer periods of time throughout the modern oceans (e.g. Forchhammer, 1865; Culkin, 1965; Riley and Tongudai, 1967). These major components of the sea water are the cations Na^+, Mg^{2+}, Ca^{2+}, K^+ and Sr^{2+} as well as the anions Cl^-, SO_4^{2-}, HCO_3^-, Br^-, CO_3^{2-}, $B(OH)_4^-$ and F^- which account for an average salinity of 35 psu. Due to this constant state of the major components any biochemical process, such as bacterial oxidation of plant material, may have effects on the properties of sea water (Millero, 1996 and 2002).

Furthermore, a number of factors may cause the composition of the sea water to change dramatically, such as processes occurring in sediments, anoxic basins, estuaries, and hydrothermal vents. Other factors that may influence sea water

chemistry include dissolution processes, evaporation, freezing, and oxidation. In the case of hydrothermal activity, for instance, Ca, Cu, Ni, Zn, Mn, and Si are enriched, while Mg and SO_4 will be reduced (von Damm, 1990; Millero, 2002).

When sea water does not contain any dissolved oxygen, it is considered anoxic. This may happen when the rate of oxidation of organic matter exceeds the oxygen supply from the atmosphere. One of the most fundamental consequences of anoxic conditions is the lower redox potentials of these environments. As a result of these conditions, trace element concentrations (e.g. released metals from the sediment) can alter the sea water on a regional scale (Richards, 1965; Zhang and Millero, 1993; Millero, 2000).

Despite the vast number of palaeo-proxies based on carbonate of foraminiferal tests, such as sea water temperature (e.g. Elderfield and Ganssen, 2000), sea-level changes (e.g. Li et al., 2000), and primary productivity (e.g. Lea and Boyle, 1989), as well as the above mentioned good knowledge about present day sea water, only a few studies take aim at the reconstruction of the chemical composition of palaeo-sea water (e.g. Marchitto et al., 2000; Nameroff et al., 2002). This is interesting, as it is important to have knowledge of past sea water composition when studying past milieu changes. If the theory applies that foraminifers preserve changes in sea water chemistry, then foraminifera will document these whether or not induced by a severe change in sedimentation conditions or any other geodynamic process. Missing experimental data for the important first row transition metals incorporated in foraminiferal calcite (except for V (Hastings et al., 1996) and Cu (de Nooijer et al., 2007)) opens the perspective for new investigations. Thus, the present study *"Utilisation of trace element contents in benthic foraminifera for reconstructing sea water composition"* aims to shed additional light on past sea water composition by means of accurate calibrations between the actual sea water conditions and the chemistry of analysed foraminiferal tests which may best be achieved by performing culturing experiments (Filipsson, 2008).

The key issues of this study are:

- Which differences can be detected in foraminiferal test carbonate when analysing specimens from distinct geochemical environments? Are oxic and anoxic conditions decipherable? Are the consequences of major Earth events (e.g. catastrophes such as at the Cretaceous/Palaeogene transition) detectable in the tests of calcareous foraminifera?
- Can benthic foraminifera provide a better proxy record than bulk sediments in palaeo-environmental reconstructions?
- To what extent is foraminiferal carbonate usable to draw conclusions about the past?
- Is it possible to incorporate key geochemical trace elements simultaneously in the carbonate of foraminifera? Does this approach affect the elemental uptake in any way?
- Is µ-synchrotron XRF a suitable method to detect trace element concentrations in foraminiferal calcite?

These main objectives shall be achieved in the following way:

- Performing two multi-element (= batch) culture experiments using the shallow-water benthic foraminifer *Ammonia tepida* simulating two specific, distinct geochemical environments. In one case oxidising conditions are reflected by increased concentrations of Mn, Co, Ni, and Cu, and in the other an anoxic milieu is simulated by adding V, Cr, As, and Mo. These experiments shall be used to calculate partition coefficients for the involved trace elements. For validation reasons in each batch experiment, one element with known partition coefficient (V in one, Cu in the other) is used as a control;
- Reconstructing the sea water compositional history using the obtained partition coefficients (complemented by published data) and applying these to recent/sub-recent foraminifera of a well-known anoxic/suboxic environment from a sediment core of ODP Site 1002. In a second step these partition

coefficients will be used to reconstruct the sea water composition by means of fossil foraminifera that span a major catastrophic event (Cretaceous/Palaeogene transition in Brazos, Texas, USA). Both sets of foraminifera will be analysed using HR-ICP-MS in order to undertake a multi-element approach (Meudt, 2004) and subsequently use multivariate statistics;

- Deciphering the variability of the sedimentary record, which is valuable for palaeo reconstructions (e.g. linkage between sedimentation rate and geochemical regime), and the corresponding foraminiferal data. Knowing the geochemical sedimentary composition facilitates conclusions as to what extent the analysed foraminiferal test chemistry may be correlated to the sediment-derived environmental conditions. To this end, bulk sediments of ODP Site 1002 are analysed by XRF;
- Utilisation of µ-synchrotron XRF to analyse the calcareous foraminiferal tests. Until now, this technique has not been used to analyse foraminiferal calcite, however, due to the small size of the foraminiferal tests, it is perfectly suited for analysing single chambers of the tests (~ 100 µm) that preserve the trace elemental information. As no published µ-synchrotron data exists, results will be verified herein using the well-established LA-ICP-MS technique (e.g. Reichart et al., 2003; Dissard et al., 2009).

The present study is structured in such a way that in the first part of Section 2 some background information about sea water and foraminifera is given. This is complemented by a short summary of crucial studies regarding isotopes and trace elements in foraminiferal calcite used as proxies. Section 3 begins with a short introduction to the foraminiferal species used in this study and provides an insight to the sampling sites and proceeds with a detailed description of the experimental procedures. In the latter part of Section 3, all instrumental applications and calculation methods are discussed. Section 4 presents all results. The first part of the discussion in Section 5 deals with the culture experiments and considers all aspects of the

experiments. The application of the results comprises the second part of Section 5 and is followed by a discussion of the practical aspects including the reconstruction of palaeo sea water from the two locations (Cariaco, Venezuela and Brazos, Texas, USA). The conclusions and an outlook for future work round up this study in Section 6 and Section 7. Detailed measurement data regarding all materials are found in the appendices A to E.

2 Essential aspects of research

2.1 Sea water

2.1.1 Composition of sea water

Sea water composition is mainly controlled by the compositions of source materials and the physicochemical principles regulating the adsorption processes of various chemical species in sea water onto oceanic pelagic clays (Li, 1991).

2.1.1.1 Major components

The composition of sea water has been the subject of numerous investigations, especially regarding the major constituents of sea water (e.g. Culkin and Cox, 1966; Morris and Riley, 1966; Carpenter and Manella, 1973; Uppström, 1974; Wilson, 1975). Major constituent means that it usually has a concentration of at least one µmol/L in sea water. Exceptions are constituents that are important for the marine realm, but do not reach that limit. Throughout the years, researchers considered 12 constituents besides water as major constituents. All 12 major components are listed in Table 1.

Table 1 - Major constituents of sea water (Pilson, 2013 and references therein)

Component	Average concentration [µmol/L]
Na^+	480,000
K^+	10,500
Mg^{2+}	54,100
Ca^{2+}	10,500
Sr^{2+}	92.0
Cl^-	559,000
SO_4^{2-}	28,900
HCO_3^-	1,890
CO_3^{2-}	189
$B(OH)_4^-$	84.0
F^-	70.0
Br^-	863
H_2O	54,880,000

Although the amount of dissolved salts may vary throughout the oceans, major constituents are called conservative as they are found in relatively constant proportions to the salinity and each to other in sea water. Additionally, these major components have long oceanic residence times – residence times that exceed the ocean mixing time of ~ 1000 years (e.g Wilson, 1975; Chester and Jickells, 2012).

Salinity is defined as the number of grams of dissolved inorganic salts in one gram of sea water and ranges between 33 and 38 per mil – with the overall average considered to be 35 per mil (Turekian, 1976). Salinity is usually not expressed in per mil, but as the so-known Practical Salinity Unit [psu]. The varying value for the salinity in the open ocean is a result of various (competing) processes, such as concentration (e.g. evaporation and ice formation) and dilution effects (e.g. melting of ice, atmospheric precipitation, and riverine input (especially in near shore waters)). If one (or more) of these processes occur, major constituents may not show conservative behaviour any more (Millero, 2002).

2.1.1.2 Trace elements

All chemical elements of the periodic table found on Earth are thought to be present in sea water at least to some extent. Major constituents of sea water have been mentioned in Section 2.1.1.1, whereas minor components of the sea water with a concentration of less than one µmol/L are usually called trace elements (e.g. Chester and Jickells, 2012). Furthermore, trace elements have much shorter residence times in the ocean than major constituents; in some cases even much shorter than the average ocean mixing time. Moreover, each trace element abides by one or more of the following distribution patterns (Li, 1991; Nozaki, 1997; Chester and Jickells, 2012):

- Conservative-type distribution: The ratio of the element to salinity is (relatively) constant throughout the water column. Such elements have only a very limited interaction with particulate matter or biological processes relative to their abundances. Hence, oceanic residence times are long (~ 100,000 years);

- Nutrient-type distribution: Elements belonging to this group show low concentrations in surface waters gradually increasing with depth just as typical nutrients (e.g. nitrate and phosphate) do because of their involvement in the biogeochemical cycle of biological uptake in surface waters and the degradation and dissolution of surface water products at depth. The oceanic residence time of nutrient-type elements are rather long (~ 10,000 years), but shorter than conservative-type elements;
- Scavenged-type distribution: Trace elements of this group display high concentrations in surface waters with continuous depletion at depth and are highly particle reactive. Therefore, these elements have only a short residence time (< 1000 years) and are subsequently removed from the water column by sinking particulate matter. Concentrations within the oceans vary considerably and reflect local inputs;
- Intermediate-type, or behaviour/mixed-type distribution: Elements whose distributions do not display the idealised end-members listed above, but show characteristics of one or the other distribution types in different locations (e.g. the element Al exhibits surface enrichment in the Pacific as well as in the Atlantic followed by a mid-depth minimum and then another increase in deep waters, while showing an altogether different pattern in the Mediterranean). Some elements also show a combination of the characteristics of the above mentioned ideal end-members due to their existence in different oxidation states.

Some trace elements are globally influenced by anthropogenetic activity. Their oceanic distribution varies with time and thus cannot be representative in any way. In some other oceanic environments, such as in those iaffected by hydrothermal activity or changing oxygen supply, the distribution patterns of trace elements may appear erroneous.

2.1.2 Special marine environments

Naturally occurring geodynamics as well as physicochemical processes may influence sea water and thus its composition. These processes are responsible for specific environments such as anoxic conditions or hydrothermal influence.

2.1.2.1 Anoxic waters

Anoxic (sea) water is defined as water that is depleted of dissolved oxygen (Richards, 1965). In areas with restricted water exchange anoxic environments may be found quite frequently, even though these conditions actually prevail in only a very small proportion (~ 0.3 %) of the world‘s oceans (Millero, 2000; Algeo, 2004).

Anoxic conditions occur when the rate of oxidation of organic matter by bacterial activity is greater than the supply of oxygen. Causes for such conditions are limited advection of oxygen induced by physical barriers, density stratification, stagnation of circulation or elevated inputs from organic material (Richards, 1965; Grasshoff, 1975; Sarmiento et al., 1988; Gerlach, 1994; Millero, 2000).

Water column anoxia may be the result of trace metal concentrations in the underlying sediments, depending on their solubility of sulphide-bearing waters which are the result of the bacterial activity leading to deoxygenation. Typically elements such as V, Co, Cu, Zn, Mo, Cd, Pb, and U are enriched in anoxic sediments and thus depleted in the overlying water column (e.g. Calvert, 1976; Jacobs et al., 1987; Algeo and Maynard, 2004).

The natural phenomenon of anoxic waters is not restricted to modern times and has occurred throughout Earth’s history. Present day locations of anoxic sea waters are for example the Black Sea (Eastern Europe), the Cariaco Basin (Venezuela), the Framvaren Fjord (Norway), the Mariager Fjord (Denmark), and the Orca Basin (Gulf of Mexico).

2.1.2.2 Hydrothermal infuenced sea water

Submarine hydrothermal solutions are a relatively common phenomen at the mid-ocean ridge complex and play an important role in the budgets of water, chemical, and heat components of the earth-ocean-atmosphere system. Sea water passes through oceanic crust independent of age and interacts with the seafloor basalts. This leads to a chemical exchange in the sea water chemistry. The often high-temperature solutions are either enriched or depleted compared to the ambient sea water (von Damm, 1990; Elderfield and Schultz, 1996; von Damm, 2000).

The chemistry of hydrothermal fluids may vary dramatically from place to place and also differs with time within the same hydrothermal system. Von Damm et al. (1985) found the following reasons that may conduce variations in the composition of hydrothermal fluids:

- Differences in temperature
- Differences in the residence time (i.e. longer residence times imply longer reaction times)
- Differences in rock type (for instance glass reacts faster than crystalline rock)
- Differences in age of the hydrothermal system
- Differences in the depth at which the rock-sea water reaction takes place

Additionally, when hydrothermal liquids exit through overlying sediments, interactions with that sediment layer may greatly modify the composition of the fluids especially if calcareous sediments that are able to neutralise acidic vent solutions are present (German and von Damm, 2004).

In general, widespread submarine hydrothermal activity has a considerable impact on the background concentration of certain elements, such as Mn, Fe, Co, Mo, Ni, Cu, Zn, As, Ba, and Pb, in the sea water on a regional (or local) scale. Metal concentrations may reach dimensions several orders of magnitude higher than in the original sea water (e.g. von Damm, 1990; Trefry et al., 1994; Elderfield and Schultz, 1996; German and von Damm, 2004).

At present, submarine hydrothermal activity predominantly occurs at oceanic back-arc spreading centres and mid-ocean ridges. Well studied locations of hydrothermal activity include the Mid-Atlantic-Ridge, the Juan de Fuca Ridge, the Galapagos Spreading Centre, the East Pacific Rise, and the Guaymas Basin.

2.2 Foraminifera

2.2.1 General aspects

Foraminifera are unicellular eukaryotic microorganisms (Protozoa), found mainly in marine environments. Many species of foraminifera secrete shells, referred to as “tests”, which in most cases are composed of calcium carbonate. Some species build a non-mineralised (organic) shell or an agglutinated test – meaning it is constructed of foreign material which is cemented by the foraminifer. Commonly the tests consist of chambers which are added systematically by growth. Some species build spiral tubes in which the individual chambers are absent. The majority of adult foraminifera are between 200 and 500 µm in size, but certain species may measure up to 20 cm (Grell, 1973; Goldstein, 1999; Röttger and Lehmann, 2009).

Regarding calcareous foraminifera, Erez (2003) describes the actual process of calcification which begins with sea water uptake into vacuoles by endocytosis. Once the sea water enters the vacuoles, the pH is increased and the elemental concentration is modified by cellular pumps before it is exocytosed into a “biomineralisation space” (Elderfield et al., 1996; Erez, 2003; de Nooijer et al., 2009). In that biomineralisation space, $CaCO_3$ precipitates on an organic matrix, thereby defining the outline of a new test chamber (Hemleben et al., 1977). Trace elements present in this modified sea water precipitate along with the calcium carbonate and thus are incorporated into the shell. In addition to this biological control, physicochemical parameters such as pH (e.g. Sanyal et al, 1996), temperature (e.g. Lea et al., 1999), salinity, and possibly pressure (e.g. Rosenthal et al, 1997) also influence the manner in which trace and minor elements are incorporated into calcium carbonate tests during shell precipitation.

Foraminifera exhibit cytoplasmic organisation and reticulated pseudopodia protruding from one or more apertures in the shell. This sticky net-like array of pseudopodia (shown in Figure 1) may cover an area up to ten times the diameter of the shell and is mainly used to collect food – such as algal cells, bacteria, diatoms, fungi, or organic detritus. Besides feeding (Figure 2), pseudopodia are essential for motility (foraminifera may move up to seven millimetres in 24 hours), and attachment purposes and are also needed for building and structuring the shells, protection and even respiration and reproduction. Thus pseudopodia enable foraminifera to interact with their surroundings (e.g. Salami, 1976; Anderson and Lee, 1991; Goldstein, 1999).

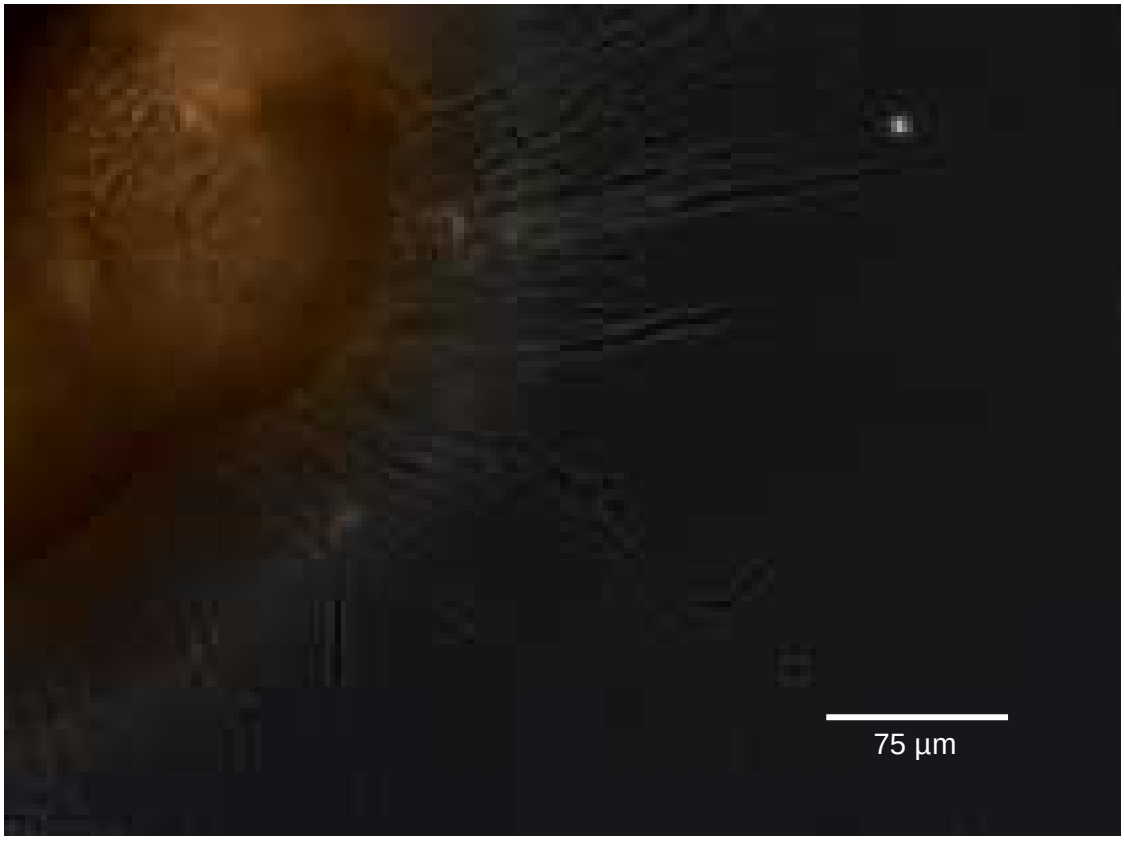

Figure 1 – Net-like structure of pseudo-podia

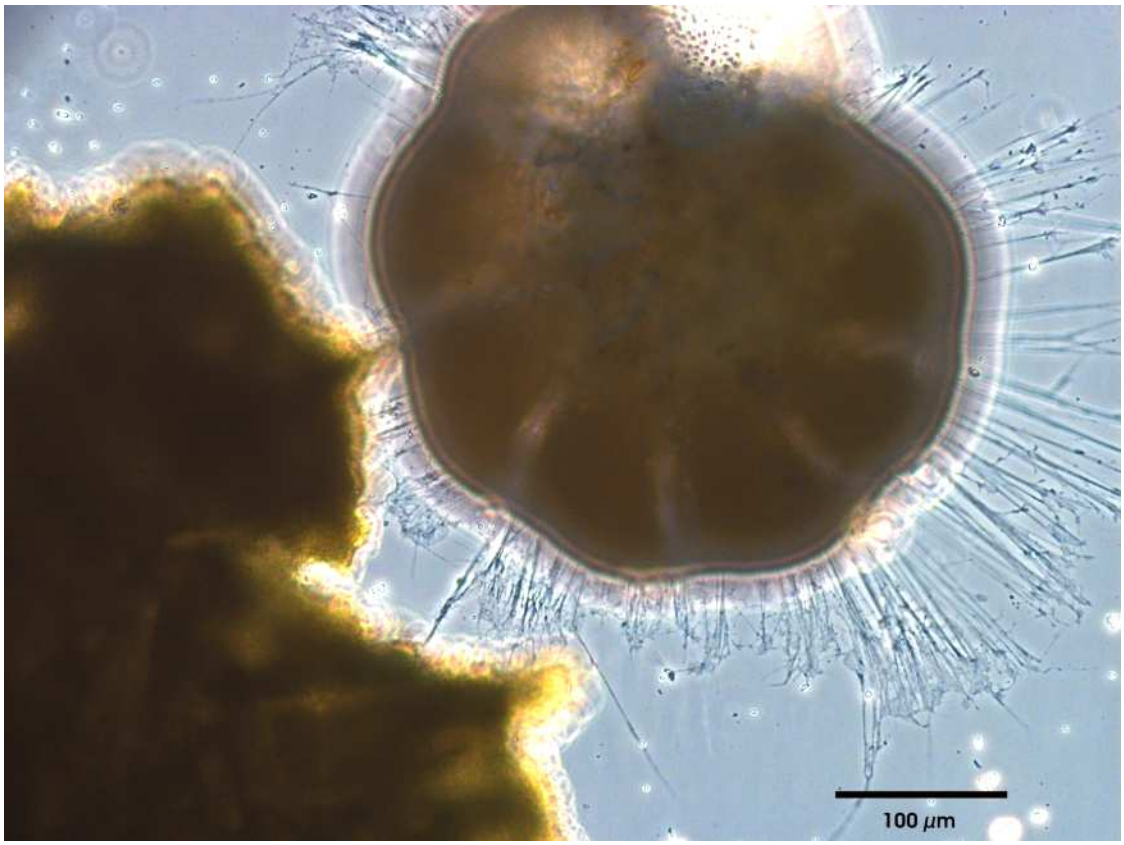

Figure 2 – Foraminifer feeding on alga

The life cycle of Foraminifera is characterised by an alteration of sexual and asexual generations. Asexual reproduction (schizogony), which is commonly observed in laboratory cultures, inevitably leads to the death of parental cells. In contrast, during sexual reproduction (gametogamy, autogamy or gamontogamy) zygotes are formed (e.g. Hemleben et al., 1989; Lee et al., 1991; Goldstein and Moodley, 1993, Goldstein, 1999).

Foraminifera are found in virtually all marine habitats (i.e. from shallow intertidal environments to deep-sea trenches and even in the antarctic sea ice) (e.g. Dieckmann et al., 1991; Murray, 1991a; Jonasson et al., 1995; Goldstein, 1999; Lipps and Langer, 1999); they exhibit adaptive radiation, which has enabled them to persistent from the earliest Cambrian to present day. Regarding their mode of life, foraminifera are considered both benthic and planktonic. Some benthic foraminifera are considered as endobenthic (meaning foraminifera live within the sediment), whereas others are epibenthic (i.e. living on the sediment). But the majority of the benthic species belong to

neither group – living at the sediment-water interface and are able to move up or down the sediment column and thus have variable microhabitats (Linke and Lutze, 1993). Planktonic foraminifera live within the water column and drift passively in the water currents. They originated from benthic foraminifera during the late Jurassic and represent about 40 – 50 living species at present, whereas the benthic record is much broader (Hemleben et al., 1989; Murray, 1991b, Sen Gupta, 1999).

2.2.2 Trace elements in foraminiferal calcite – an overview

2.2.2.1 Crucial geochemical proxy studies

Urey (1947), who studied thermodynamic properties of isotopes, opened the door to geochemical proxy studies by his calculations regarding the isotopes of oxygen. It was his idea to use the variations with temperature of the fractionation factors in isotopic exchange equilibria as a thermometer. This idea was picked up in 1955, when Emiliani advanced Urey's idea to the first empirical equation regarding sea water temperatures calculated from oxygen isotopic analyses of Pleistocene pelagic foraminifera from deep-sea cores of the Atlantic and Pacific Oceans as well as from the Caribbean Sea.

Emilianis equation is still the basis for palaeo sea water calculations by means of oxygen isotope analyses from foraminifera even though it has been extended and revised for various species of planktonic and also some benthic foraminifera (Erez and Luz, 1983; Bemis et al. 1998). Many foraminiferal studies include oxygen isotopic analyses today – examining both planktonic and benthic species (e.g. Lea, 2004; Filipsson et al., 2010).

For palaeothermometry applications of foraminiferal species that have not been studied in detail yet, the equation of Erez and Luz (1983) is commonly used.

The proxy toolbox has increased enormously ever since. More recently, proxies based on Mg/Ca ratios for palaeothermometry have been developed knowing that Mg is a conservative element in the sea water, i.e. the Mg/Ca ratio is constant with depth (e.g. Broecker and Peng, 1982). Additonally, Mg incorporation in biogenic carbonate is

related to the sea water temperature (e.g. de Deckker and Corrège, 1992). An increase of temperature leads to an increase in Mg content in the carbonate while the $\delta^{18}O$ values are decreasing and vice versa. This linkage between the Mg content and the $\delta^{18}O$ value is not linear though, as the Mg content in the tests increases slightly exponentially relative to the $\delta^{18}O$ (Anand et al., 2003). The Mg/Ca proxy is also widely used, just as the oxygen isotopes for both planktonic (e.g. Lea et al., 1999) and benthic foraminifera (e.g. Filipsson et al., 2010).

The newest attempt to reconstruct surface water temperatures is by Ca isotopes. The advantage of the $\delta^{44}Ca$ proxy on the one hand is the constant content of Ca in the ocean water through time and its long residence time compared to the mixing time of ocean water (~ 1 Ma compared to ~ 1000 years, respectively (e.g. Broecker and Peng, 1982; Zhu and MacDougall, 1998)). On the other hand the biological fractionation of Ca is relatively uniform in magnitude among different types of marine organisms (Skulan et al., 1997) and Ca isotopic data significantly varies with oceanic temperature (Zhu and MacDougall, 1998). Nägler et al. (2000), clearly identified that Ca isotopic ratios are preserved in foraminiferal test carbonate and are in general accord with Mg/Ca ratios, with $\delta^{44}Ca$ values tending to predict slightly higher temperatures.

Other geochemical proxies useful in environmental reconstructions include B isotopes, which are used to determine pH changes in the ocean water on glacial/interglacial timescales (e.g Sanyal and Bijma, 1999). The idea behind this is that in sea water boron exists as a mixture of the two species boric acid ($B(OH)_3$) and borate ($B(OH)_4^-$) which are pH-dependent. Hemming and Hanson (1992) found that in marine carbonates the isotopic composition of boron is close to the one of borate; the latter of which is thought to be incorporated into the carbonates. This, combined with the fact that in modern oceans borate is proportional to pH, turn boron isotopic measurements of marine biogenic carbonate, such as foraminifera (Sanyal et al., 2001; Yu et al., 2007), into a tool for estimating palaeo-pH values of sea water.

Alongside these isotopic studies, trace elements incorporated in foraminiferal calcite gained general interest after Boyle's pioneer study (1981) manifested the potentials of trace elements in palaeo-oceanography. Especially elements that clearly can be allocated to specific oceanographic features, such nutrients were thoroughly studied. Special attention was given to the element Cd, which is used as a tracer for available nutrients (*sensu lato* primary productivity) in the past ocean (e.g. Boyle and Keigwin, 1982; Boyle, 1988; Martin and Lea, 1998; Rickaby and Elderfield, 1999). Cadmium shows a global linear relationship with the limiting micronutrient P in the modern ocean (Bruland et al., 1978) and is, just as P, removed from the surface ocean by organisms and then rapidly (that is, nearly quantitively) regenerated from sinking biological debris in the upper water column (Collier and Edmond, 1984). The parallel oceanic distribution of Cd and P thus results from similar behaviour in terms of uptake and remineralisation (Boyle, 1988).

Another well studied element is Ba, which has a distribution similar to that of dissolved silica in the sea. Because Ba is remineralised in deeper waters, it tends to track alkalinity (Lynch-Stieglitz, 2004). Thus, Ba is used to trace oceanic alkalinity and to refractory nutrients, accordingly. Lea and Boyle (1989) found that the behaviour of Ba and alkalinity in various oceanic sites is quite similar. Although both are dominated by different cycling mechanisms (e.g. Bishop, 1988), they share similar sites of uptake. Additionally, regeneration in deep waters results in strong co-variance of Ba and alkalinity throughout the ocean (Bishop, 1988; Lea and Boyle, 1989).

A promising, but rarely used proxy for sea level fluctuations is the elment Sr – more precisely, using the Sr/Ca ratio. Especially for the Cretaceous (e.g. Stoll and Schrag, 1996; Li et al., 2000) this proxy has been used, because during that time of sea level highstand, up to 90% of the marine carbonate was deposited on the continental shelves, which provide the major sinks and sources for Sr accumulation compared to about 20% in modern oceans. High Sr concentrations in sea water reflect diagenesis of Sr-rich aragonite on continental shelves (Schlanger, 1988). When sea level is low, that

aragonite is exposed to weathering and readily releases the majority of its Sr to the sea water in a short time (< 100 ka) (e.g. Gavish and Friedman, 1969) which in turn is removed from the sea water by marine organisms such as foraminifera and subsequently incorporated into their calcite shells. Thus, short term sea level changes may be recorded by varying Sr/Ca ratios in foraminiferal tests.

The most recent attempts in palaeo-reconstuction studies is using more than one method/proxy for one parameter to cross-check the data set (e.g. Li et al., 2000) or so known multi-proxy or multi-parameter studies which use more than one proxy to gain information about various aspects at the same time, such as temperature and salinity (e.g. Elderfield and Gansson, 2000). The present study will also consider this multi-proxy approach to reconstruct the sea water of two past oceanic sites.

2.2.2.2 Towards culturing foraminifera

Most calibrations of foraminiferal proxies are based on correlating average ambient conditions to the analyses of foraminifera isolated from recent (e.g. core-top) sediment samples. Not only does this approach rely on the assumption that conditions have remained stable for a considerable length of time, but in order to eliminate secondary contaminations and overgrowths, complex cleaning protocols are usually implemented (e.g. Boyle and Keigwin, 1985/1986; Lea and Boyle, 1991; Martin and Lea, 2002). Moreover, under natural conditions environmental parameters often co-vary and thus are difficult to disentangle. The use of controlled laboratory cultures is the most promising way to circumvent such complications and provides insights to controls on foraminiferal shell chemistry (Filipsson, 2008).

Culture studies with planktonic foraminifera were pioneered by Alan Bé (USA) and Christoph Hemleben (Germany). They performed the first systematic culture experiments with an emphasis on shell growth and chamber formation (Bé et al., 1977). Techniques have been improved since then and research aspects on culturing have been broadend. Culture-based thermometry, for example, was introduced by Erez

and Luz (1982) and has been complemented by Bijma et al. (1990), expanded (Spero and Lea, 1993), and revised (Bemis et al., 1998). The discovery of the so known “carbonate ion effect” (Spero et al., 1997) has shed light on the impact of varying carbonate concentrations on C and O isotopes.

The first culturing experiments focusing on quantifying foraminiferal elemental uptake were performed by Delaney et al. (1985) who found the first relationships between foraminiferal test chemistry and (culture) solution composition. They performed culture experiments with the elements Li, Sr, Mg, and Na.

Subsequent studies on the uptake of Ba (Lea and Spero, 1992 and 1994) and Cd (Mashiotta et al., 1997) showed further relationships between foraminiferal elemental shell concentration and sea water contents of these elements and opened the door for quantitve sea water reconstruction studies by calculating distribution coefficients for the mentioned elements, being then able to quantify past nutrient and alkalinity patterns.

Russell et al. (1994) examined the uptake of U into foraminiferal calcite. They found that the U/Ca may be used to trace past U concentrations in the ocean just as Hastings et al. (1996) did for V. Both groups concluded that their experiments indicate an incorporation of the mentioned elements in proportion to the elemental concentration of the culture solutions. Both elements may be used to detect changing sea water conditions in terms of oxygen depletion.

The fact that planktonic foraminifera may only reconstruct surface waters, more attention has drifted to culture experiments using benthic foraminifera as these are representatives of deeper waters (Filipsson, 2008).

The first attempts at culturing benthic foraminifera were made in the 1950’s by Arnold (1954) and Bradshaw (1955) with a main emphasis on ecological aspects using shallow water benthic foraminifera. This kind of culturing has continued until today with diverse species from different depths. Since the pioneer days various culture studies on different issues have been performed, unfortunately without identical culture

protocols, however. In various recent studies microcosms such as natural sediment (e.g. de Nooijer, et al., 2007) have been used, in others artificial sediment (e.g. Hintz et al., 2004) or no sediment at all (e.g. Toyofuku and Kitazato, 2005; Dissard et al., 2010a and 2010b). Depending on the species and the habitat of the cultured foraminifer, special culturing systems have been developed (e.g. Hintz et al., 2004) or simple aquaria have been used (e.g. Dissard et al., 2010a and 2010b).

Among the first culturing studies with shallow-dwelling benthic foraminifera with respect to palaeo oceanography was the above mentioned study by Russell et al. (1994) dealing with U uptake of foraminifera. Hastings et al. (1996) also performed a combined planktonic/shallow benthic foraminifera study; this one pertaining to V uptake. The first research regarding isotopic aspects was performed by Wilson-Finelli et al. (1998) and examined the behaviour of C and O isotopes in four species of foraminifera, while Toyofuku et al. (2000) worked on palaeothermometry using Mg/Ca ratios, comparing cultured and natural foraminifera.

Havach et al. (2001) continued work on trace metal uptake in deep sea foraminifera by culturing four different species and calculating the distribution coefficients of Ba and Cd for these. Further culturing experiments regarding partition coefficients of Cd were conducted for shallow water benthic foraminifera (Maréchal-Abram et al.; 2004). Hintz et al. (2006a and 2006b) also calculated Cd coefficients for various species using artificial microcosms.

One of the most recent studies published addressed Cu uptake by shallow benthic foraminifera (de Nooijer et al., 2007). That study included a fraction of sieved natural sediment and reported the first distribution coefficients of Cu.

The present study focuses on trace metal uptake of shallow benthic foraminifera using no sediment in order to rule out pore water influences. It shall be the first attempt using multi-element culture solutions to mimic natural conditions of specific geochemical environments.

2.2.2.3 Abiotic factors influencing trace element composition

The trace metal distribution, which often exhibits a nutrient-type depth profile within the water column, is strongly impacted by biological productivity in the ocean. In particular, low concentrations of some first row transition metals are known to be essential for productivity. However, the distribution of trace metals in the ocean is affected by certain geogenic processes (e.g. hydrothermal activity) and anthropogenic influences (e.g. pollution), as described below. Locally, geogenic processes such as hydrothermal activity can dramatically enrich the trace element composition of sea water for up to several kilometres from the active hydrothermal vent (German and von Damm, 2004). Although foraminifera do not reside within hydrothermal vents, the overall increase of trace metal concentrations in the surrounding sea water due to hydrothermal activity will affect foraminifera, particularly those living near the vent (e.g. Panieri, 2006). These hydrothermal effects are recorded in foraminiferal tests. For example, a field site which is known to be influenced by hydrothermal activity (DSDP Site 216, Ninety-east Ridge) yields specimens of benthic foraminifera that are enriched in “hydrothermal” trace elements such as Cu, Co, and Pb (Meudt, 2004). Changes in redox conditions (e.g. Morford and Emerson, 1999) or anthropogenic pollution sources may also influence trace and minor element distribution in sea water and will be recorded by foraminifera. Despite this, most pollution studies focus exclusively on bulk sediment analyses and/or foraminiferal distribution patterns (e.g. Alve, 1991 and 1995; Vilela et al., 2004; Buzas-Stephens and Buzas, 2005; Carnahan et al., 2008), partly due to the fact that accurate distribution coefficients have not yet been determined for linking sea water chemistry with foraminiferal carbonates for many of the elements of interest. As polluted sediments are usually suboxic or anoxic due to enrichment in organic matter with high levels of sulphate reduction, heavy metals are often accumulated and bound to highly insoluble minerals such as sulphides. Hence, these metals are not bio-available and as a result, true pollution levels remain unknown. Heavy metals can only be remobilised in the sediment and diffused into the water with increasing oxygen levels. Analyses of

foraminiferal calcite and partition coefficients of minor and trace metals could potentially reveal true trace metal availability. Thus foraminiferal calcite has the potential to become an excellent tool for monitoring marine pollution.

3 Material and methods

3.1 Foraminifera used in this study

3.1.1. *Ammonia tepida*

Ammonia beccarii (Linné) forma *tepida* (Cushman), referred to as *Ammonia tepida* in the following, is a symbiont-barren species of benthic foraminifera. The form used in this study is of the molecular type T6E (Hayward et al., 2004). It is one of the most common genera of benthic foraminifera and is found worldwide in a wide variety of environments – such as the inner shelf, in estuarine (e.g. Goldstein and Moodley, 1993; Alve and Murray, 1999; Cearreta et al., 2002; Pascual et al., 2002), and even salt-marsh environments (e.g. Goldstein and Moodley, 1993; Pascual et al., 2002; Leorri et al., 2010). *Ammonia tepida* is known to have a broad tolerance range for temperature and salinity, to withstand strong seasonal regimes, and to survive severe environmental conditions. Furthermore, this species is also easy to grow in the laboratory, where it can form new chambers and even reproduce (Bradshaw, 1957; Schnitker, 1974; Goldstein and Moodley, 1993; Alve and Murray, 1999; Stouff et al., 1999; Pascual et al., 2002; le Cadre and Debenay, 2006; de Nooijer et al., 2007). Thus, easy culturing and its robustness makes *Ammonia tepida* a very suitable species to conduct experiments concerning its surrounding environmental conditions.

3.1.2 *Bulimina spp.*

Bulimina is a genus of benthic foraminifera and is considered to be endobenthic. It appeared first in the Palaeocene and various symbiont barren free species of *Bulimina* are found at present. Culture experiments conducted by Barras et al. (2009) and Filipsson et al. (2010) showed that the best living conditions for *Bulimina* are between 4 and 19 ℃ and reproduction occurred best at natural environment temperature (7 and 14 ℃). Salinity may range between 27 and 40 ‰.

The species used in this study were *Bulimina aculeata* and *Bulimina marginata* expressed as *Bulimina spp.* throughout this study. Just as *Ammonia*, *Bulimina* has a

fairly widespread geographic distribution and can be found in various environments such as outershelf of Venezuela (e.g. Hedberg, 1934), in brackish environments such as estuaries like of the river Rhône (Mojtahid et al. 2010), deep environments such as adjacent to the Great Bahama Bank (460 – 814 m) (Filipsson et al. 2010), or the Cantabrian Sea (450 – 650 m) (Barras et al., 2010). *Bulimina* is reported to tolerate oxygen-depleted (i.e. dysoxic) regimes and is recognised in various depths (e.g. van der Zwaan et al., 1999; Pérez-Asensio and Aguirre, 2010).

3.1.3 *Lenticulina spp.*

Lenticulina is another genus of benthic foraminifera. Its first appearance was in the Triassic and it is still found in the Holocene. During Cretaceous times *Lenticulina* had a cosmopolitan distribution and is considered a dominant genus (e.g. Loeblich and Tappan, 1988; Friedrich, 2010). *Lenticulina* lives on the sediment and thus is classified as epibenthic.

For the present study *Lenticulina spp.* (= *Lenticulina gaultina*, *Lenticulina rotulata* and *Lenticulina sternalis*) were analysed.

3.2 Site description and temporal classification

3.2.1 Mullinax-1 core, Brazos, USA

The core Mullinax-1 (31°07.530'N, 96°49.301'W) was recovered on a meadow of the Rosebud Farm about 370 m downstream from the bridge (Highway 413 Bridge) over the Brazos River, Falls County, Texas, USA (Figure 3). The core has a length of about 45 m and provides a continuous and undisturbed sediment sequence through the upper Maastrichtian to early Danian (Keller et al., 2007). It thus allows an investigation of the Cretaceous-Palaeogene boundary including the so known "event deposit" (e.g. Schulte et al., 2006; Keller et al., 2007) also referred to as "boundary (event) complex" (e.g. Yancey, 1996), a graded, mostly coarse-grained sandstone complex.

The whole investigated part of the core is divided stratigraphically into three intervals: The Maastrichtian, the sandstone complex, and the Danian.

The late Maastrichtian samples in this core are generally characterised by grey to dark grey horizontally bedded mudstones with few intercalations of fissile shales and contain variable contents of foraminifera and other invertebrate assemblages such as nannofossils, and palynomorphs. Throughout the core, especially in the latest Maastrichtian, altering strata (in terms of granulometric data) of clay and silt occurs, which is considered normal for the Late Maastrichtian (mid-outer shelf sedimentation). The water depth of these mudstones was 100-200 m, whereas the uppermost Maastrichtian sediments are considered to have been deposited in 75-100 m depth. Mineralogically, the investigated part of the core reveals stable contents of calcite and trends to slightly lower calcite contents up-core, followed by an abrupt decrease at the sandstone-complex. Phyllosilicates show the opposite behaviour and increase up to 60 % at the event deposit. Relatively high C_{org} values (0.8-1.0 %) occur throughout the investigated samples (Keller et al., 2007; Hart et al., 2012).

The aforementioned sandstone complex is a highly controversial issue in research. On the one hand it is interpreted as a consequence of the Chicxulub impact on Yucatán, deposited within a short time period by mega-tsunami waves induced by the impact (e.g. Bourgeois et al., 1988; Smit el al., 1992; Arenillas et al., 2006; Schulte et al., 2006). On the other hand deposition over a considerable time interval is also discussed (e.g. Adatte et al., 1996; Keller et al., 2003; Gale, 2006; Keller et al., 2009). No matter which of the two scenarios actually took place, a complete change in depositional conditions occurred during this time.

The sandstone complex is deposited above the Corsicana Formation (weakly bedded, dark grey mudstones with dispersed shell fragments) and is divided roughly into five lithological units (Yancey, 1996):

- A basal conglomerate composed of clasts of mudstone embedded in a matrix of shell hash;
- A spherulitic conglomerate unit, composed of green to brown coloured loosely cemented sandstones;

- A more compact sandstone and two resistant, grey to light grey coloured, spherule-bearing layers overlain by sandstones barren of spherules, which imbed a thin glauconitic clay layer;
- Hummocky cross-bedded sandstones split up into a lower and an upper part by grey glauconitic sandstones;
- The final unit – a marly limestone.

Danian deposits begin with sandy mudstones (medium to dark grey). These are poorly sorted and weakly bedded though some irregular thin bedding is found. The overlaying dark grey mudstones show some dark bands, small burrows with dark infillings and a rich microfauna consisting of diverse foraminifera, ostracods, bivalves, and gastropods. Further up, varying mud-, silt- and sandstones are deposited and are overlain by a thin interval of claystones (Keller et al., 2007; Hart et al., 2012).

Figure 3 – Location of Mullinax-1 core (Rosebud Farm, Brazos, Texas, USA) marked by the yellow dot (●)

In this study 61 samples (hand picked tests of benthic foraminifera) of core material were analysed – beginning at the depth of 6.22 m and ending at 22.16 m. Due to the extremely small size of the specimens combined analyses of *Lenticulina spp.* (= *Lenticulina gaultina*, *Lenticulina rotulata* and *Lenticulina sternalis*) were conducted.

3.2.2 ODP Site 1002, Hole C, Cariaco Basin (Venezuela)

The Cariaco Basin (Figure 4) is located on the northern continental shelf of eastern Venezuela and is one of the world's largest anoxic marine basins. It is an east-west-trending pull-apart basin and covers an area of approximately 10,000 km^2 (Schubert, 1982). The Cariaco Basin has a length of 160 km and a width of 50 km and is divided by a saddle into two sub-basins. The maximum depth at the saddle is about 900 m, whereas the two sub-basins have a maximum depth of approximately 1400 m. From the Caribbean Sea, the Cariaco Basin is separated by a shallow sill (depth about 150 m) to the north. This sill allows surface waters to exchange freely with Caribbean surface waters, but waters below the sill depth are poorly ventilated (Scranton et al., 1987). The excessive oxygen demand created by high upwelling-induced surface productivity and restricted mixing result in anoxia below 300 m (Deuser, 1973; Peterson et al., 1991).

The Venezuelan rivers Manzanares, Neveri, Unare and Tuy presently are the major source of terrigenous sediment delivery to the basin, whereas water from the Amazon and Orinoco Rivers has little influence on the hydrography of the Cariaco Basin (Müller-Karger et al., 1989).

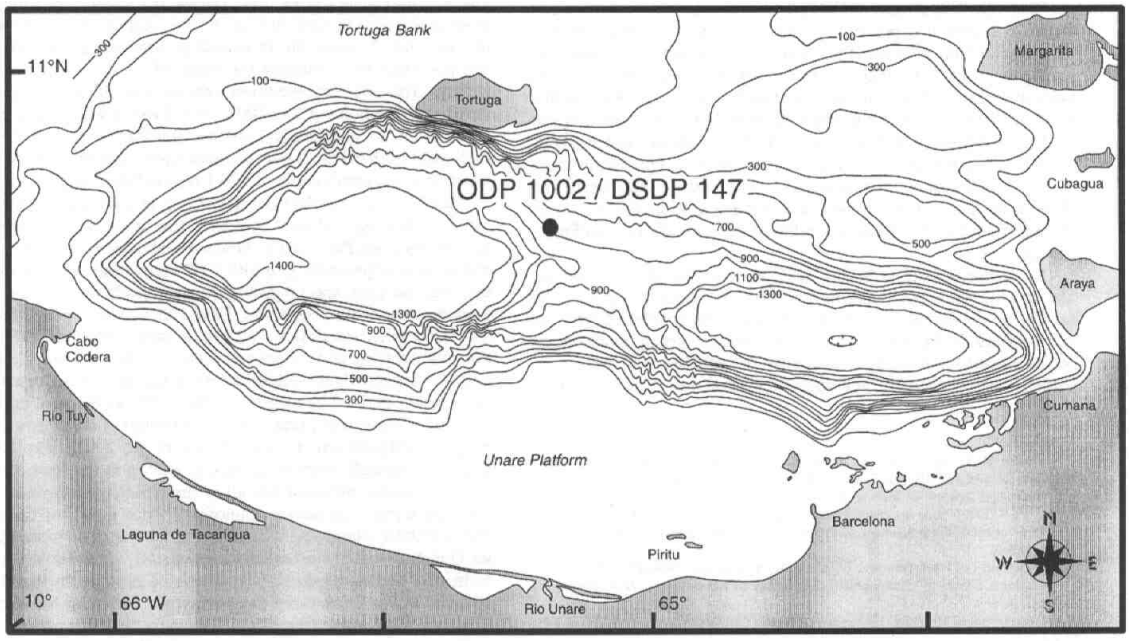

Figure 4 – The Cariaco Basin (Peterson et al., 2000). The position of ODP Site 1002 Hole C is marked by the black dot (●)

Recent to sub-recent sediment from Cariaco was chosen for this study as it documents a change in sedimentation conditions from oxic to anoxic and it is devoid of diagenetic influence. If the theory applies that foraminifers preserve changes in sea water chemistry, which are, for instance, induced by a dramatic change in sedimentation conditions, then foraminifera from this location will document the well known present day anoxic conditions, too. Additionally, these foraminifers may verify the culture experiments that were performed within this study.

The exact position of OPD Site 1002 Hole C is 10°42 .366'N, 65°10.166'W (black dot in Figure 4). The total core from Site 1002 C measures 170.1 m and generally consists of a continuous sedimentary sequence of nannofossil-rich silty clay (mostly olive grey to greenish grey in colour) that spans from Pleistocene (maximum age = 578,000 years) to present day Holocene. The top of the core was located 892.6 m below sea level (Sigurdsson et al., 1997).

For the present study 70 samples beginning at 12.04 and ending at 0.34 mbsf were investigated. The deepest sample is equivalent to an age of 19,130 years (Peterson et al., 2000). Generally, a lot of the recovered material is laminated which indicates

deposition under largely anoxic, bioturbation-free conditions, but these are interrupted by massive (= oxic) intervals. Within the oxic intervals laminated parts are frequently found (Sigurdsson et al., 1997).

Figure 5 shows the part of the core which was used in this study. In the lower part the core (12.1 to 8.5 m) consists primarily of olive grey (5Y 4/2) nannofossil-rich silty clay. Very slight bioturbation is found and laminations are common throughout this part. The most pronounced laminae are grey (5Y 5/1) thin, silty layers. Foraminifera and pteropod fragments are commonly visible. Between 11.0 and 9.5 m, two thin silty turbidites occur with thicknesses of 4 and 8 cm respectively. Further up (between 9.5 and 8.0 m) three clay layers of different colours are present: A light grey (10Y 6/2) 5 cm thick layer, the second is a 3 cm thick light grey (5Y 7/1) clay layer, and a 3 cm thick light reddish brown (5YR 6/4) clay layer marks the end of this interval. From 8.5 m on core-up the sediments mainly consist of dark olive grey silty clay (5Y 3/2) with nannofossils, foraminifera, and diatoms. Olive grey (5Y 4/2), diatom rich clayey mixed sediments and light greenish grey (5GY 7/1) to yellowish brown (10Y 5/4) clay parts are also present. Bioturbation is visible in the clay parts, but the laminated intervals (mm-scale in thickness) are undisturbed. Laminations are found mostly in the top three meters of the core and are very distinct between 6.5 and 3.0 m – between 8.5 and 6.5 m no laminations are found. Besides foraminifera, diatoms (especially the top 5.0 m of the core are considered as extremely rich in diatoms) and nannofossils, pteropod fragments, and some whole specimens are present. Additionally, from 5.84 to 5.86 m a thin, fine-grained turbidite occurs (Sigurdsson et al., 1997; Peterson et al., 2000).

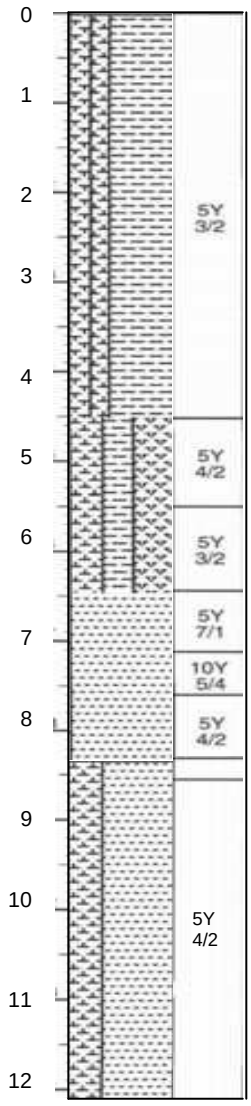

Figure 5 – Core from ODP Site 1002, Hole C, Cariaco Basin (modified after Sigurdsson et al., 1997). Numbers on the left: Depth [mbsf]

3.2.3 Live foraminifera – Dorum-Neufeld, Germany

Live specimens of *Ammonia tepida* were collected by sampling the upper 0.5 cm of sediment (Wadden mud – with a mud and clay content of greater than 50 % (Köster 1998/1999)) using Petri dishes at low-tide in an intertidal mudflat of the Wadden Sea, part of the North Sea. The locality is situated near the Lower Saxony town of Dorum-Neufeld, Germany. Dorum-Neufeld is located 20 km N of Bremerhaven within the *Nationalpark Niedersächsisches Wattenmeer*. Figure 6 shows the location.

Figure 6 – Locality of Dorum and the Nationalpark Niedersächsisches Wattenmeer

3.2.3.1 Preparing live foraminifera for culturing

In the laboratory, the sediment was sieved using a 125 µm mesh sieve and was washed with filtered (0.2 µm) North Sea water. Foraminifera were hand picked under a binocular microscope using a very fine brush and screened under a Zeiss Axiovert 200M inverted microscope for pseudopodial activity – which expresses vitality. Seven hundred live individuals in total were transferred into and divided evenly among 14 small Petri dishes (see Figure 7) and then covered with plankton net. Two dishes were set in each of the seven sediment-free aquaria, each containing 1.575 L of culture solution (= mixture of filtered North Sea water and 175 ml of a mix of stock solution and reverse osmosis water (ROW, conductivity < 0.067 µScm^{-1}) – further details below). Before use, the aquaria were thoroughly cleaned with 10 vol.-% HNO_3 and rinsed with ROW.

Figure 7 – Foraminifera in a petri dish with a lens on the bottom

3.2.3.2 Culturing procedures

Two stock solutions (350 ml each), with defined concentrations of Mn, Co, Ni, and Cu for one experiment (= Batch I experiment), and with As, Cr, V, and Mo for another experiment (= Batch II experiment) were prepared using ICP-standard solutions (1000 µg/mL in 5 vol.-% HNO_3 each) (Specpure, Alfa Aesar, Germany). For Batch I, the stock solution was prepared by filling 42 µl Mn, 45 µl Co, 146 µl Ni, and 935 µl Cu ICP-standard solutions into an Erlenmeyer flask, which was filled up to 350 ml with ROW. The stock solution for Batch II was prepared in the same way, but using 182 µl V, 38 µl Cr, 250 µl As, and 881 µl Mo ICP-standard solution instead. Table 2 shows an overview of the stock solutions.

Table 2 – Components of the stock solutions used in Batch I experiment (= Stock I) and Batch II Experiment (= Stock II) [µl]

	Mn	Co	Ni	Cu	V	Cr	As	Mo
Stock I (350 mL)	42	45	146	935				
Stock II (350 mL)					182	38	250	881

The pH of the stock solutions was raised to 8.0 ± 0.1 with 1M NaOH (p.a.) in order to match the pH of the natural sea water. Then, 175 mL stock solution was added to 1.40 L North Sea water, which was equivalent to a 20-fold sea water concentration. For the 10-fold and the 5-fold concentration experiments, 87.5 mL stock solution and 87.5 mL ROW, as well as 43.75 mL stock solution and 131.25 mL ROW, respectively were each added to 1.40 L North Sea water. In addition, a reference tank without any additional trace element was prepared. Finally, the culture solutions were filtered again using a 0.2 µm membrane filter to avoid introducing possible inorganic precipitates in the aquaria. Table 3 summarises the volumes of each component in the different aquaria for each concentration.

Table 3 – Composition of the culture solution for the different aquaria in the conducted experiments. The amounts of stock solution and ROW for the diverse concentrations are identical for Batch I- and Batch II experiment

	Stock solution [mL]	**Reverse osmosis water [mL]**	**North Sea water [L]**
5-fold concentration	43.75	131.25	1.40
10-fold concentration	87.5	87.5	1.40
20-fold concentration	175	0	1.40

Before the filtered North Sea water was mixed with the stock solution, the fluorescent label calcein (bis[N,N-bis(carboxymethyl)aminomethyl]-fluorescein) (Sigma-Aldrich) was added to the sea water at a concentration of 5 mg/L to mark newly grown chambers of the foraminifera (Figure 8), (Bernhard et al., 2004).

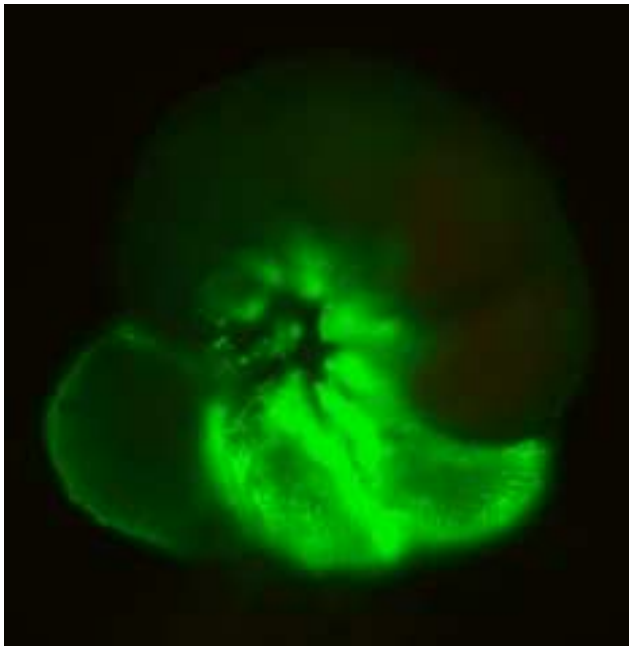

Figure 8 – Newly grown chambers (light green) marked by calcein

Foraminiferal cultures were performed without sediments or any other substrate to avoid artifacts, which could be induced for instance by pore water from sediments. Consequently, only the water chemistry had to be controlled and monitored. The seven aquaria were covered with a fibre-glass plate, to minimise evaporation, and then were placed in a temperature controlled cabinet (Figure 9). Salinity, pH and temperature were monitored every other day to ensure stable conditions (Figures 12 and 13), Section 4.1).

- Salinity was measured using a salimeter (type Cond 330i fitted with a TertaCon 325 electrode, both from WTW, Germany). Precision of these measurements was accounted by repeated measurements and was found to be better than 1.00 %;
- pH and temperature were measured with a combined instrument (type Multi 340i equipped with a SenTix 41 electrode, both from WTW, Germany). Precision for both was accounted by repetitive measurements. Precision for pH and temperature were better than 1.20 % and 1.40 %, respectively.

To prevent bacterial build-up, the culture solutions were changed every 4 weeks. Vitality of specimens was checked bi-weekly: Ten specimens were randomly selected from each tank and screened for pseudopodial activity with the aid of an inverted microscope. Food, which consisted of approximately 5 mg of a mixture of air dried

algae (*Phaeodactylum triconortum*, *Dunaliella salina* and *Isochrisis galbana*), was added to the aquaria at the beginning of the experiment and every time food was no longer visible (4 and 8 weeks after the start of the experiment). The total duration of this experiment was 82 days.

Figure 9 – Aquaria in temperature controlled cabinet

The elemental composition of the culture solutions were measured weekly using High Resolution Inductively Coupled Plasma Mass Spectroscopy (HR-ICP-MS, type Axiom from VG Elemental). The analyses showed that the mean trace element concentrations remained within an acceptable range throughout the experiment (Table 6, Figures 10 and 11). Accuracy of the analyses was verified by measuring the certified water reference sample CRM-TMWD-A (High Purity Standards, USA) in every analytical batch.

At the end of the experiment, all specimens were screened for pseudopodial activity before the tests were cleaned of organic material by soaking the specimens in a solution of 6-8 vol.-% NaOCl (Merck), twice, for two to three hours at a time (Mashiotta et al., 1999; Pak et al., 2004). Finally, the tests were rinsed four times with ROW and allowed to dry thoroughly before being analysed.

3.3 Treatment of foraminiferal tests from core samples

Before foraminifera from core samples were analysed, these had to undergo a complex cleaning protocol to produce a primary signal. Organic matter (e.g. Martin et al., 2002) as well as precipitation of metals on the tests may influence the content of some minor and trace elements (e.g. Boyle, 1981; Boyle and Keigwin, 1985/1986; Elderfield et al., 1996; Hastings et al., 1996). For this study a multi-stage cleaning protocol was applied, based on the procedure developed by Boyle (1981) and Boyle and Keigwin (1985/1986), complemented by Hastings et al. (1996) and modified by Meudt (2004) to meet the requirements needed for very small amounts of sample material.

Briefly, after weighing (30 µg as the low limit) as well as cracking the tests between two glass plates the fragments were transferred into 1.5 mL polypropylene (PP) micro-tubes.

To remove the clay particles, micro-tubes were filled with 0.5 mL of double distilled water (H_2O_{bidest}). Bubbles of air were eliminated by tapping the micro-vessels carefully against the rack. Vessels were then sealed and the rack was placed in an ultrasonic bath for one to two minutes. After letting the fragments settle down for half a minute, the water was pipetted off. This washing was repeated once with H_2O_{bidest} and twice with 100 µL methanol (p.a. quality). Three rinses with 1 mL H_2O_{bidest} followed to wash out the methanol. Then the samples were dried overnight in a hot-air cabinet at 40 °C.

To reduce metal oxides, a 1 M solution of $[NH_3OH]Cl$, using a 5 % NH_3 solution (p.a. quality), was produced. Each micro-tube was filled with 0.5 mL reagent and emerging bubbles were eliminated as mentioned before. Micro-tubes were then sealed and the

rack was placed in a 60 °C heated ultrasonic bath for four to five minutes. After this the samples rested for a minute and the reagent was removed using a pipette. Subsequently the samples were rinsed three times with 1 mL H_2O_{bidest} before they were transferred to the hot-air cabinet (40 °C) overnight.

Then 100 µL H_2O_2 were added to 30 mL 0.1 N NaOH (both in p.a. quality). Each micro-tube was filled with 250 µL of this reagent. After closing the tubes, the rack again was placed in a 60 °C heated ultrasonic bath for four to five minutes. After settling, 0.5 mL H_2O_{bidest} was added to each vessel. After one minute the solution was pipetted off and the samples were rinsed three times with 1 mL H_2O_{bidest}. Subsequently all samples were transferred to the hot-air cabinet (40 °C) overnight again.

To eliminate the residual metal contamination at the surface of the test fragments, 25 µL of 0.25 % HNO_3 (ultra pure quality) were added to each sample. Two minutes later, 1 mL H_2O_{bidest} was added and pipetted off again. To rinse the fragments, three times 1 mL of H_2O_{bidest} was added and removed again.

As a last step, the samples were dissolved by adding 100 µL 1 % HNO_3 (ultra pure quality). To accelerate the dissolution, the rack with the micro-tubes was placed in the ultrasonic bath for 15 minutes. If any fragments were left over, another 100 µL HNO_3 (1 %, ultra pure quality) were added and the ultrasonic bath was repeated. After a short settling phase, the dissolved samples were pipetted into 5 mL teflon beakers and 1 % HNO_3 (ultra pure quality) was added until a total volume of 2.5 mL was reached.

3.4 HR-ICP-MS

The High Resolution Inductively Coupled Plasma Mass Spectroscopy (HR-ICP-MS) (type Axiom from VG Elemental, Germany) was used to measure the trace element content of the culture solutions as well as of the foraminifera from ODP Site 1002 C and the Mullinax-1 core.

For the culture solutions, weekly measurements of the elemental composition confirmed that the target concentrations remained constant within an acceptable range

(Figures 10 and 11). The accuracy of the analyses was assessed by measuring the certified water reference sample CRM-TMWD-A (High Purity Standards, USA) in every analytical batch. Each sample was analysed three times with a dwell time of 25 ms for all elements except for As, which was 30 ms. The internal standards used were ^{169}Tm for Mo, ^{115}In for As, and ^{103}Rh for the other analysed elements (Ca, V, Cr, Mn, Co, Ni, and Cu). For all measurements of the culture solutions a concentric nebuliser with a flux rate of 1 mL/min and Ni cones were used. Table 4 lists the detection limits and the accuracy of the measurements.

For the analyses of the foraminiferal tests, generally the same conditions were applied and the same elements as internal standards were used (^{103}Rh for the elements Mg, Al, P, S, Ca, V, Cr, Mn, Fe, Co, Ni, Cu, Zn, and Rb, ^{115}In for As and ^{169}Tm for the elements Mo, Sr, Cd, Ba, Pb, and U. For all foraminiferal measurements a micro-concentric nebuliser (flux rate: 100 µL/min) was used. Detection limits and accuracy is shown in Table 5.

Table 4 – Detection limit and accuracy (standard deviation) of the performed measurements (culture solutions)

Element	Detection limit [µg/L]	Standard deviation	Element	Detection limit [µg/L]	Standard deviation
Ca	3.77	0.001	Ni	0.12	0.04
V	0.002	0.001	Cu	0.11	0.04
Cr	0.004	0.001	As	0.15	0.05
Mn	0.03	0.01	Mo	0.3	0.1
Co	0.02	0.01			

Table 5 – Detection limit and accuracy (standard deviation) of the performed measurements (foraminiferal calcite)

Element	Detection limit [µg/L]	Standard deviation	Element	Detection limit [µg/L]	Standard deviation
Mg	0.62	0.21	Cu	0.12	0.03
P	0.08	0.03	Zn	0.2	0.07
S	1.46	0.49	As	0.18	0.05
Ca	6.46	2.55	Rb	0.03	0.01
V	0.01	0.01	Sr	0.02	0.01
Cr	0.02	0.01	Mo	0.4	0.07
Mn	0.1	0.03	Cd	0.002	0.001
Fe	0.16	0.05	Ba	0.04	0.01
Co	0.03	0.01	Pb	0.02	0.01
Ni	0.14	0.04	U	0.002	0.001

3.5 µ-synchrotron XRF

At the synchrotron facilities in Hamburg (DESY, HASYLAB beamline L) and Karlsruhe (ANKA, FLUO-beamline) µ-synchrotron X-Ray Fluorescence Spectroscopy (µ-synchrotron XRF) measurements were performed to determine the trace element content in the tests of the cultured foraminifera.

Using a liquid glue (Tesa, Beiersdorfer, Germany), two rows (each consisting of five individuals) of tests were affixed with their spiral side onto a 3 µm mylar film that was attached to plastic slide mounts. The glue as well as the mylar film were tested for their

trace element constituents before use. The abundances of all elements of interest were clearly below the detection limits of µ-synchrotron XRF determinations. Newly grown chambers as well as some old chambers were analysed. For line-focus measurements, an excitation energy of 12.5 keV was adjusted – just below the Pb LIII absorption edge to avoid interferences of the Pb LIIIMV line on the As KLIII line. Focusing by refractive lenses gave a point size of 2 x 5 µm and the chambers were analysed by line scans, averaging five points per line in newly grown chambers and three points per line in old chambers. In unfiltered sample spectra, the Ni-K lines were strongly overlain by the intense Ca sum-peak due to the calcium carbonate matrix of the investigated foraminiferal tests. To reduce this interference, a 20 µm secondary beam aluminium filter was mounted in front of the fluorescence detector. Due to low trace element concentrations in the sub µg/g and lower µg/g range, long measuring times (500 s) were necessary at each point. Trace element contents in the tests were quantified by fundamental parameters using PyMCA 4.3.0 (Solé et al., 2007). The fundamental parameter calculations were recalibrated for trace element calibration purposes by using a pressed calcite pellet (containing 756 µg/g Cr and 727 µg/g As) and the MPI-DING reference glass StHS6/80-G standard (Max-Planck-Institut für Chemie, Germany) (Jochum et al., 2000) as primary standards. Geometry effects caused by the uneven shape of the tests were corrected by calculating the absorption of the incoming beam from the count rate of the primary monitor (in front of the sample) and the secondary monitor (behind the sample). Since the calcium concentration (40 wt %) is constant in calcite, the average path length of the outgoing beam could be calculated using Ca as internal standard (Kramar et al., 2010). Replicate measurements of the same spots lay within 5 % relatively, while errors resulting from the path length calculations through the chamber walls are estimated to 10-20 % relatively. Kramar et al. (2010) discussed these effects in detail.

To obtain information about the spatial distribution of the trace elements, pseudo 3-D scans using confocal poly-capillary optics across newly grown and field grown

chambers were carried out. At ANKA FLUO-beamline excitation energies of 12.5 keV and at HASYLAB beamline L (DESY) 25 keV were applied. A focus of 15 µm for the primary capillary and 6 µm for the secondary capillary produce a voxel size of 15 x 15 x 6 µm. The measuring time could be reduced to 30-50 s per measuring point due to a higher obtained flux using poly-capillaries. The 3-D meshes had a spacing of 25 µm x 25 µm in the plane and step sizes of 20 µm in the top and the bottom region of the tests. In the middle part the step size was 50 µm to prevent measuring empty space. For the semi-quantitative trace element evaluation each voxel was calculated by the fundamental parameter method using PyMCA 4.3.0 (Solé et al., 2007). It should be noted that a 20 µm thick Al foil was used as a filter to eliminate the Ca sum-peaks.

For trace element calibration purposes a pressed calcite pellet and the MPI-DING reference glass StHS6/80-G standard (Max-Planck-Institut für Chemie, Germany) (Jochum et al., 2000) were measured.

3.6 LA-ICP-MS

Laser Ablation Inductively Coupled Plasma Mass Spectroscopy (LA-ICP-MS) measurements were conducted to determine the trace element content in the tests of the cultured foraminifera. The non-destructive nature of µ-synchrotron XRF allowed measurements with LA-ICP-MS on the same chambers and thus to compare or rather corroborate the µ-synchrotron measurements. For the LA-ICP-MS measurements, specimens were fixed on a double-sided adhesive tape and mounted on plastic stubs.

The LA-ICP-MS analyses were conducted at Utrecht University (Department of Earth Sciences) by means of an excimer laser (Lambda Physik, Germany) equipped with GeoLas 200Q optics at a wavelength of 193 nm. The ablation was conducted in a helium atmosphere. Pulse rate was adjusted to six pulses per second with an energy density of 1 J/cm^2 at the surface of the sample. The laser beam was set to a diameter of 80 µm. The ablated material was analysed with a quadrupole ICP-MS (Micromass Platform). A collision and reaction cell was used to minimise spectral interferences on

the minor isotopes of Ca (Mason and Kraan, 2002). Calcium was used as an internal standard, via the ^{44}Ca isotope, with simultaneous monitoring of ^{42}Ca and ^{43}Ca. For calibration of trace element contents, the NIST SRM 610 glass standard (National Institute of Science and Technology, USA) (Pearce et al., 1997) and an in-house matrix-matched calcite standard (GJR) were applied. Concentrations of Cu and Ni were calculated using the ^{63}Cu and ^{60}Ni isotopes. Mn was quantified using its only natural isotope, ^{55}Mn. Internal relative precision of Mn, Ni, and Cu was better than 4.5 %, 4.7 %, and 4.8 %, respectively.

3.7 XAFS

Due to the nature of As occurring in more than one oxidation state, X-ray Absorption Fine Structure spectroscopy (including XANES (X-Ray Absorption Near-Edge Structure spectroscopy) and EXAFS (Extended X-ray Absorption Fine Structure spectroscopy)) measurements were performed at the synchrotron light source Ångströmquelle Karlsruhe (ANKA, Karlsruhe) SUL-X beamline to detect the species of As incorporated into the tests of the cultured foraminifera. XAFS is a non-destructive, element-selective method providing information about oxidation state, interatomic distances, coordination number and ligand's identity. Due to its high brilliance, deduced from the synchrotron beam, which is well focused and has low noise, it is a suitable tool for analysing sample material containing small amounts of the detected element.

At the SUL-X beamline a wiggler acts as radiation source. For energy monochromatisation, a silicon (111) crystal pair was used with data being recorded by a 7 element Si(Li) detector – parallel in transmission with an ionisation chamber in front of the sample and another ionisation chamber behind the sample. To calibrate energy, a thin reference foil (As metal) was placed between the second and the third ionisation chamber and the energy was adjusted to 11876 eV.

Before measuring EXAFS and XANES spectra, the samples were scanned by micro-XRF at the same beamline to find the regions with the highest As concentration. To

eliminate Ca sum-peaks, a 40 µm thick Al foil was used as a filter. The applied energy during measurement was 12 keV and the XAFS spectra were collected at room temperature. The spot size of the analysed regions was 100 µm x 100 µm and the peak time was 2 µs. For statistical purposes and to increase the signal-to-noise ratio in the EXAFS region (until k = 12), 12 individual scans were collected for each sample. Spectra were collected at 0.2 eV steps in the edge region. Averaging of line scans and calibrating energy was performed using the Artemis 0.8.014 software, while Athena 0.8.061 software was used for shell fitting – both part of the IFEFFIT software package (Newville, 2001; Ravel and Newville, 2005).

A pressed calcite pellet with a defined As concentration (727 µg/g) and the reference glass StHS6/80-G (mentioned in Section 3.2) were used as standards.

3.8 XRF

70 bulk sediment samples of the ODP core were analysed for major and trace element chemistry. Major elements were quantified by wavelength dispersive X-ray fluorescence (WD-XRF) using an S4 Explorer WD-XRF spectrometer (Bruker AXS, Germany). Measurements were conducted on fused glass discs prepared by mixing the powdered sample with SPECTROFlux (Alfa Aesar) in a ratio of 1:10. For the determination of trace element concentrations energy dispersive X-ray fluorescence (ED-XRF) was applied using an Epsilon 5 (PANalytical, The Netherlands) ED-XRF spectrometer was used. The powdered sample material was placed in cups and covered with a 6 µm thick mylar film. Accuracy and precision were assessed by repeated measurements of certified reference materials (AGV-1, SOIL-VII, SL-1, GXR-1, GXR-2, GXR-3 for ED-XRF and AGV-1, BE-N, GXR-2 for WD-XRF). Precision was found to be generally better than 2 % and 5 % for WD-XRF and ED-XRF, respectively. Detection limits for most of the trace elements are in the range of 3-5 mg/kg.

3.9 IR-MS

Isotope ratio mass spectrometry (IR-MS) was used to measure the isotopic composition of C and O in the calcareous foraminiferal tests (70 samples of ODP Site 1002 and 43 samples of Mullinax-1 core). Measurements were performed by a Delta Advantage IRMS (Thermo Finnigan) coupled online with a GasBench II device for automated carbonate analysis. Each sample run consisted of the measurement of five distinct pulses generated by a reference gas, followed by recording the signals from ten aliquots of CO_2 produced by reaction of the sample with phosphoric acid. Internal precision, based on the standard deviation of the ten peaks is typically < 0.05 ‰ for $\delta^{13}C$ and < 0.08 ‰ for $\delta^{18}O$. Raw data were calibrated against the VPDB scale, by measuring the calcite reference material NBS-19 three times after every ten samples.

3.10 Carbon and sulphur analysis

Carbon and sulphur analysis was performed to determine the total S and C contents of the ODP core sediments. The analyses were conducted by a carbon-sulphur analyser CSA 5003 (Leybold Heraeus) based on non-dispersive infrared spectrometric detection, while the amount of inorganic/carbonate carbon was determined with a carbon-water-analyser (CWA 5003, Leybold Heraeus). The fraction of organic carbon was assessed by calculating the difference between total and inorganic carbon. Detection limits for both C and S were at 100 ppm.

3.11 Calculation of partition coefficients

Partition coefficients were calculated using the resulting trace element (TE) and calcium concentrations according to the following expression:

$$D_{TE} = (TE/Ca)_{calcite} / (TE/Ca)_{sea\ water}.$$

D_{TE} were calculated using the medians of each set of concentration measurements. Because the analytical data did not show a Gaussian distribution, the medians are a more reliable and robust parameter (e.g. Hoaglin et al., 1983; Zhou, 1987) than the means. Subsequently, the mean of the medians of the reference, 5-, and 10-fold

concentrations was calculated as the distribution coefficient. The error envelope was calculated using the standard error of the mean (e.g. Howarth, 1983). The results of the 20-fold concentration solution experiment (considering the Batch I experiment) were not included in the calculations. For more details see section 3.5.1 and the Discussion.

3.12 Calculation of palaeo temperatures

In order to reconstruct past sea water temperatures, temperature calculations according to Erez and Luz (1983) were performed, as their equation is suited best for benthic foraminifera (Zahn and Mix, 1991; Bemis et al., 1998).

The equation is based on the $\delta^{18}O$ value of foraminiferal calcite. The calculation is as follows:

$$17 - 4.52 \times (\delta^{18}O_{fc} - \delta^{18}O_{sw}) + 0.003 \times (\delta^{18}O_{fc} - \delta^{18}O_{sw})^2$$

with:

fc = foraminiferal calcite

sw = sea water.

3.13 Statistical data evaluation

The behaviour of trace elements is controlled by a number of different factors. Complex interaction of these factors makes interpretation of geochemical data difficult. The use of multivariate statistical methods is beneficial whilst deciphering complex interactions and effects considering geochemical processes. Before applying statistical methods to the data, outliers were eliminated by Grubbs' test.

Thus, multivariate statistical methods (i.e. hierarchical cluster analysis and factor analysis) were carried out, using the software package Statistica (Version 6.1, StatSoft Inc.), to obtain more details of geochemical data (the tests of calcareous foraminifera and also of bulk sediment samples). Foraminiferal trace element data were Ca-normalised because of the calcareous matrix of the tests (tests consist of nearly 100 % calcite) before using statistical methods.

Cluster analysis is a statistical tool which groups the objects (or elements) of investigation in a way that the individual elements of a group (= clusters) are more similar to each other, but different to objects of another cluster. For hierarchical cluster analysis, which was used for the geochemical data of the foraminiferal calcite tests in the present study, Ward's method (Ward, 1963) was applied. This method uses Pearson correlation coefficients from an initially created data matrix as a basis. Preliminarily, data from this data matrix was z-transformed so that geometrical (i.e. Euclidean) distances between the grouped elements (i.e. clusters) could be calculated. Ward's method, based on analysis of variances, gradually combines those clusters by iteration, which contribute least to the sum of squares. Repetitive iteration leads to hierarchical clusters with minimum distances. The final number of clusters corresponds to the number of iterations. Results of hierarchical cluster analysis are graphically summarised in dendrograms.

Factor analysis is a heuristic, hypotheses generating statistical method that reduces the number of initial correlated variables and groups these in independent variables – the factors. These factors are mutually independent and express correlations between the variables by the factor loading, which corresponds to the correlation between a variable and a factor. The factor loading has values between -1 and 1, meaning strong negative and strong positive correlation, respectively. In general, the better the variables are correlating with each other, the fewer factors are needed to explain the total variance. Additionally, a so called factor score is calculated for each case (e.g. samples in the core) that expresses the estimated values of factors for the specific case.

In this study, factor analysis was applied to the geochemical data of bulk sediment samples of the ODP Site 1002, Hole C core and the geochemistry of the foraminiferal tests of the Mullinax-1 core.

Prior to performing factor analysis, a correlation matrix is created. Subsequently, factors are extracted gradually from this matrix until an eigenvalue of 1 is reached,

which marks the end of the factor extraction. The eigenvalue of a factor expresses the amount of the total variance of all variables that is explained by this factor. In order to maximise the variance of the factor loadings, Varimax standardised rotation was applied to the data.

Further details and the mathematical theory about the applied multivariate statistical methods may be obtained for instance from Ward (1963), Stoyan et al. (1997), and Bortz (1999).

4 Results

4.1 Culture solutions

Continuous monitoring of the culture solutions revealed that the trace element concentrations correspond well to the initial concentrations within the range of the standard deviation. The elements of the stock solutions therefore did not precipitate or absorb to a significant amount when mixed with the ROW and the North Sea water, nor were they consumed to an appreciable degree over the course of the experiments (Figures 10 and 11, Table 6).

Furthermore, salinity (24.0 ± 0.1), pH (8.0 ± 0.1) and temperature (14.5℃ ± 0.2℃) were monitored every other day and were stable within the given standard deviations over the course of the experiments. These measurements are shown in Figures 12 and 13.

Table 6 – Mean concentrations of Mn, Ni, Cu, V, and As in the culture solutions. Reference = North Sea Water without added trace elements, 5-, 10-, and 20-fold indicate 5-, 10-, and 20-fold concentrations of natural North Sea water. B I = Batch I experiment, B II = Batch II experiment

	Manganese [nmol/L]	Nickel [nmol/L]	Copper [µmol/L]	Vanadium [nmol/L]	Arsenic [nmol/L]
Mean reference	30 ± 13	48 ± 14	0.195 ± 0.027	36 ± 4	63 ± 21
Mean 5-fold (B I)	86 ± 33	231 ± 70	1.01 ± 0.233		
Mean 10-fold (B I)	113 ± 45	371 ± 52	1.70 ± 0.155		
Mean 20-fold (B I)	209 ± 56	649 ± 105	3.29 ± 0.263		
Mean 5-fold (B II)				331 ± 16	295 ± 64
Mean 10-fold (B II)				617 ± 30	512 ± 58
Mean 20-fold (B II)				1189 ± 37	952 ± 92

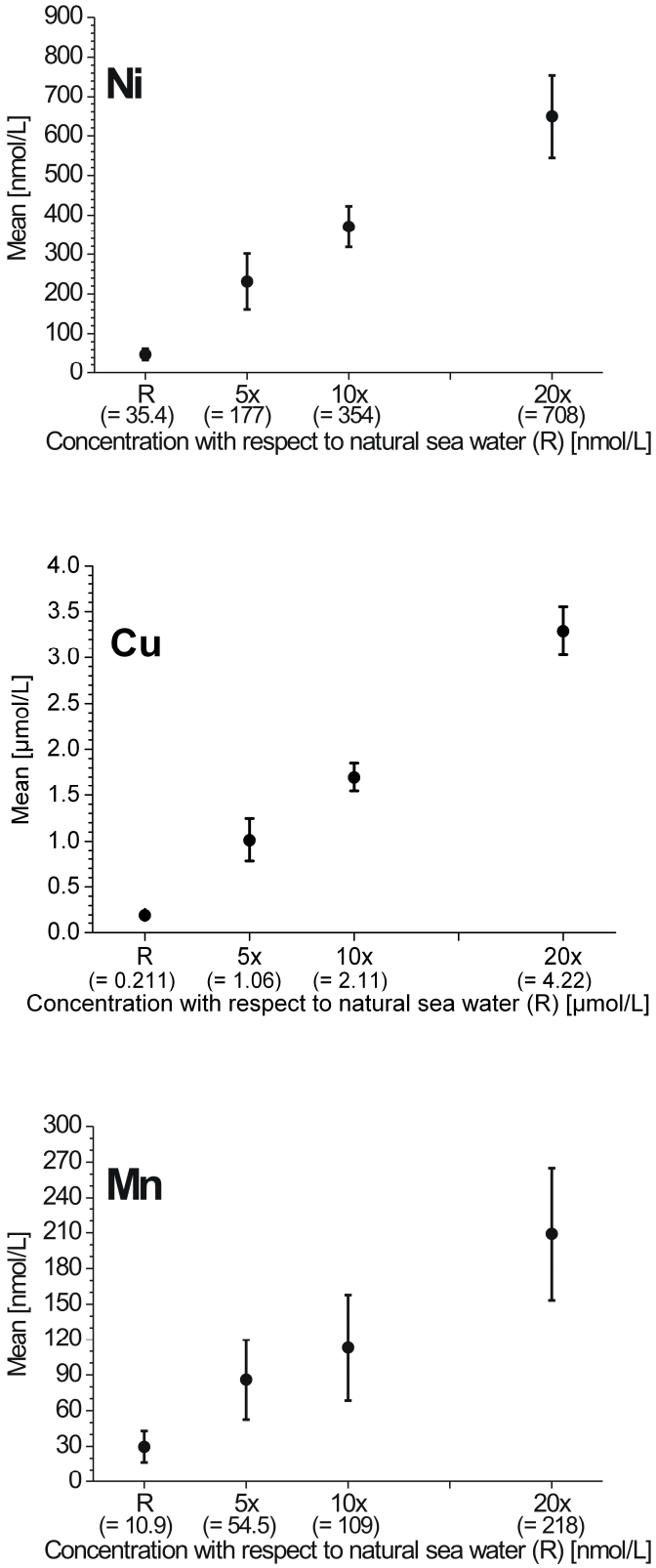

Figure 10 – Variation (expressed as standard deviation) in the concentration of Ni (top), Cu (centre), and Mn (bottom) of the culture solutions during Batch I experiment; R = reference (natural North Sea water). Values in parentheses are calculated values based on pure sea water measurements performed before the experiments

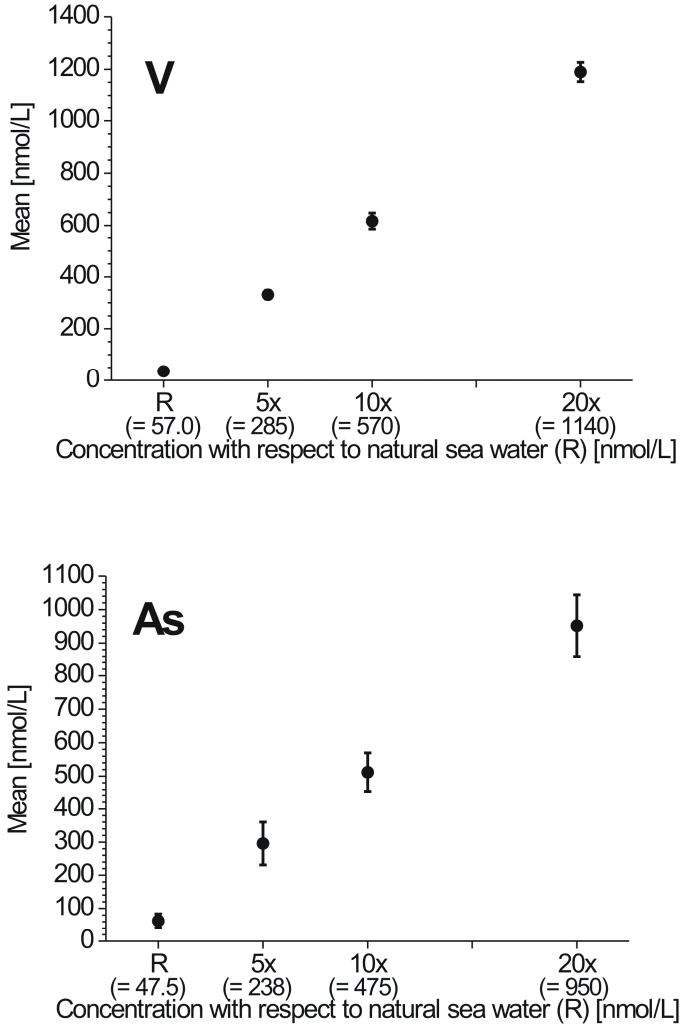

Figure 11 – Variation (expressed as standard deviation) in the concentration of V (top) and As (bottom) of the culture solutions during Batch II experiment; R = reference (natural North Sea water). Values in parentheses are calculated values based on pure sea water measurements performed before the experiments

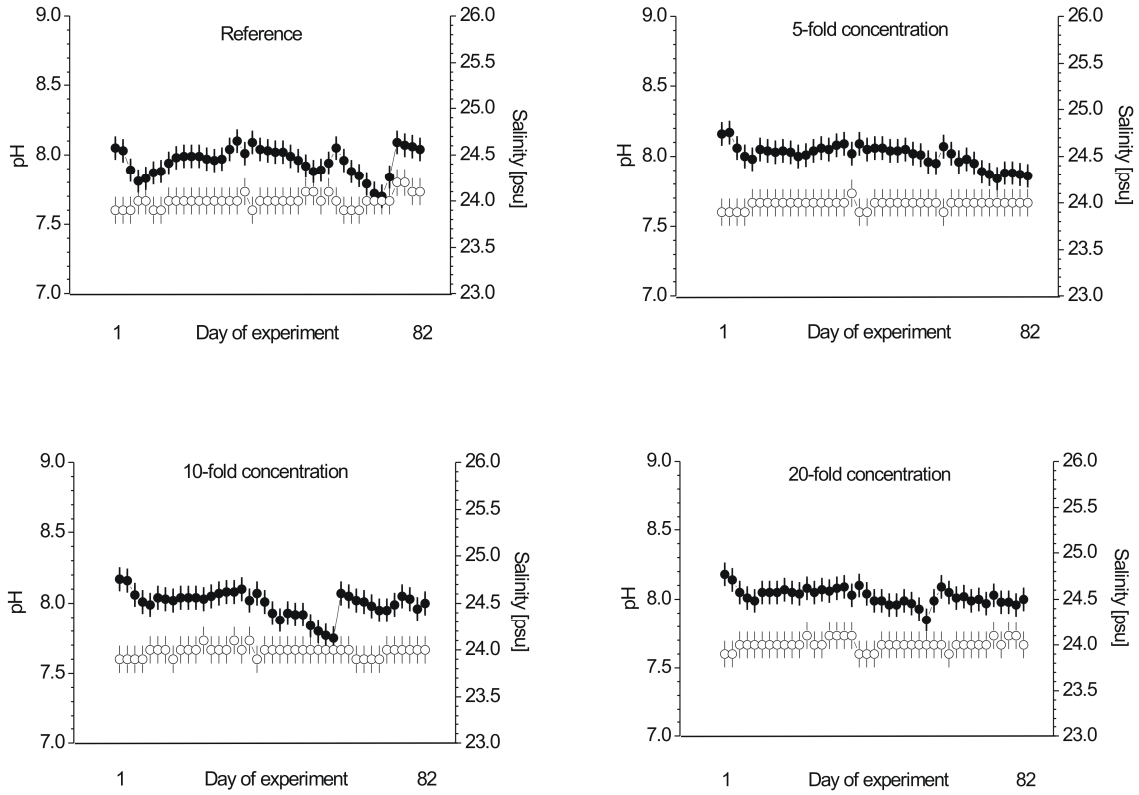

Figure 12- – pH (●) and salinity [psu] (○) monitoring of each culture solution during the course of the experiment (Batch I experiment: Top left = Reference, top right = 5-fold concentration, bottom left = 10-fold concentration, and bottom right = 20-fold concentration)

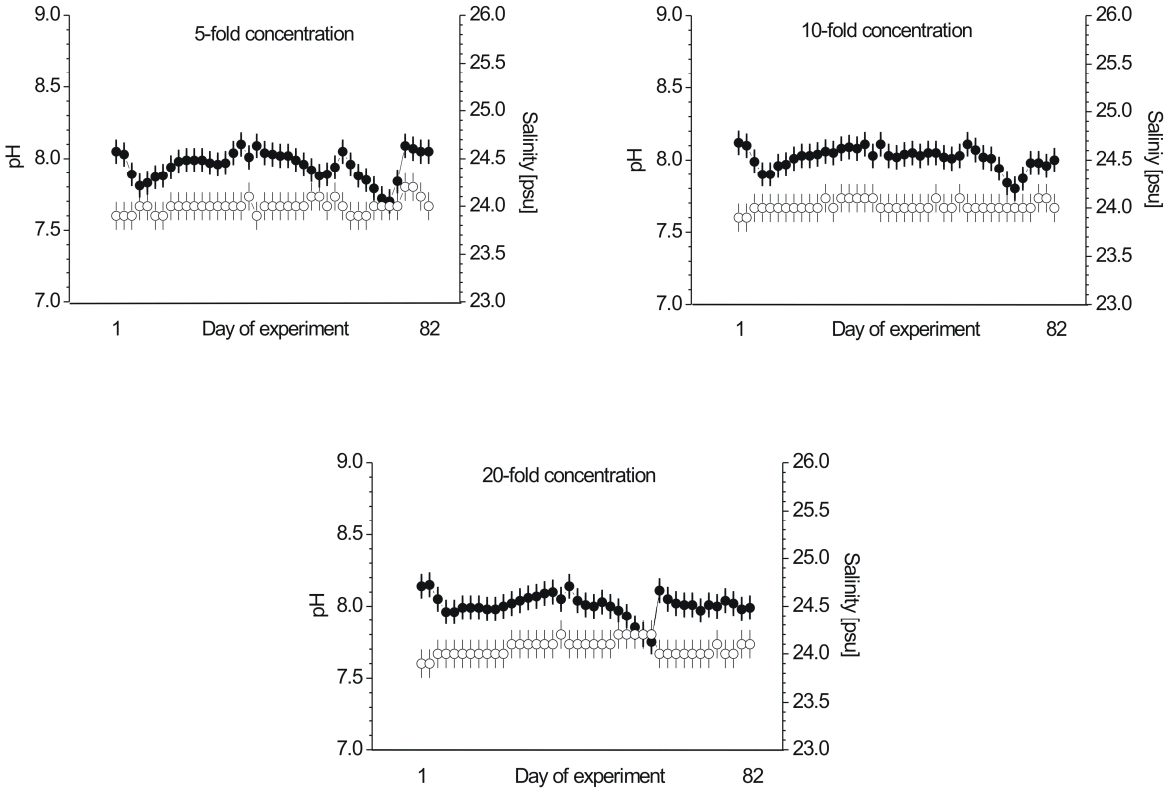

Figure 13 – pH (●) and salinity [psu] (○) monitoring of each culture solution during the course of the experiment (Batch II experiment: Top left = 5-fold concentration, top right = 10-fold concentration, and bottom = 20-fold concentration. Reference is shown in Figure 12)

4.2 Newly grown foraminiferal calcite

Regarding Batch I, nearly all specimens (95.5 % on average) survived the culture period of 82 days. Exact values for each experiment are listed in Table 7. In one of the aquaria (10-fold concentration), even reproduction occurred, but only one juvenile foraminifer was recovered after termination of the experiments. Seven individuals of the 5-fold concentration experiment were lost during water changes. New chambers formed in all experiments. For the reference experiment, 47.0 % of the specimens formed at least one new chamber. In the 5-, 10- and 20-fold concentration experiments, 53.0 %, 41.0 %, and 29.0 % of the individuals formed at least one new chamber, respectively (Table 7 and Figure 14).

For Batch II, 92.0 % of the specimens (on average) survived the culture period of 82 days. Detailed values may be obtained from Table 7. In two aquaria reproduction occurred: One individual in the 5-fold and the 10-fold concentrated tanks and three individuals in the tank with the highest trace element concentrations. New biogenic calcite was formed in all aquaria. In the 5-, 10-, and 20-fold concentration tanks this rate was 51.0 %, 45.0 %, and 37.0 % of specimens, respectively (Table 7). Absolute numbers are shown in Figure 14.

Thus, for both experiments it is true that decreasing calcite production and a decreasing survivor's rate along with increasing trace element concentrations can be obtained.

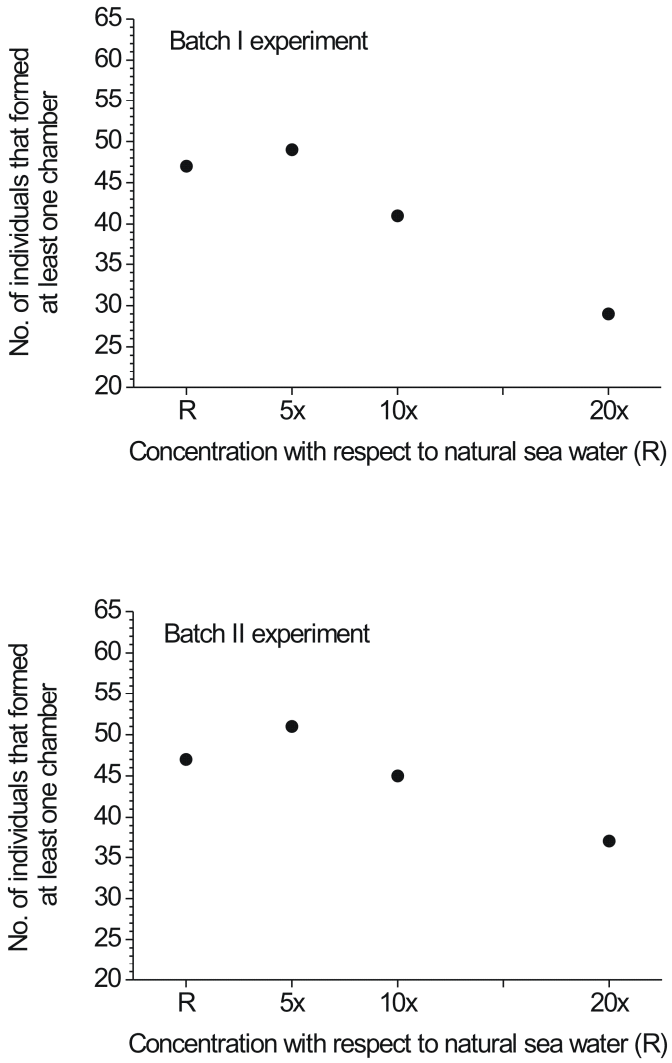

Figure 14 – Total number of individuals that formed new chambers. Top: Batch I experiment, bottom: Batch II experiment

Table 7 – Chamber addition and offspring data of the cultured *Ammonia tepida*. NSW = North Sea water; 5-, 10-, and 20-fold indicate 5-, 10-, and 20-fold concentration of natural North Sea water; B I = Batch I experiment; B II = Batch II experiment

Aquarium	No. of individuals (start of experiment)	Living individuals (end of experiment) [%]	No. of individuals that formed new chambers					Individuals that formed new chambers [%]	Total no. of formed chambers	No. of offspring
			1	2	3	4	5			
Reference	100	98.0	10	14	12	9	2	47.0	120	0
5-fold NSW B I	100*	96.7	22	19	8	0	0	53.0	84	0
10-fold NSW B I	100	94.0	22	16	0	0	0	41.0	54	1
20-fold NSW B I	100	93.0	20	9	0	0	0	29.0	38	0
5-fold NSW B II	100	93.0	31	16	4	0	0	51.0	75	1
10-fold NSW B II	100	87.0	25	14	6	0	0	45.0	71	1
20-fold NSW B II	100	90.0	25	11	1	0	0	37.0	50	3

* Seven individuals were lost during water changes.

4.3 Comparison of µ-synchrotron XRF and LA-ICP-MS

The precision of measurements for Co, Mo and Cr analyses was low as the measured concentrations were too close to or under the detection limit for both analytical methods. Arsenic and V measurements were only confidently obtained using the µ-synchrotron XRF, while for these elements the LA-ICP-MS measurements showed a non-satisfying signal to noise ratio. For the elements of Batch I experiment though (especially Cu and Ni), the LA-ICP-MS measurements match well with those of µ-synchrotron XRF.

Although the analyses show a wide range of variability in trace metal uptake among individual specimens, clear trends are observed for Cu, Ni, As, and V. Specimens

grown under identical conditions show for both Mg and Sr (e.g. Reichart et al., 2003; Dueñas-Bohórquez et al., 2009; Dissard et al. 2010a and 2010b) similar element uptake and seem to reflect differences in elemental uptake between individuals rather than analytical variability. This is confirmed by the fact that irrespective of the analytical technique used (LA-ICP-MS or µ-synchrotron XRF), the concentrations of Ni and Cu in the calcite increase with increasing concentrations in the sea water (Table 6, Figure 10, Figures 16 and 17), except for the tests grown at the highest concentration (20-fold). For As and V this is true for at least one of the applied analytical techniques (Table 6, Figures 11 and 19).

4.4 Speciation of arsenic

Arsenic occurs as As (V) in the foraminiferal calcite tests. This is indicated by measurements of absorption edge positions shown as a normalised spectrum in Figure 15. The K-edge spectrum of the As (V) standard (grey line in Figure 15) is very similar to the one from the foraminiferal calcite. Both peak at 11,876 eV and thus clearly reveal the incorporated species as As (V) (red line in Figure 15). In contrast, the likewise measured As (III) standard reaches its maximum at 11,873 eV (black line in Figure 15). Additionally, Fourier-transformed EXAFS spectra (no graph available) showed a prominent peak at ~3.3 Å, which corresponds to an As-Ca distance – evidence for the incorporation of As into the foraminiferal calcite tests (personal communication with U. Kramar, 2011).

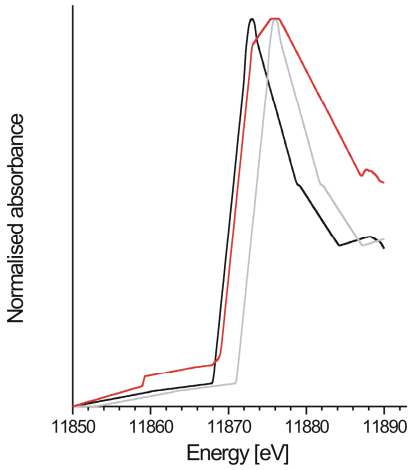

Figure 15 – Arsenic in foraminiferal calcite (red line), As (III) standard (black line), and As (V) standard (grey line)

4.5 Partition coefficients

Partition coefficients for all trace elements were deduced from molar foraminiferal test TE/Ca ratios and the corresponding sea water values (Figures 16 – 19). The solid lines in Figures 16 – 19 represent calculated partition values, based on the calculated medians for the different experiments. The dotted lines show the highest upper and the lowest lower quartile values, which display the area of uncertainty.

For the elements Co and Cr not even vague estimates for D_{TE} are possible as the concentration of these trace elements were very low in the foraminiferal tests – more precisely, the measured concentrations of these elements were not evaluable as they showed such low signal-to-noise ratios that they could not clearly be calculated. Thus, these two elements won't be discussed in Section 5.

In the case of Mo, only a few sporadic signals could be detected probably meaning that the element was only adsorbed onto the surface of some tests – the big ionic radius of Mo is definitely not the reason why Mo was not incorporated into the tests as Cd, a frequently analysed element in foraminiferal carbonate, has a larger ionic radius. Molybdenum also won't be discussed any further.

4.5.1 Nickel, Copper, and Manganese

The partition coefficients for Ni (D_{Ni}) and Cu (D_{Cu}) were calculated based on data measured with two different analytical methods, µ-synchrotron XRF and LA-ICP-MS. According to both methods, D_{Ni} varied between 0.4 and 2.0 (average D_{Ni} = 1.0 ± 0.5) and between 0.5 and 1.7 (average D_{Ni} = 1.0 ± 0.4) using µ-synchrotron XRF and LA-ICP-MS, respectively. Results from both analytical techniques are found to agree. Combining D_{Ni} from both analytical methods gives a value of 1.0 ± 0.5. Figure 16 shows the partition coefficients of Ni for both applied techniques.

The partition coefficient for Cu (D_{Cu}) lies between 0.08 and 0.25. Based on the µ-synchrotron XRF measurements, D_{Cu} was found to be 0.16 ± 0.04, whereas a value of 0.12 ± 0.02 was determined using the LA-ICP-MS. Hence, the average D_{Cu} is 0.14 ± 0.02. This is slightly lower than, but in the same range as the previously determined partition coefficient for Cu by de Nooijer et al. (2007: 0.25 ± 0.15 using the same LA-ICP-MS configuration as the current study). D_{Cu} values are presented in Figure 17.

Because both analytical techniques yield very similar results, it is valid to calculate a total *D* for Ni and Cu by taking the mean of the individually calculated partition coefficients from both methods. In this way, possible systematic errors of both analytical techniques are reduced.

A systematic decline in the concentration of Ni and Cu incorporated in newly grown chambers was observed in the specimens from the 20-fold experiment in comparison to those cultured in the 10-fold solution (Figures 16 and 17). This suggests that an additional process may have affected the incorporation of Ni and Cu at high concentrations (see Section 5.1.2). For this reason the partition coefficients were calculated without the data of the 20-fold concentration experiment. The decrease in values was quantified by both the µ-synchrotron XRF and the LA-ICP-MS analytical techniques.

The scatter in the Mn data (displayed in Figure 18) only allows an estimate of D_{Mn}, being at least 2.4.

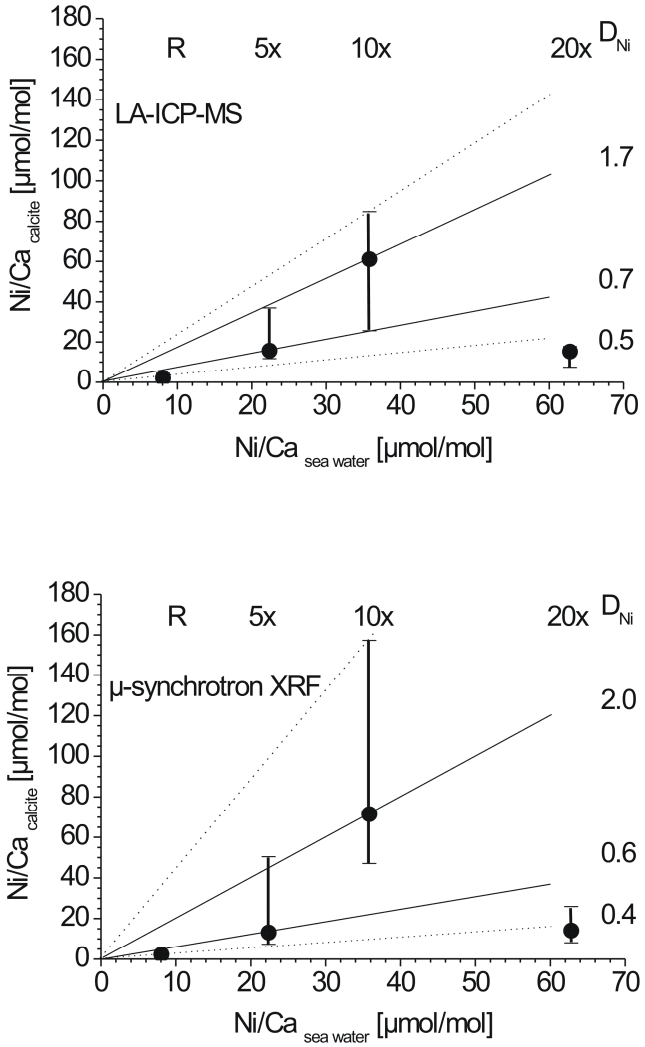

Figure 16 – Calculated partition coefficients of Ni – based on LA-ICP-MS (top) and µ-synchrotron XRF (bottom) measurements. Black filled circles (●) display the median value of the observed concentration ratios, short horizontal lines (–) symbolise the 25 % (lower line) and the 75 % quartile (upper line). Solid lines show the range in median values for reference, 5-, and 10-fold concentration solutions; dotted lines display the upper and lower quartiles and demarcate the area of uncertainty

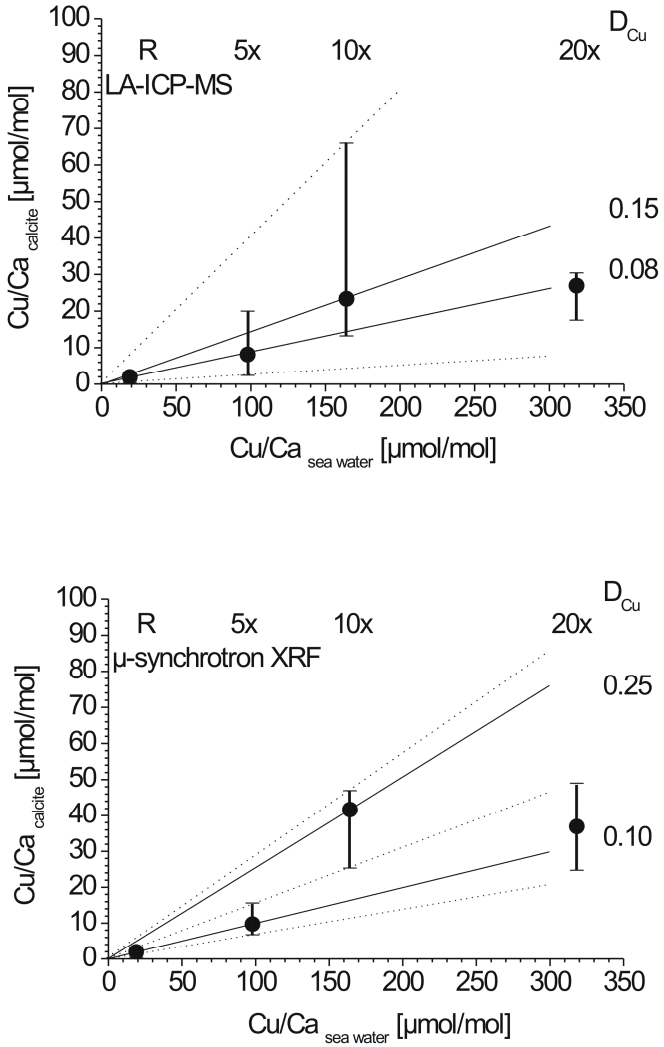

Figure 17 – Calculated partition coefficients of Cu – based on LA-ICP-MS (top) and µ-synchrotron XRF (bottom) measurements. Explanation of symbols as in Figure 16

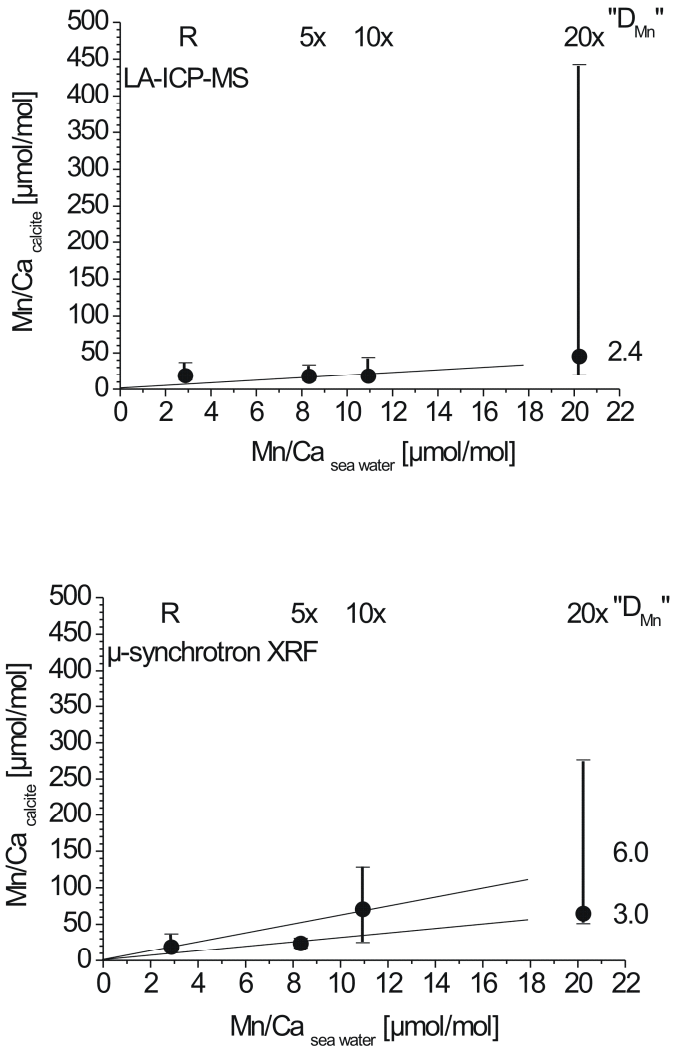

Figure 18 – Estimated partition coefficients for Mn – based on LA-ICP-MS (left side) and µ-synchrotron XRF (right side) measurements. Explanation of symbols as in Figure 16

4.5.2 Arsenic and Vanadium

For the element As the D_{As} ranged between 3.0 and 7.0 x 10^{-2} (calculated to 5.0 ± 1.0 (x 10^{-2})). The partition coefficient was calculated only on the basis of µ-synchrotron XRF measurements. Using LA-ICP-MS, the measured values could not be separated from background signals.

The element V displayed a slightly broader range of values. D_v showed a variation between 8.0 and 15.0 x 10^{-3}, which calculates to a partition coefficient of 12.0 ± 2.0 x 10^{-3}. This value is slightly higher, but within the same order of magnitude as the determined D_v of Hastings et al. (1996: 2.8 x 10^{-3}). Vanadium was also measured using both µ-synchrotron XRF and LA-ICP-MS. Similar to the case with As,

only the µ-synchrotron results were valid for use in determining the partition coefficient for V as the signal/noise ratio was not resolvable for the LA-ICP-MS measurements. Thus, only µ-synchrotron measurements were used for the D_V calculation. The partition coefficients for both elements (As and V) are shown in Figure 19.

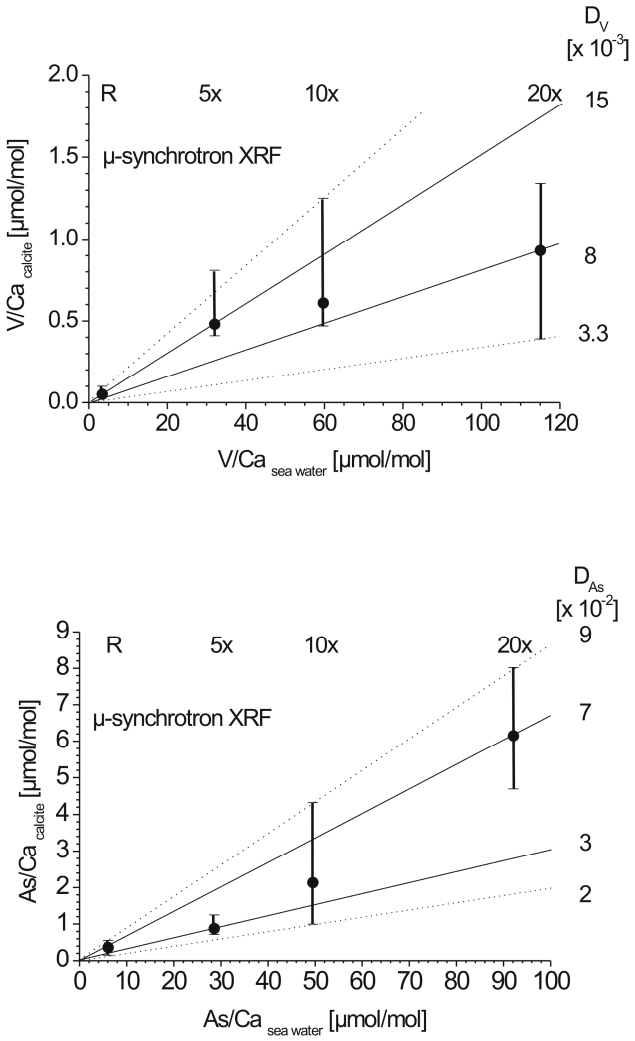

Figure 19 – Calculated partition coefficients for V (top) and As (bottom) by µ-synchrotron XRF. For the explanation of the symbols, see Figure 16

4.6 Sediments from ODP Site 1002C

The core from ODP Site 1002C can generally be divided into three zones (regarding geochemical data), labelled 1, 2, and 3 in Figures 20 – 22. Zone 1 begins at the bottom of the investigated part of the core (12.04 m) and continues up to a depth of 8.43 m. Zone 2 is clearly smaller and covers the interval from 8.43 m to 6.41 m, whereas the

top part of the core (Zone 3 in Figures 20 – 22) from 6.41 m to 0.34 m covers the biggest interval of the analysed core.

4.6.1 Major, minor, and trace elements

Major, minor, and trace elements of the sediments of ODP Site 1002, Hole C, display five general distribution patterns:

- Silicon (SiO_2), $Fe_2O_{3\ t}$, MnO, and Zr show a maximum distribution in Zone 1 reducing continually up-core, with Zone 2 values being only slightly below Zone 1 levels. Copper generally shows an equivalent distribution pattern in most instances, but compared to the above mentioned elements it exhibits a jig-saw pattern in the upper part of Zone 1;
- Titanium (TiO_2), Al_2O_3, Y, La, Ce, Nb, and to a lesser extent Ba, show maximum concentration values in Zone 2, with further high concentrations in Zone 1 and clearly lower concentrations in Zone 3. Additionally, Ba exhibits two high concentrated samples in the upper zone;
- Magnesium (MgO), Zn, and Ga reveal a fairly stable concentration trend throughout the investigated part of the core. The concentrations are generally slightly higher in Zone 1 than in Zone 2 and Zone 3, but are approximately of the same level in all three zones. Zinc as well as MgO show a clear maximum at the end of Zone 1; Ga peaks in Zone 2;
- Sodium (Na_2O), K_2O, V, Ni, Cr, and Rb show concentrations of the level in zones 1 and 2, but increasing concentrations in Zone 3 core-upwards. All elements display maximum values in the upper part of Zone 3 except for K_2O which shows a maximum in concentration in Zone 2. The general trend for all six elements is very similar though;
- Organic carbon (C_{org}), Mo, Cd, and Cd as well as (to a lesser extent) CaO, P_2O_5, Sc, As, and Sr show small concentrations in Zone 1 and Zone 2 with a clear minimum in Zone 2 and increasing concentrations in Zone 3 up-core. Molybdenum, Cd, and U clearly display two maximum peaks in Zone 3, while

CaO, P_2O_5, and Sr show a fairly stable, but clearly higher concentration than in the lower zones, with one maximum in Zone 3. The pattern of Sc, and to a considerably lesser extent that of As is characterised by a jig-saw distribution in Zone 3;

- Lead and S cannot be attributed to any of the above mentioned distribution patterns.

All details of the elemental distribution patterns can be observed in Figures 20 – 22.

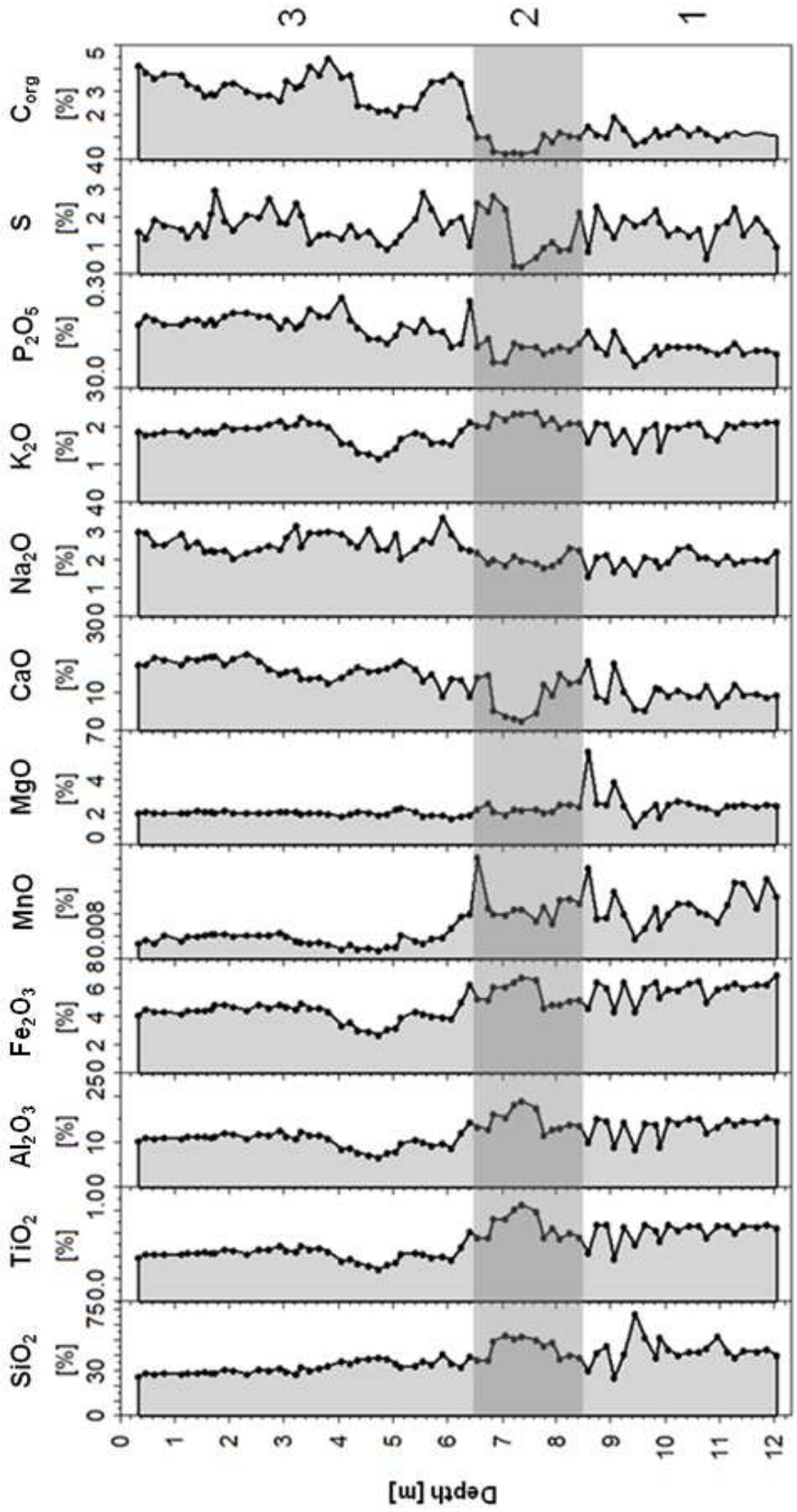

Figure 20 – Major element distribution with depth in the sediments of ODP Site 1002, Hole C. All concentrations in wt. %. Zones 1, 2, and 3 are indicated at the top.

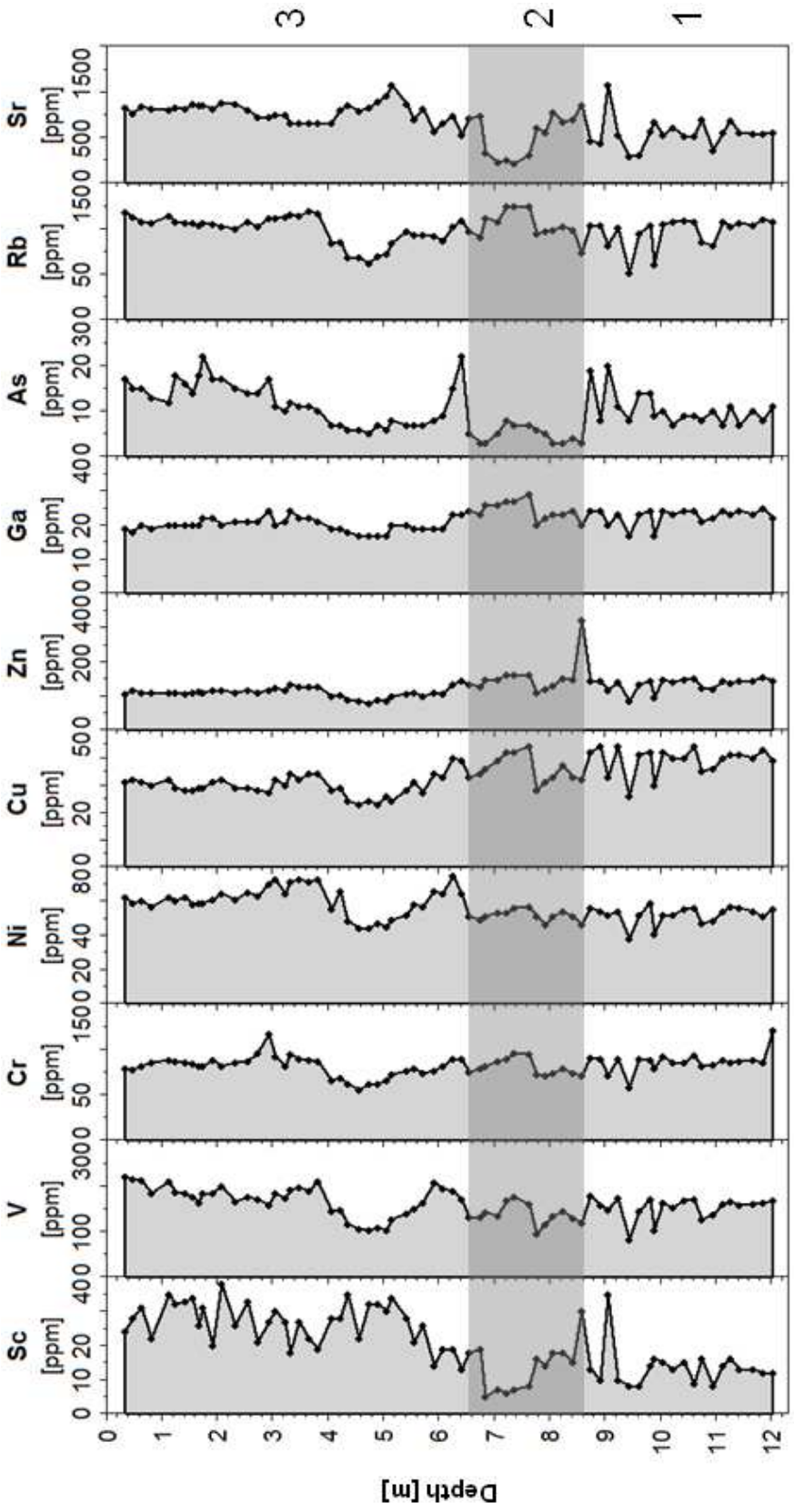

Figure 21 – Part 1 of the trace element distribution patterns with depth of the sediments from ODP Site 1002, Hole C. All concentrations in ppm (= mg/kg). Zones 1, 2, and 3 are indicated along the top

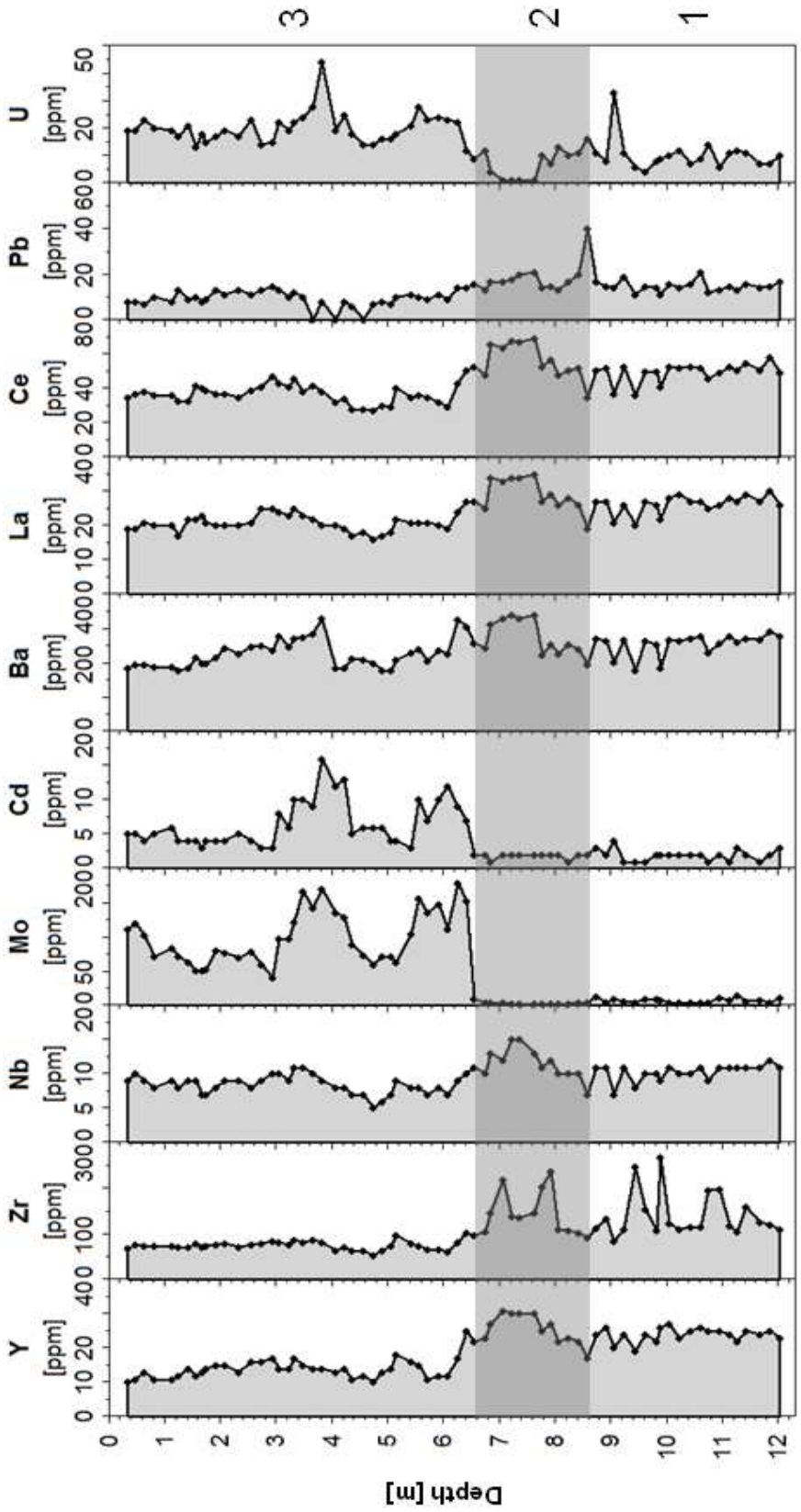

Figure 22 – Part 2 of the trace element distribution patterns with depth of the sediments from ODP Site 1002, Hole C. All concentrations in ppm (= mg/kg). Zones 1, 2, and 3 are indicated along the top

4.6.2 Depositional environment – degree of water oxygenation

Cross-plots of elements that usually show a good correlation, such as Ni and Cu, clearly demonstrate that the data is divided into two populations (Figure 23) even though the core may be divided into three geochemical distinctive zones as shown in the depth profiles of sections 4.6.1 (Figures 20 – 22).

When regarding Figure 25 (Section 4.6.3) in this context, it becomes evident that the data represent two distinct geochemical environments.

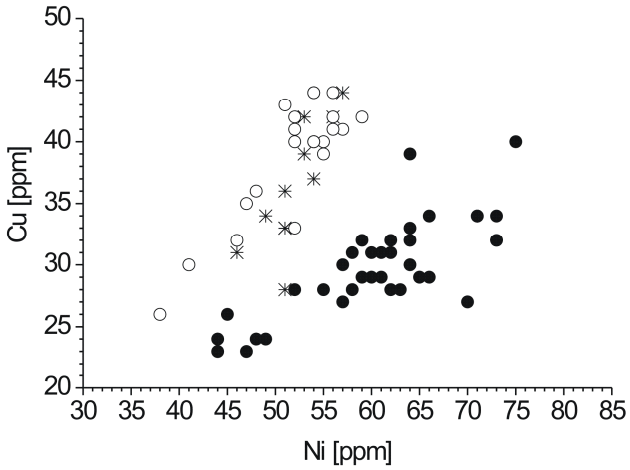

Figure 23 – Ni/Cu cross-plot showing two separate data populations: Zone 3 (●) and Zone 2 (⁕) together with Zone 1 (○)

These zones can clearly be identified when considering milieu specific elements. For instance Mo, U, and C_{org} are indicators for anoxic environments as they are connected to each other. In anoxic environments, sediments reveal higher C_{org} contents than oxic sediments. Molybdenum and U become mobile at low redox conditions and C_{org} acts either as a carrier or a ligand building organo-metallic complexes with the two metals (Morford and Emerson, 1999; Algeo and Maynard, 2004; McManus et al., 2005; Tribollivard et al., 2006). Thus, C_{org} and Mo show a good correlation in anoxic environments, C_{org} and U a good correlation throughout the whole core (both are significant correlations at $p = 0.05$). Figure 24 shows the cross-plots of Mo and U with C_{org} and identifies an anoxic and an oxic environment. A complete list of the chemical composition of the core is shown in Appendix C.

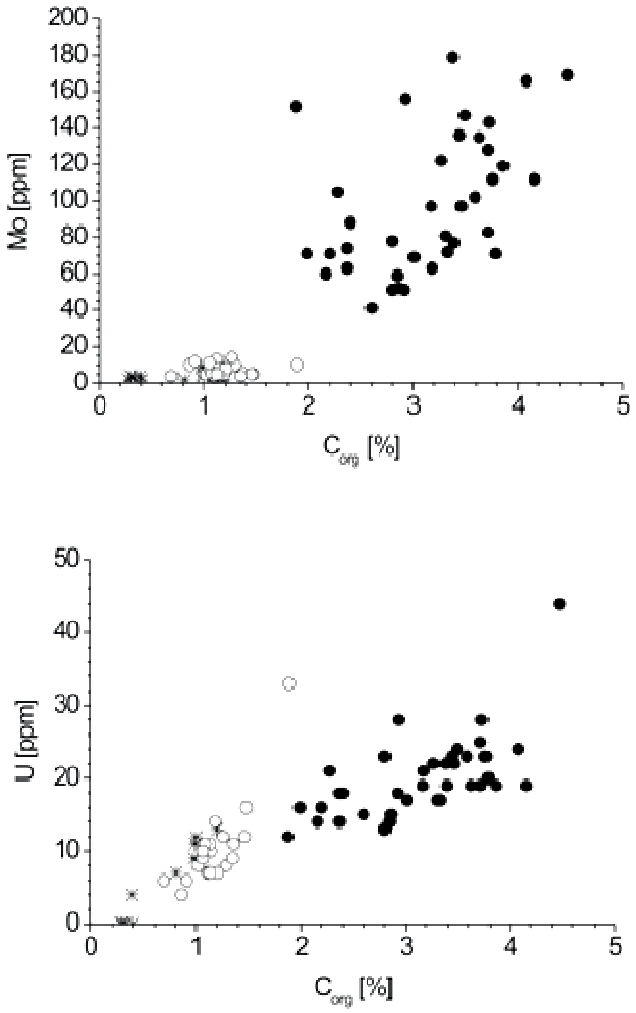

Figure 24 – Milieu specific element cross-plots showing an oxic (○) and an anoxic (●) environment. Samples of Zone 2 ("Transition zone") (*) go along with the samples of the oxic population

4.6.3 Sedimentation rate

Figure 25 shows the calculated sedimentation rates for the analysed sediments of ODP Site 1002 (Hole C). As a basis for the calculation of the sedimentation rates the dated sediment samples of the core of ODP Site 1002C (Peterson et al., 2000) were used. Sedimentation rates were calculated as follows:

$$\text{sedimentation rate [cm/ka]} = d_B - d_A / a_B - a_A \times 100$$

with:

d = depth [m],

a = age [ka],

A and B = two consecutive samples (B following A down-core)

Subsequently, the ages were derived from correlation to the SPECMAP time scale (Imbrie et al., 1984).

The sedimentation rate is associated to the oceanic productivity – with high sedimentation rates being observed in regions of high productivity (Diester-Haass and Schrader, 1979). In anoxic environments though, high contents of C_{org} in the sediments are preserved due to oxygen deficiency. Then low sedimentation rates are associated with high amounts of organic matter (Canfield, 1994). In the Cariaco Trench the sedimentation rate changed dramatically at about 12,600 years BP, when strong upwelling over the basin and a rapid rise of the sea level coincided induced by meltwater discharge from the Laurentide Ice Sheet into the Gulf of Mexico and oxic turned into anoxic conditions (Peterson et al., 1991). In turn the sedimentation rate decreased from more than 180 cm/ka up-core down to approximately 45 cm/ka. This vast reduction of sedimentation goes along with the clear changes in concentrations of most major and trace element contents (Figures 20 – 22).

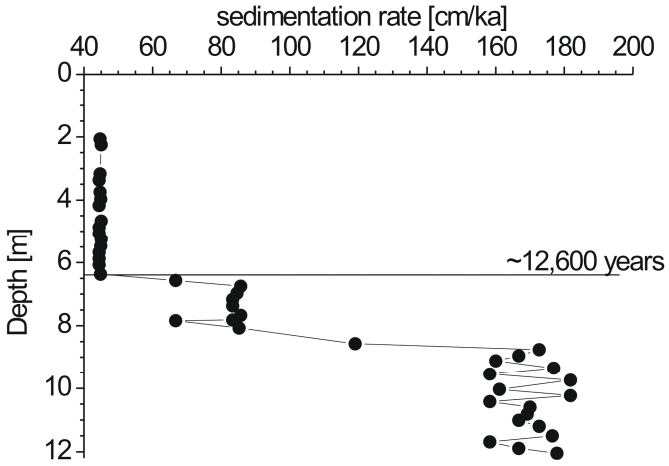

Figure 25 – Calculated sedimentation rate of the sediments of ODP Site 1002, Hole C, for the analysed 12.04 m

4.7 Foraminifera from cores

4.7.1 Foraminifera from ODP Site 1002 C

In general, the depth profiles of the Ca-normalised concentrations of the major, minor, and trace elements of the benthic foraminifera (Figures 26 and 27) reveal in most cases the three zones (displayed for the sediments in Figures 20 – 22). The following element distribution patterns are identifiable:

- Molybdenum and Cd clearly display a minimum distribution throughout the oxic and the transition part of the core (i.e. zones 1 and 2). In the upper, anoxic part of the core, however, the tests are enriched considerably in these two elements and show maximum distributions at depths between 3.0 and 4.0 m; in the case of Cd an additional maximum peak shows up at 2.0 m depth;
- Lead shows a similar trend as Mo and Cd in Zone 1 with the exception that in the upper part of Zone 1 the concentration begins to increase and stays at an intermediate level until the top of Zone 2. In Zone 3 the distribution reaches its maximum at ~3.5 m. From then on Pb distribution decreases to a level equivalent to the lower part of Zone 1;

- The elements Mg, Cr, Co, as well as Ni and to a lesser extent P, S, and Sr, show a stable distribution throughout the three zones of the core. Magnesium, Co, and S display their maximum concentrations in Zone 2 at ~7.0 m depth with S showing a second clear maximum concentration right at the top of the core. Nickel and Cr have their maxima in the anoxic part of the core at ~4 m and ~6.0 m depth respectively. Phosphorus has three clear maximum concentration peaks: One in the oxic part (at ~10.0 m depth) and two in Zone 3 (at ~4.0 and ~6.0 m depth). Strontium displays the most even pattern throughout the whole core with no clear maximum point of concentration;
- Vanadium, As, and Ba show in the lower part (Zone 3 and Zone 2) considerably higher concentrations than in the upper part. For V and As the distribution generally decreases up-core with an exception of the top 2 m of the core, where concentrations of both elements rise significantly, even though they do not reach the level of either Zone 2 or Zone 3. In case of Ba, which displays three maxima in the lower part (at ~8.0, ~8.5, and ~10.5 m depth); an additional high concentration peak is present in Zone 3 at ~4.5 m depth;
- Zinc, Rb, and to a lesser extent Cu display a distribution pattern with low (or in case of Rb very low) concentrations in Zone 3. In Zone 2 the distributions reach their maxima in average before the concentrations decrease clearly in Zone 1 again. Just for Zn and Rb a clear maximum peak at ~4.0 m depth can be observed, which also reveals the highest concentration of these elements in the core;
- Uranium concentrations and $\delta^{13}C$ values reveal a very similar distribution pattern. In Zone 1 intermediate to high concentrations can be observed. In Zone 2 concentrations reach a minimum before they in Zone 3 again and reach maximum values in that anoxic part of the core;
- Oxygen ($\delta^{18}O$) shows a general core-up depletion of the $\delta^{18}O$ values. The minimum can be observed at ~7.0 m depth, the maximum at ~9.0 m;

- Manganese and Fe display a distribution pattern that shows high concentrations in the oxic part with a clear maximum concentration at a depth of ~7.0 m in the transition zone can be observed while in the anoxic part (Zone 3) the concentrations are very low.

A striking feature in the distribution depth profiles is that concentrations of some redox-sensitive elements seem to display unexpected or seemingly erroneous patterns. For instance Fe and Mn or Ba and As should show higher concentrations in low redox conditions than in an oxic environment. For U and V it should be the other way around. This will be discussed in Section 5.2.1.2.

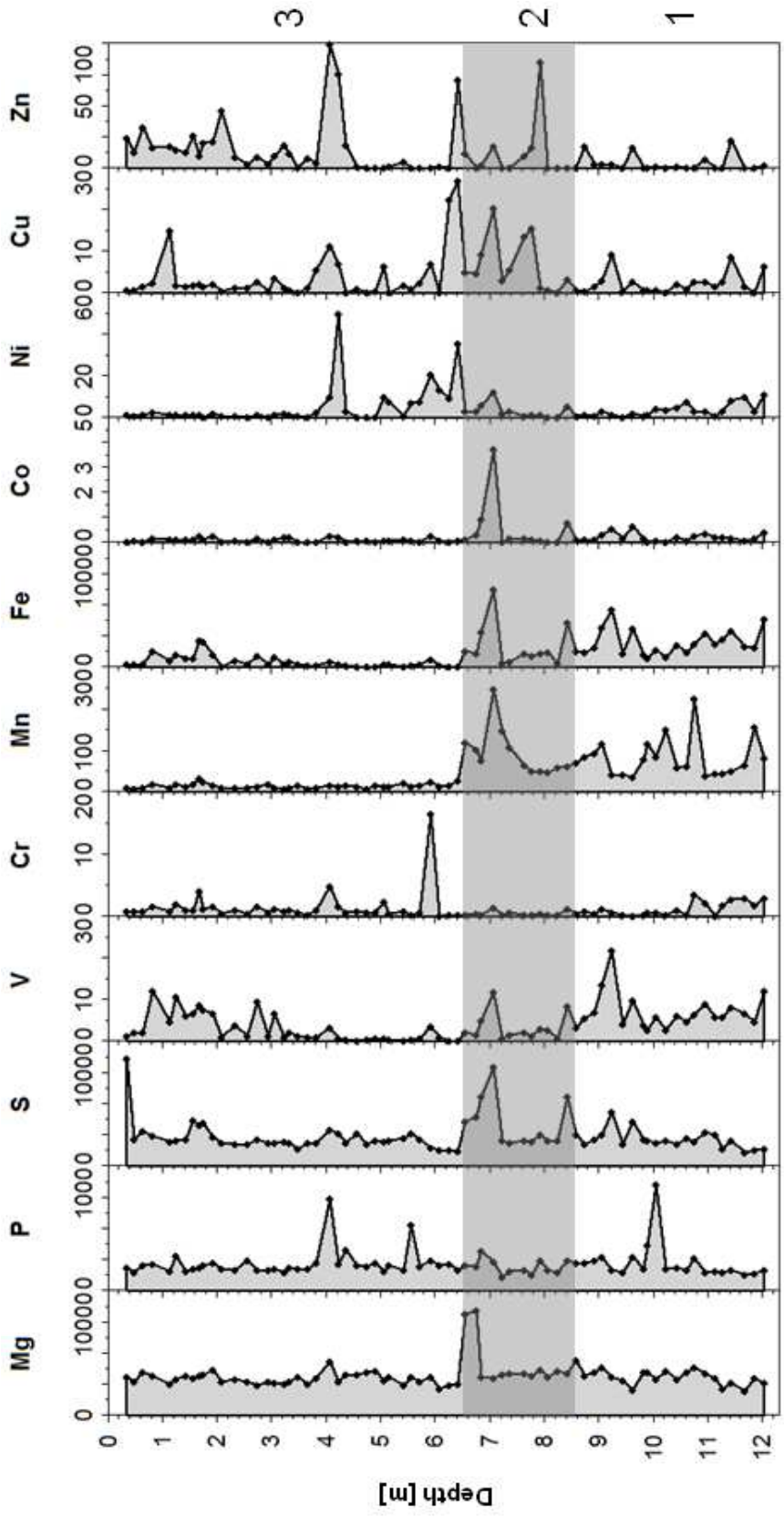

Figure 26 – Depth profiles (part I) of *Bulimina spp.* at ODP Site 1002, Hole C. Zones 1, 2, and 3 are indicated by the accordant number and are explained on page 60 (Figure 20). Concentrations of all elements are in µmol/mol Ca

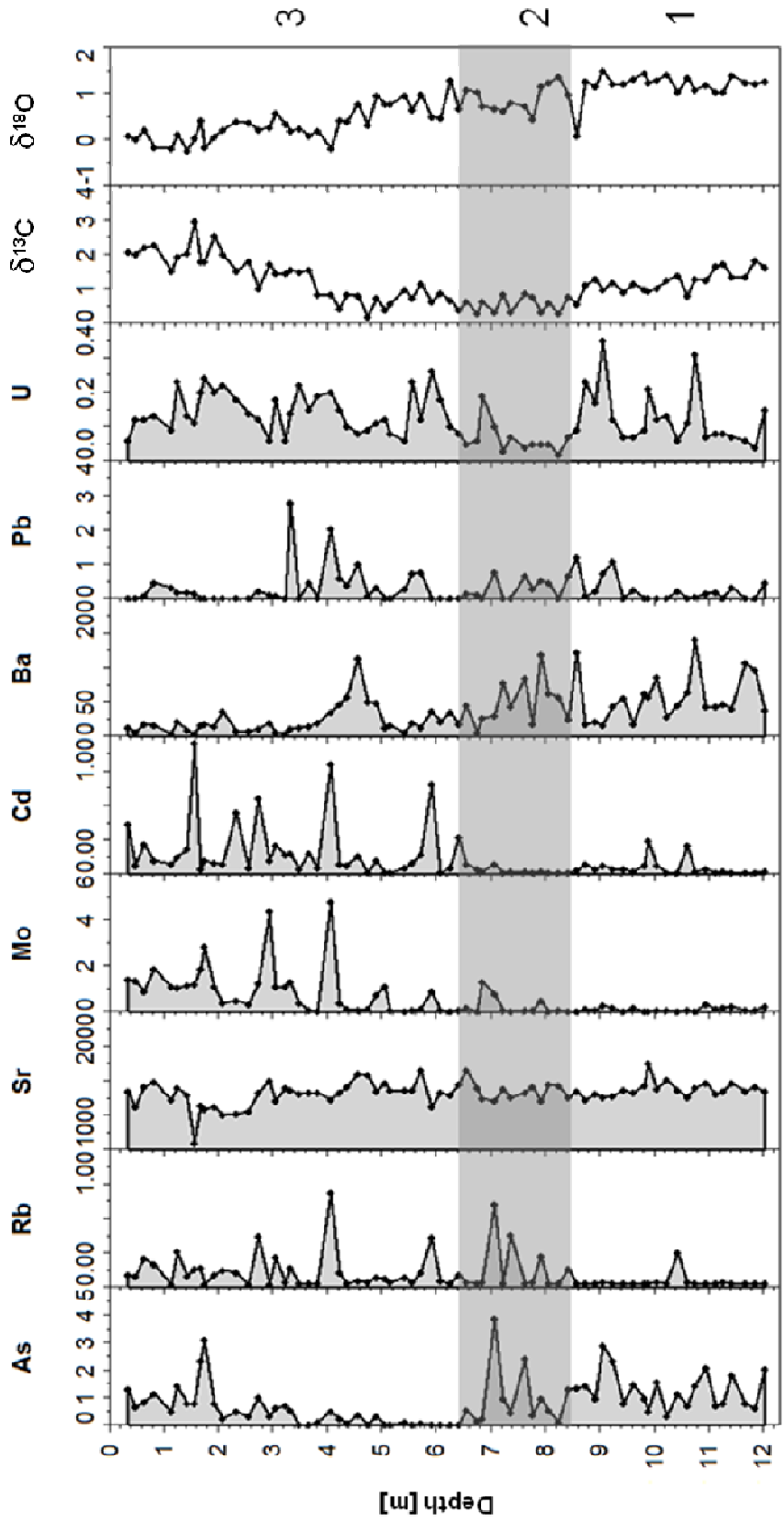

Figure 27 – Depth profiles (part II) of *Bulimina spp.* at ODP Site 1002, Hole C. Marked zones as in Figure 26. Concentrations of all trace elements are in µmol/mol Ca

4.7.2 Foraminifera from Texas (core Mullinax-1)

The analysed benthic foraminifera (*Lenticulina spp.*) were very well preserved. Only some tests from the upper part of the core (Palaeogene section) showed dissolution effects. These tests were not analysed. Most of the Ca-normalised element concentrations of the foraminiferal tests show that the sea water chemistry must have changed upon the event at the Cretaceous-Palaeogene transition (Figure 29). Generally, most elements show a clear drop in concentration in the event deposit below the Cretaceous-Palaeogene border, where mainly sandstones and also some clays are deposited (details in Section 3.2.1) – just Mn concentrations are notably enriched. Furthermore, the following trends can be observed:

- Magnesium, V, Cr, and U show very similar concentration trends. In the bottom of the section, high concentrations are present. Up-core these slightly decrease; nevertheless, values remain on relatively stable. At a depth of about 13.0 m they show their highest concentrations before decreasing notably in the event deposit. For V and Cr minimum concentrations are observed in the Palaeogene part of the core, whereby V concentrations increase in the uppermost part of the core just as does Mg. U concentrations remain at a low level throughout the Palaeogene;
- A second trend is displayed by Co, Ni, and Cu. These three elements generally show higher concentrations in the Maastrichtian than in the Danian. Between 17.0 and 18.0 m depth Co and Ni reveal their maximum concentrations, whereas Cu shows high concentrations, but its maximum is found between 12.0 and 13.0 m depth. In the event deposit all three display lowest concentrations which only are enriched at minimally in the Palaeogene part;
- Arsenic, Cd, and to a lesser extent Ba and Zn, show low concentrations throughout the whole section. Cadmium and As only reveal one big excursion at 13.5 m depth, while concentrations in the event deposit are near zero. In the Palaeogene part, Cd stays at lowest levels whereas As increases slightly. Ba

is also fairly constant, but does not show its maximum in the Cretaceous. In the event deposit its concentrations are slightly reduced, but clearly increase in the Palaeogene with its maximum concentration at approximately 9.0 m depth. Zn values, displaying a trend similar to those of As, are higher in the Cretaceous, but show two excursions at 12.5 and 17.0 m depth. Palaeogene concentrations remain low as in the event deposit;

- Molybdenum and Pb display a jig-saw pattern with clearly higher concentrations in the Cretaceous part of the core. While Mo reduces notably in the event deposit, Pb remains on an intermediate level, but both show higher concentrations in the Palaeogene again;
- Carbon and O isotopes generally show stable high values in the Maastrichtian section, but including a drop between 16.0 and 17.0 m depth, where an intercalation of shale is present. In the event deosit the isotopic values decraes again before in the Palaeogene the former high levels are reached again. Only in the uppermost part of the core (between 6.0 and 7.0 m depth) values reduce clearly;
- Manganese and Sr concentrations do not match any of the other patterns. In case of Mn, concentrations often display opposite features compared to the other elements. It partly displays high values in the Maastrichtian part of the core, but also in the sandstone complex and the uppermost part of the Danian. In contrast, Sr shows a fairly stable behaviour, practically only displaying slightly lower concentrations in the event deposit.

The detailed depth profiles are presented in Figures 28 and 29.

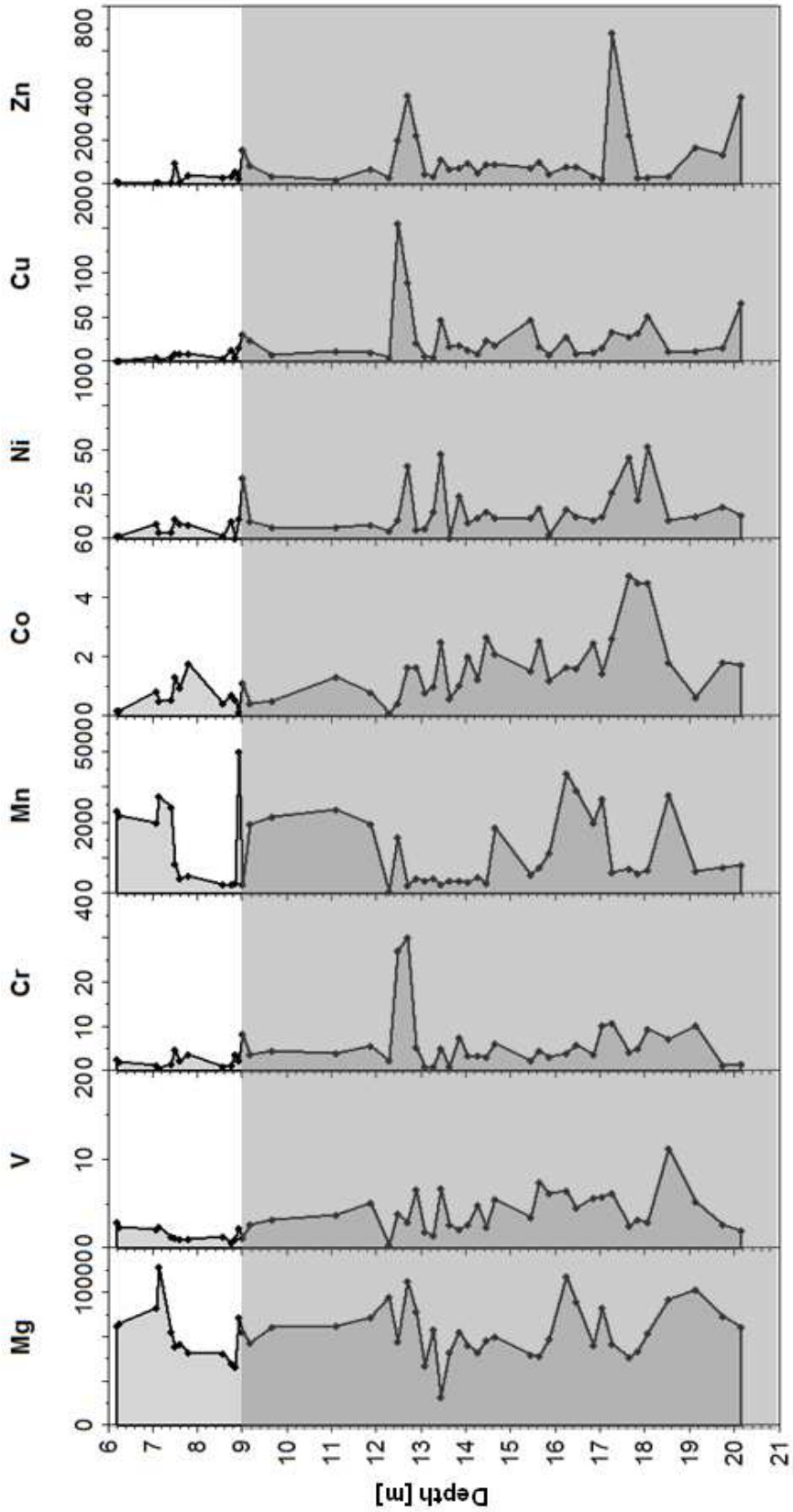

Figure 28 – Depth profile of Ca-normalised trace elements (part 1) in the tests of Lenticulina spp. at Brazos (Mullinax-1 core). Grey background = Cretaceous, white background = Palaeogene

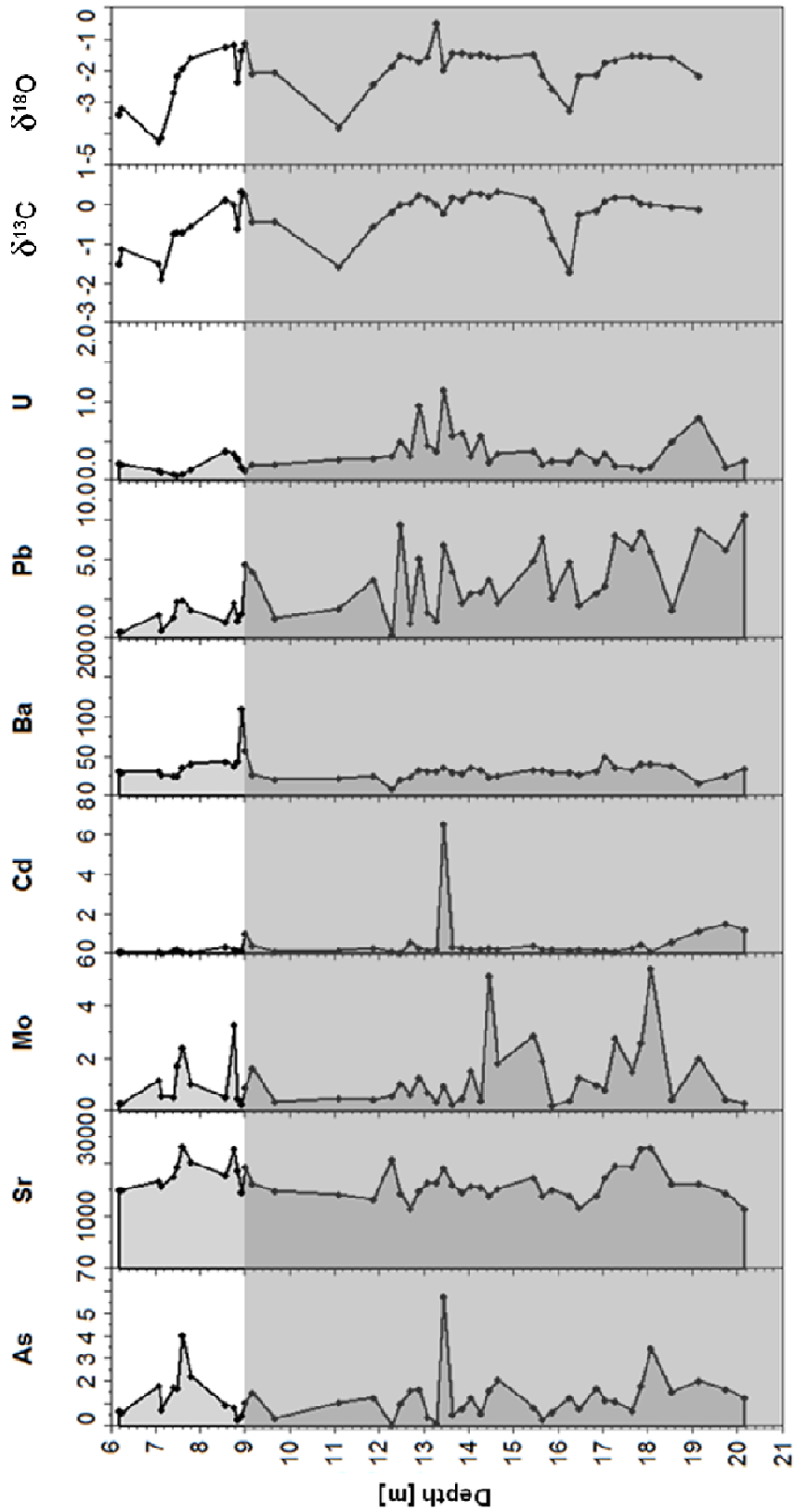

Figure 29 – Depth profile of Ca-normalised trace elements (part 2) in the tests of *Lenticulina spp.* at Brazos (Mullinax-1 core). Background colours as in Figure 28

5 Discussion

5.1 Experimental part

5.1.1 Considerations of experimental uncertainties

5.1.1.1 General considerations

The element concentrations in the culture solutions were remarkably stable, and values for Cu, Ni, As and V concentrations show only minor scatter (Figures 10 and 11; Table 6). The variability observed in Mn is somewhat more significant, possibly because Mn readily forms oxides and hydroxides under oxic conditions (e.g. Middelburg and de Lange, 1988; Heiser et al., 2001).

Calcein binds to Ca as calcium carbonate is precipitated and is therefore incorporated into the mineralised structure (Bernhard et al., 2004). Although Lu and Allen (2002) report that Cu incorporation competes with Mg and Ca (its incorporation is reduced at increased Ca and/or Mg concentrations), Hintz et al. (2004) as well as Dissard et al. (2009) suggest that the (trace) element incorporation is not affected by the use of calcein. De Nooijer et al. (2007) also report that Cu binding to calcein is negligible. Hintz et al. (2004) argue that measured Mg/Ca ratios in calcein labelled chambers were of the same magnitude as the ratios in unlabelled chambers. Similarly, Dissard et al. (2009) showed that calcein does not affect the incorporation of the elements Mg and Sr into foraminiferal calcite. Concurrently measured Mg/Ca ratios (not shown here) confirm this assumption.

As shown in Table 7, in Batch I experiment 41.0 % of the foraminifers in the culture solutions grew at least one chamber, with the exception of the 20-fold solutions in which a lower percentage (29.0 %) added new chambers. Data for Batch II experiment (Table 7) shows a similar behaviour. In the tank with the highest concentration the lowest percentage (37.0 %) grew at least one chamber. In the latter tank, however, the highest reproduction rate (three individuals) was observed. No malformed chambers were identified during the experiments and nearly all individuals (95.5 % of Batch I

experiment and 92.5 % of Batch II experiment, Table 7) survived. In pollution studies, malformed chambers of foraminiferal tests are often considered indicative of great stress, for instance resulting from pollution by heavy metals (e.g. Alve, 1991; Yanko et al., 1998). Given that the chamber formation and survivor rate were still quite high, and the absence of malformed chambers, it may be assumed that the experimental conditions were satisfactory for *Ammonia tepida.* The low reproduction rates observed here may indicate that the overall conditions for the experiment were perhaps suboptimal for this species, but that is not necessarily the case. Microcosm experiments similar to those conducted by Havach et al. (2001) or Hintz et al. (2006) might have improved the overall survival and chamber formation rate, but would have also introduced other complications, particularly with regard to keeping the trace element concentrations constant.

Trace element data remains inconclusive for some of the individual tests. This can primarily be explained by the fact that some chambers had very thin walls (Figures 30 and 31), which resulted in a reduction of the ablation time as less material was available to ablate and thus yielded poor signal statistics. Additionally, the chamber walls show variable thickness within one chamber so that gaining proper signal statistics is complicated. If chamber walls are evenly developed, ablation craters are more smoothly rounded as for instance shown by Reichart et al. (2003). Figure 31 clearly illustrates rough crater edges due to broken wall material which is a result of very thin chamber walls.

Unfortunately, the limited size (size of newly formed chambers <100 µm – see Figure 32) of the newly added chambers prevented multiple analyses on a single chamber with LA-ICP-MS.

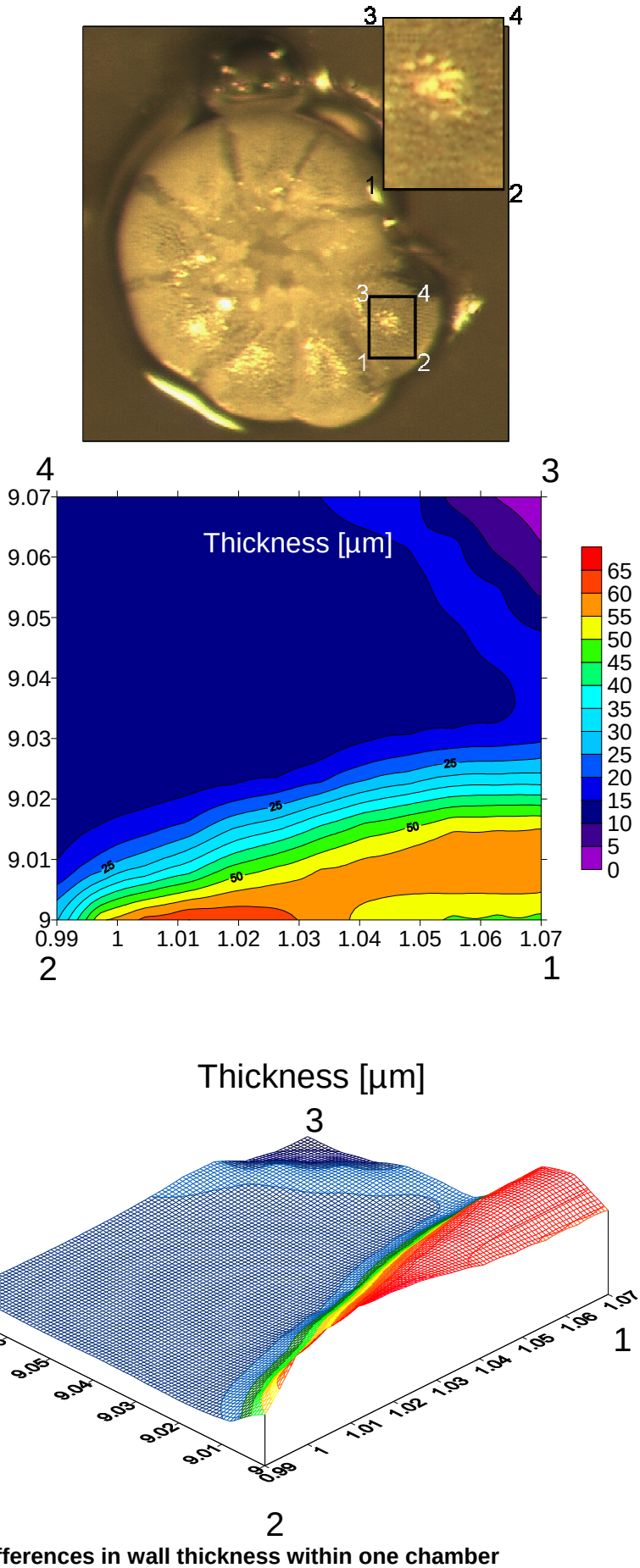

Figure 30 – Differences in wall thickness within one chamber

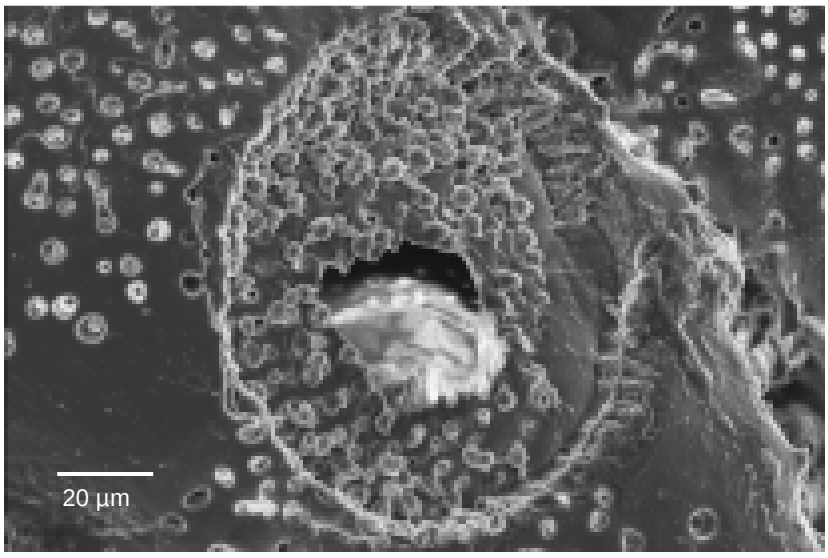

Figure 31 – SEM micrograph of broken ablation crater edge due to very thin chamber wall

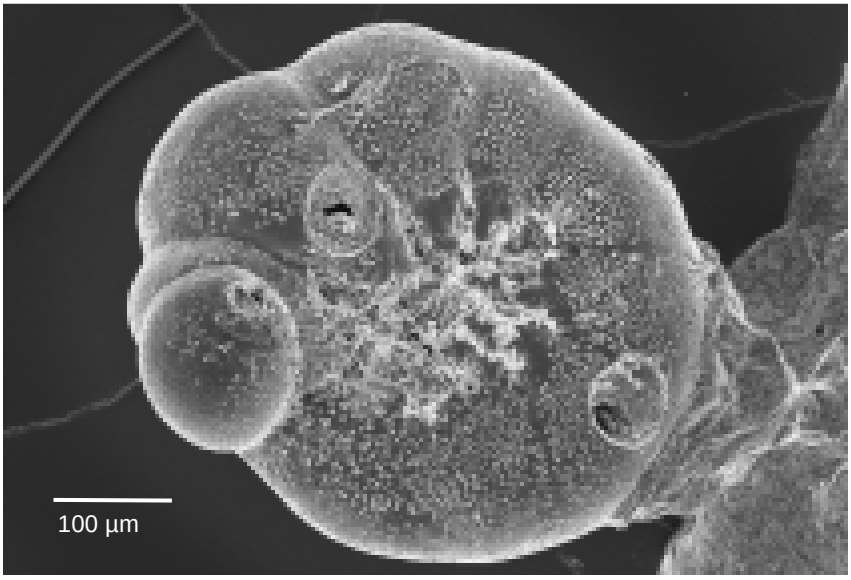

Figure 32 – SEM micrograph of a foraminifer with ablation craters showing balloon-like newly formed chamber in the front

5.1.1.2 Incorporation of arsenic into carbonate

5.1.1.2.1 General aspects of As in aquatic environments

Arsenic, a metalloid, has more than one possible oxidation state in the natural environment. These naturally occurring species are arsenide (As (-III)), elemental arsenic (As (0)), arsenite (As (III)), and arsenate (As (V)).

Although the applied ICP-MS standard solution for the culturing experiment consisted of As (III), all the detected incorporated As was of the pentavalent species though. FIAS control measurements (not displayed here) of the ICP-MS standard solution yet clearly showed that the solution does, in fact, consist solely of arsenite.

Arsenic oxidation in aquatic systems is not unusual as As (III) is only stable in low redox environments. The oxidation is generally a slow process and depends on the initial arsenite concentration as well as on temperature, salinity, pH and microbial activity (e.g. Johnson and Pilson, 1975; Cullen and Reimer, 1989). For instance, in thermal waters at room temperature oxidation kinetics are rather slow, but increase with rising temperatures (Schwenzer et al., 2001).

Regarding the intervals of change and the stable temperature (14.5 ± 0.2 °C) of the culture solutions of this study, it seems very unlikely that within that short period the whole volume of the culture tanks was oxidised by the chemical oxidation due to contact with oxygen. The described abiotic oxidation rates of Scudlark and Johnson (1982) would not account for the total conversion of As (III) to As (V). It is rather likely that due to microbial activity by bacteria the oxidation proceeded, as various kinds of bacteria were found in the culture solutions despite the fact that the culture solutions were changed in regular intervals (cf. Section 3.2.3.2). Bacterial activity considerably accelerates arsenic oxidation (e.g. Scudlark and Johnson, 1982) and may be divided into chemoautotrophic (e.g. Hamamura et al., 2009; Prasad et al., 2009; Valenzuela et al., 2009; Chang et al., 2010) and heterotrophic (e.g. Silver and Phung, 2005; Stolz et al., 2006) oxidation. In the case of chemoautotrophic oxidation

the prokaryotes conserve energy for growth in contrast to heterotrophic As (III) oxidation, in which the process is used for detoxification (e.g. Handley et al., 2009). The main enzyme that induces As (III) oxidation in either group has been shown to be As (III) oxidase (e.g. Lieutaud et al., 2010). It may be assumed that for the purpose of detoxification As (III) oxidation occurred. This process might have happened inside the foraminifera – the individuals took up the toxic As (III) into its calcifying reservoir and by detoxification the arsenite was oxidised to As (V). The arsenate then was incorporated into the calcite and the As (V)-$CaCO_3$ package subsequently was extruded for the calcification process.

On the other hand, microbial reduction of As (V) to As (III) is also known in some environments. This process is not considered for the present study though as no evidence for it could be observed.

5.1.1.2.2 Binding of inorganic arsenic

Arsenite ions have a pyramidal trigonal shape and occupy the carbonate lattice sites with a small spatial displacement of the As position from the ideal C position when incorporated into the calcite surface (Cheng et al., 1999).

Laboratory experiments have shown that the binding of the tetrahedral As (V) oxyanion to calcite also takes place as a substitution reaction similar to Se (VI). By this, As (V) is accommodated at the carbonate sites in the calcite structure (Reeder et al., 1994; Alexandratos et al., 2007). EXAFS characterisation of incorporated (by substitution) As (V) indicates that this species preferentially is incorporated at the kink sites of calcite. Arsenate adsorption is another possibility for the As (V) to be bound to calcite. In this case Alexandratos et al. (2007) found that most commonly corner-sharing coordination occurs between the AsO_4 tetrahedra and surface calcite at kink sites.

Even though the most common binding of arsenate is surface adsorption, it is possible to find As (V) within the foraminiferal calcite. This can be explained by the typical process of chamber formation. For *Ammonia tepida* the calcification process consists

of a few steps during which an *anlage* of cytoplasm is constructed. This *anlage* lines out the new chamber followed by organic lining. An extrusion of frothy cytoplasm builds a sheath around the entire test which is succeeded by the calcification (Goldstein, 1999). Thus, a thin layer of calcite covers the new formed chamber with various trace elements incorporated into the calcite – in this case As (V). As the EXAFS studies herein (Section 3.7) clearly showed a Ca-As bonding distance and the confocal µ-XRF measurements of Kramar et al. (2010) confirmed highest As concentrations in newly grown chambers.

5.1.2 Biological effects and influences

The elements Mn, Ni, Cu, V, and As usually are present only at very low levels in sea water (e.g. Table 2 or Table 6). Of these, Mn occurs at lowest concentration in the North Sea water that was used (see Table 6). Manganese, Cu, and Ni seem to be essential for the growth of primary producers and exhibit a nutrient-type distribution or a hybrid distribution (a combination of nutrient-type and scavenged-type distributions) in the oceans (Jones and Murray, 1984; Bruland and Lohan, 2004; Morel et al., 2004). Although well below concentrations generally considered toxic (e.g. Hunt et al., 2002; Croteau and Luoma, 2009), the severe drop in trace element concentrations in the tests grown in the 20-fold concentration tank of Batch I experiment (shown in Figures 16 and 17) suggests that a biological protection mechanism is involved. The trace metals considered are all somehow involved in different enzymatic activities (Nelson and Donkin, 1985). Whereas a deficiency in these elements may lead to limited productivity, conversely, an excess of these elements may inhibit growth (Sunda, 1988-1989; Bruland et. al, 1991). The lower number of chambers added in these experiments, particularly in the 20-fold experiment (see Table 7 for details), seems to point in this direction as well. As a consequence of using a multi-element mixture in the culture medium, it is possible that one (or more) of the added elements reached its toxic (although non-lethal) level with respect to *Ammonia tepida*.

Nickel is known to be a highly toxic element even though it is very common in nature as a cofactor in the urease enzyme that hydrolyses urea, which is an important source of nitrogen in the oceans (Oliveira and Anita, 1986). Nickel also serves as a cofactor in various other enzymes. Accordingly, Ni must be considered an important prerequisite for growth (Syrett and Peplinska, 1988). Syrett and Peplinska (1988) observed this for diatoms, while Dyhrman and Anderson (2003) made similar observations with respect to Ni for some dinoflagellate species. Apart from this, Ni is also essential for microbiologically-induced calcite precipitation. Culture experiments with *Escherichia coli* reveal that adding 5 µM Ni enhances calcite precipitation considerably, whereas an addition of more than 100 µM Ni will inhibit calcite precipitation (Bachmeier et al., 2002). Thus, this may also apply for foraminifera as similar observations were made during this study. The chamber growth rate for specimens cultured in the 5-fold sea water solution increased 6 % over those cultured in the reference solution, whereas the rate decreased 6 % below reference values in the 10-fold solution; the rate decreased even more dramatically in the highest concentrated solution (Table 7 and Figure 14).

Results of Mann et al. (2002) indicate that Cu may be toxic and/or harmful to various phytoplankton species. In this particular case, however, it is rather unlikely that Cu inhibited shell development as de Nooijer et al. (2007) used significantly higher concentrations in their experiments (up to 17.8 µmol of Cu was applied, which would be equivalent to a 100-fold concentration increase compared to the sea water used in this study) and still achieved new chamber growth. However, interactions between trace metals, in which one element becomes toxic due to the limitation of another, have been observed. For example, Egleston and Morel (2008) reported that Ni became toxic due to the limitation of Zn, resulting in toxicity to diatoms. Bruland et al. (1991) found that synergistic and antagonistic interactions between Cu and potential biolimiting metals, such as Fe, Mn, and Zn, might have large effects on the production of marine biota. Such an antagonistic effect, also described by Sunda and Huntsman (1998b) for

Cu and Mn, seems to be present in the experiments of the current study as well. Figures 16 – 18 show that tests from the 20-fold sea water concentration experiments might display such an antagonism between Cu (as well as Ni) and Mn.

The fact that high concentrations of Ni and Cu may harm marine life could potentially trigger a cellular expulsion or blocking mechanism in order to prevent foraminifera from incorporating these metals in proportion to their sea water concentrations. It is also known that toxic metals such as Cu, Cd, Ni, or Zn inhibit Mn uptake, when Mn is present in low concentrations (e.g. Sunda and Huntsman, 1998a and 1998b). In terms of chemical competition, Mn binding is blocked by (toxic) trace metals, which bind to the receptor sites on transport-specialised membrane proteins designed for the acquisition of nutrients (Sunda and Huntsman, 1983; 1996 and 1998a). Once the toxins are bound, the membrane nutrient-metal uptake system cannot distinguish between nutrient and toxicant.

Submarine hydrothermal systems are often enriched in biologically toxic trace elements – amongst these As (Price and Pichler, 2005; Varnavas and Cronan, 1988; von Damm 1990), a common heavy metalloid and oxyanion-forming element also found in organisms, soils, rocks, the atmosphere, and natural waters. It has an oceanic residence time with respect to riverine input of approximately 39,000 years (Broecker and Peng, 1982). Through a combination of natural processes such as biological activity, volcanic emissions as well as weathering reactions As may be mobilised under reducing as well as oxidising conditions. In sea water mostly the inorganic trivalent and pentavalent forms are present, whereas the latter is predominant (e.g. Andreae, 1978 and 1979). The concentration of As in sea water typically is up to 4 µg/L (e.g. Cullen and Reimer, 1989; Navarro et al., 1993). Near hydrothermal activity this value can be exceeded 200 times (Johnson and Cronan, 2001).

In contrast to other oxyanion-forming elements As stays mobile under reducing conditions, whereas others tend be mobile only in oxidising environments. Under reducing conditions As (V) may be reduced to the more toxic As (III) by bacterial

activity or marine phytoplankton (Andreae and Klumpp, 1979; Cullen and Reimer, 1989). This way As is available in anoxic/suboxic waters and could be used as an indicator for such environments.

Biologically, arsenic may play a very complex role as it is essential for some biological processes, but concentrations above a certain level have adverse effects, thereby converting an essential element into a toxin (e.g. Ni Dhubhghaill and Sadler, 1991). The As (III) and As (V) oxyanions are the predominant naturally occurring inorganic forms of water-soluble arsenic; As (III) species are more soluble and toxic than As (V) species (Cullen and Reimer, 1989; Nriago, 1994). Due to this it is not unrealistic that bacterial activity accounted for the oxidation of As (III) to As (V) as this oxidation leads to detoxification. Then foraminifera could incorporate arsenic without being harmed. Looking at Table 7, it is interesting that the foraminifera had the most offsprings in the tank with the highest concentration. Also chamber formation, at 37.0 %, is of a considerably higher level than in the concurrently run Batch I experiment (c.f. Table 7).

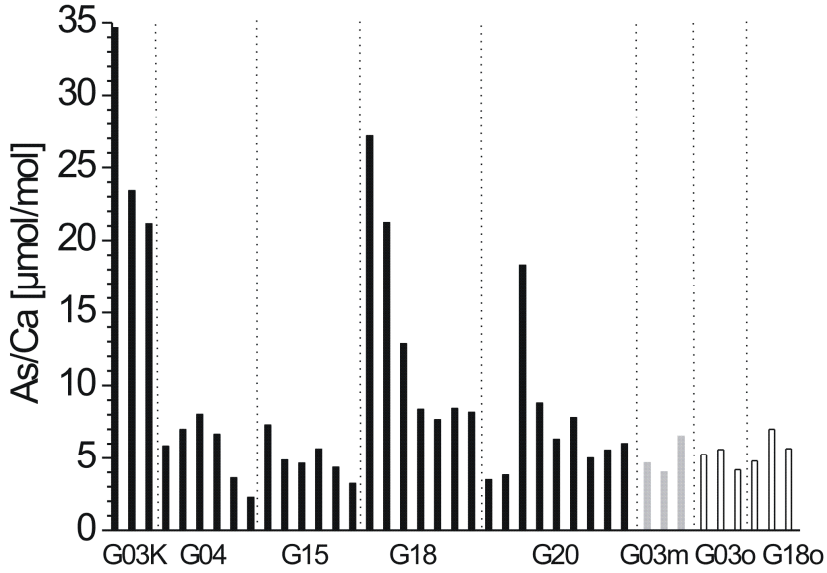

Figure 33 – Variation of As/Ca concentration within one pool tank (G – 20-fold concentration). Colours: Black = chambers formed in culture medium, light grey = (mixed grown) chambers that initiated formation in natural sea water and completed formation in culture solution (= m), and white = (old) chambers completely formed in natural sea water (= o). Numbers indicate specimen

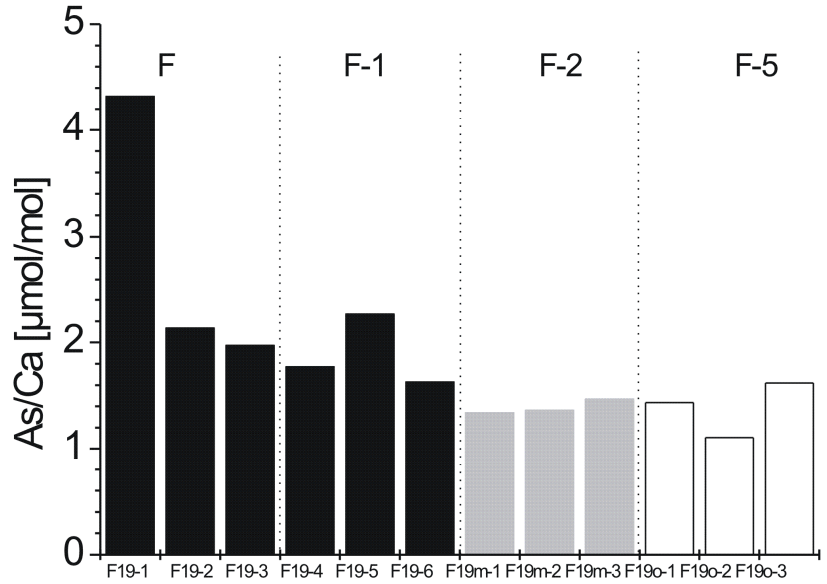

Figure 34 – As/Ca [µmol/mol] concentrations of one individual test (sample F-19 from the 10-fold concentration tank). F = last chamber, F-1 = 2nd last chamber, F-2 = 3rd last chamber, F-5 = 6th last chamber. Numbers indicate measuring point; colours as in Figure 25

The displayed results in Figures 33 and 34 partly show a wide scattering of the data, which is not unusual in biological experiments (e.g. Erez, 2003; Reichart et al., 2003; Dueñas-Bohórquez et al., 2009). Not only do differences between the analysed tests occur (Figure 33), but even within one foraminiferal chamber the measured concentration of a certain element may vary as shown in Figure 34. It can be observed that a chamber that started its formation in nature has a concentration of more or less at the natural level as only a small proportion of the culture solution was involved in the formation. For that reason, only newly formed chambers cultured entirely in batch solutions were considered for the calculation of the partitioning coefficient.

The very low concentrations of vanadium in sea water (e.g. Table 2) indicate that V is continuously removed from sea water, but the actual mechanisms are largely unknown. The behaviour of V in sea water is considered as nearly conservative (Collier, 1984) – meaning that no significant changes in concentrations occur and that these elements have the longest ocean residence times. Even hydrothermal activity only acts indirectly as a sink for vanadium (Jeandel et al., 1987; Trefry and Metz, 1989). During the course of the culture experiments it was possible to enrich V in the culture solution up to its 20-fold concentration compared to its natural occurance in sea water (Table 6 and Figure 11) without being precipitated.

Vanadium is an essential bioactive trace metal for a lot of macroalgae (e.g. Patrick, 1978; Nalewajko et al., 1995; Butler, 1998) and a great variety of marine phytoplankton species (Moore et al., 1996). In many metabolic processes, such as cell division (Meisch and Benzschawel, 1978), photosynthesis and cell motility (e.g. Meisch and Becker, 1981; Gilmore et al., 1985), sulfoxidation (e.g. ten Brink et al., 2001) or chlorophyll synthesis (e.g. Wilhelm and Wild, 1984), V may be involved. This is probably the reason why in the pool with the highest V concentration (in Batch II experiment) the highest reproduction rate was observed.

At high concentrations V is toxic (e.g. Riley et al., 2003; Bellenger et al., 2008). Thus its uptake is critical as V may be needed, for instance, for growth by N_2-fixing

cyanobacterium *Anabaena variabilis* (Pratte and Thiel, 2006) or the green alga *Scenedesmus* (Arnon and Wessel, 1953). As V becomes toxic (i.e. V reaches its toxic level), V uptake is cut off rapidly (Bellenger et al., 2008). This might also apply to foraminifera, but the toxic level for the cultured foraminifera was not reached in the experiments of the present study (Figure 19).

The V uptake of *Ammonia tepida* is just slightly reduced in the highest concentrated pool, but this could be due to the As, Cr, and/or Mo which were also used in Batch II experiment. Additionally, the fact that in all pools of Batch II experiment reproduction occurred (Table 7) might imply that foraminifera need V for growth, just as some bacteria (e.g. *Anabaena variabilis* (Pratte and Thiel, 2006) or *Azotobacter vinelandii* (Bellenger et al., 2008)).

5.2 Application

5.2.1 Recent/sub-recent material – ODP Site 1002, Hole C

5.2.1.1 Sediment of ODP Site 1002 C

Principal component analysis (PCA) was carried out, using the software Statistica (V 6.1, StatSoft, Inc.) in order to detect the main factors which account for the variance of the geochemical parameters in the core. Due to its distinct geochemical environments (see Section 4.6.2), the section was divided into three parts: An oxic part, a transition zone, and an anoxic part. For PCA the oxic part and the transition zone were analysed together, as Figures 23 and 24 (Section 4.6.2) clearly show that the samples of the transition zone plot together with the samples of the oxic part and they make up one population. For the anoxic part, a separate PCA was run in order to account for the distinct milieu and thus not to falsify interpretation.

5.2.1.1.1 Oxic part

For the oxic part of the section 28 geochemical parameters were considered and could be reduced by the PCA to three factors, which explain 86 % of the variance expressed by the initial data matrix.

The first factor (42 % of the variance) includes a set of major and trace elements (Ti, Al, Fe, K, V, Cr, Ni, Cu, Ga, Rb, and Ba) that are typical for detrital components of the sediment. All these elements have high loadings (≥ 0.7). The very high values for Ni, Cu, and V combined with the high values of Ti and Cr suggest a non-sulfidic mafic silicate component such as hornblende or biotite. Due to high K_2O contents biotite is more probable than hornblende. The association Rb and Ba, which both may substitute for K in mica or K-feldspar, together with high loadings for Al and Ga indicate further aluminosilicates such as mica, feldspars, and clay minerals as detrital components. The high loadings for the elements Nb, La, and Ce in this factor suggest some accessory minerals as another detrital constituent.

The second factor, which explains 31 % of the total variance, is characterised by high values of Mn, Mg, Ca, P, Sc, Sr, U, C, and C_{org}. This association of elements reflects the carbonate component of the sediment, which consists of calcite. Mn and Mg may substitute for Ca in calcite. A very good correlation between Sr and CaO (r = 0.95 throughout the whole core; Figure 35) clearly shows that Sr readily substitutes Ca in the carbonate phase. The very high C_{org} value denotes a period of high productivity including a high rate of carbonate building and high organic production (with a lot of organic matter settling down). In this factor the high loading of U is easily explicable because of its good correlation with C_{org} throughout the whole core (r = 0.84; Figure 35). Also with very high value, but negative algebraic sign, SiO_2 is present. This shows that during intensive biogenic carbonate deposition the sedimentation of (detrital) SiO_2 was low. A good correlation (r = 0.81) between SiO_2 and Zr (statistically significant for the p = 0.05 level) clearly shows that the majority of the Si is of detrital origin (Figure 35).

Factor three (13 % of the variance) is characterised by three elements with high loadings – As, Mo, and Sb. These elements may be adsorbed on Fe oxides as arsenate, molybdate, and antimoniate. This factor also reflects the anoxic component

of the oxic part of the core as repeatedly short anoxic periods occur during the oxic periods Sigurdsson et al., 1997).

The factor loadings of all three factors are shown in Figure 36.

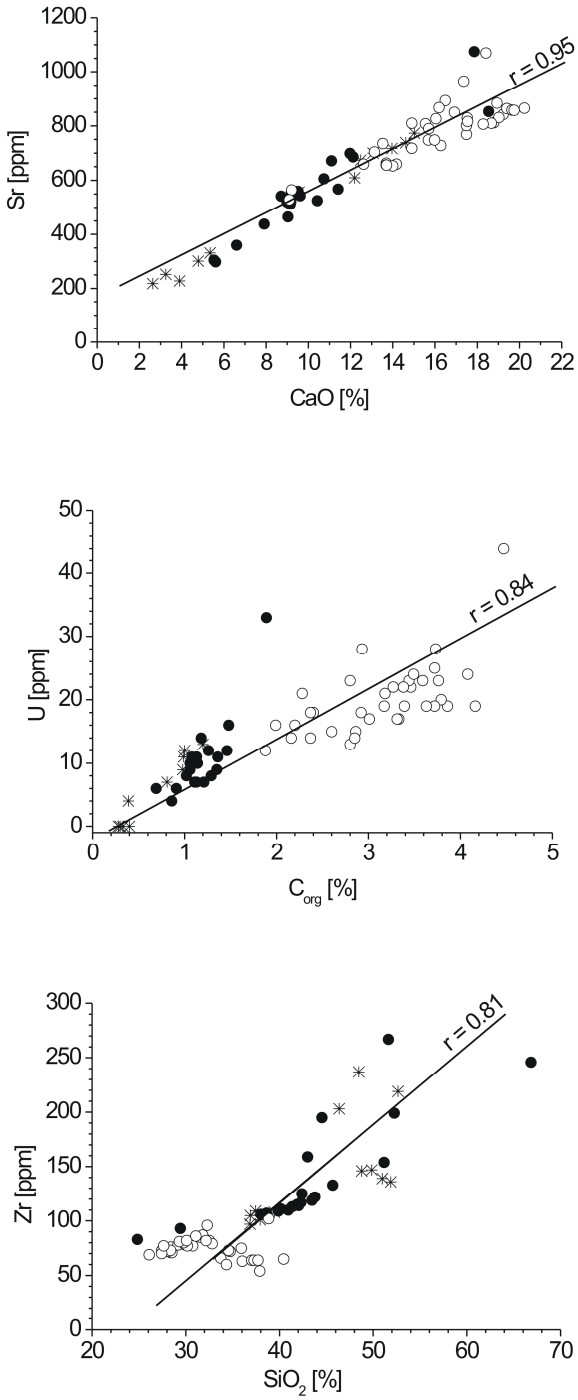

Figure 35 – Correlation graphs of CaO-Sr (top), and C_{org}-U (centre), and Zr-SiO_2 (bottom) of the sediments of the core of ODP Site 1002, Hole C. All correlations are significant at level p = 0.05. Samples: Oxic part (○), transition zone (⁕) and anoxic part (●)

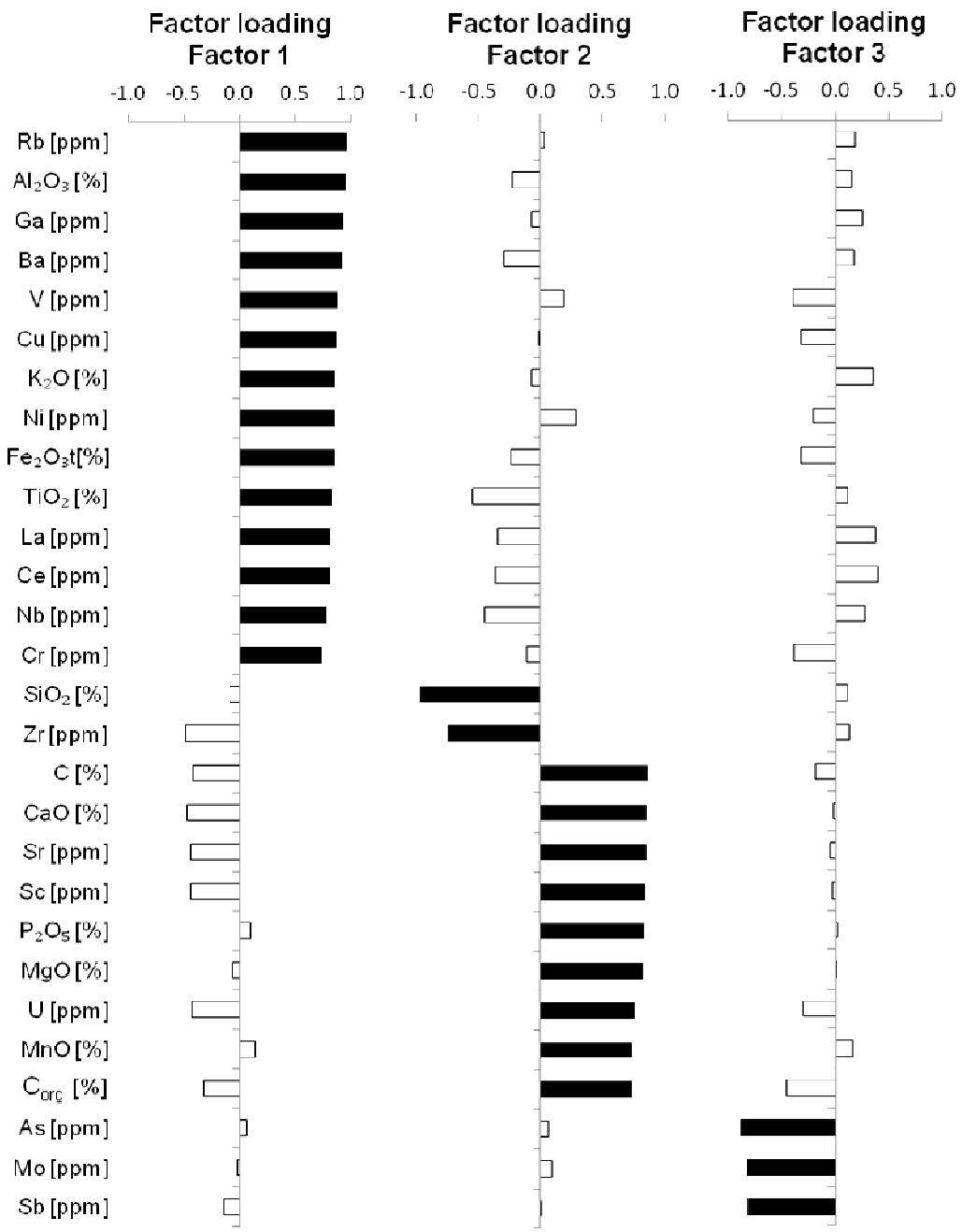

Figure 36 – Factor loadings of the three factors of the oxic sediments of ODP Site 1002 C. Colours: Black = high factor loading, white = low factor loading

5.2.1.1.2 Anoxic part

For the anoxic part of the core 22 geochemical parameters were considered and could be reduced by the PCA to only three factors, which explain 85 % of the variance expressed by the initial data matrix. Factor loadings are shown in Figure 37.

Factor one explains 48 % of the variance. It is characterised by a whole set of major and trace elements with high factor loading (Ti, Al, Fe, K, Cr, Zn, Ga, As, Rb, Zr, Nb,

La, Ce) and a moderate factor loading of V. These elements all have high positive loadings and reflect the detrital component of the sediment. Zirconium may account for a minor heavy mineral component – then also the appearance of the REE in this factor would be explained.

The second factor (20 % of the variance) includes on the one hand typical elements that explain a biogenic carbonate component of the sediment with very high negative loadings of Ca. Also the typical substitutes for Ca, Mg and Sr, are represented by this factor. On the other hand Mo, the typical diagnostic element for anoxic environments (e.g. Emerson and Huested, 1991; Piper and Dean, 2002) is also included in this factor revealing a high positive factor loading.

Factor three (17 % of the total variance) includes high factor loadings of V and C_{org}, which account for high productivity and a high rate of organic matter “sedimentation”. The intermediate factor loading of Si supports the high productivity in terms of diatoms, which are found frequently in the anoxic sediments (Sigurdsson et al., 1997).

Figure 37 shows the factor loadings of the anoxic part of the section.

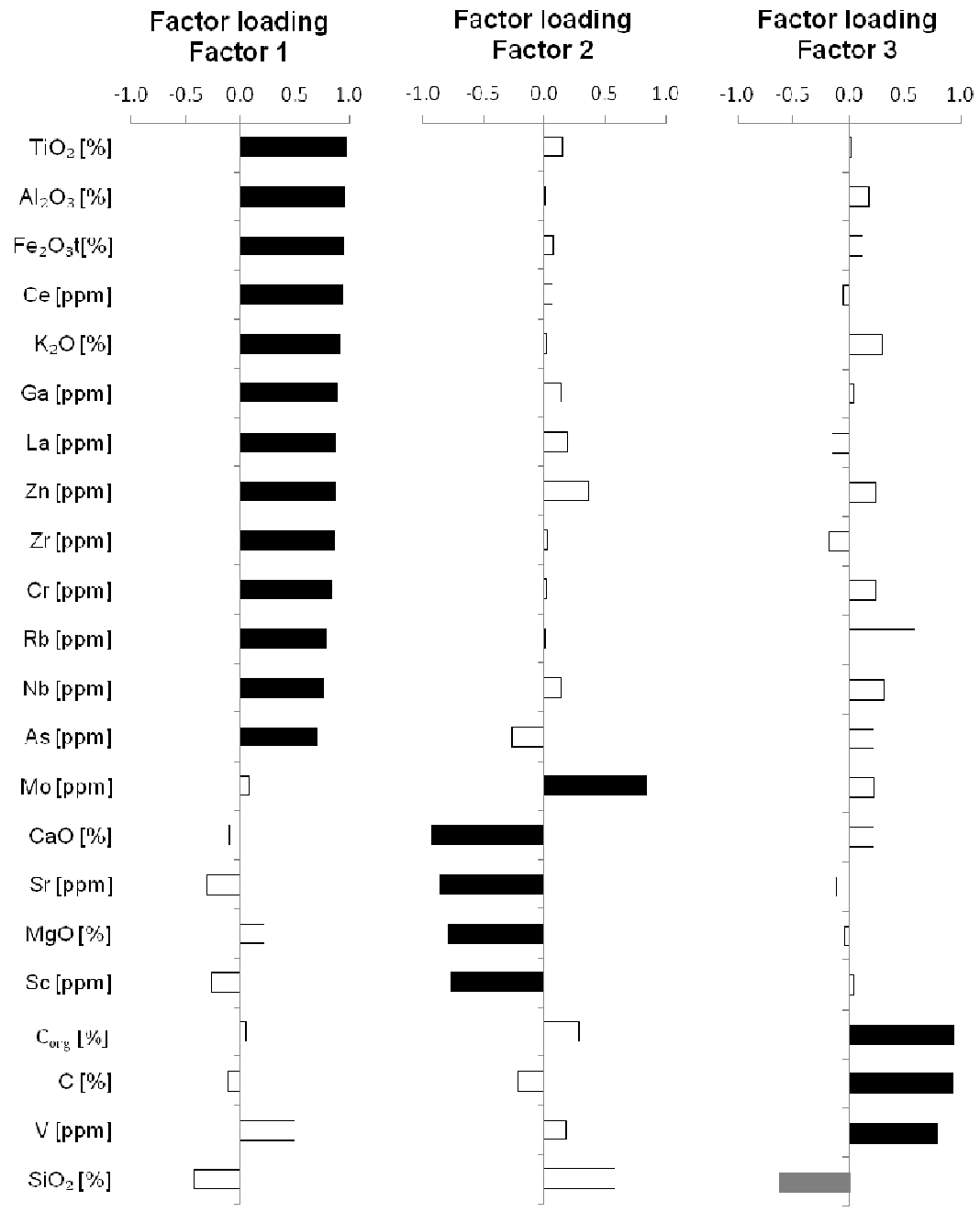

Figure 37 – Factor loadings of the factors from the anoxic sediments of ODP Site 1002 C. Black = high factor loading, grey = intermediate factor loading, white = low factor loading

5.2.1.2 Foraminifera from ODP Site 1002 C

For the benthic foraminifera hierarchical cluster analysis was performed as PCA did not show reasonable results with an inexplicable extremely low total variance. Separate cluster analyses of the two parts of the core (anoxic and oxic together with the transition zone) did not show any differences. Thus, a combined cluster analysis was performed. The obtained three main clusters are in line with geochemical reasoning.

The first main cluster unites the elements Co, Mn, As, Fe, and V. It may provide an indication for “secondary processes” such as sorption, as V and As are known to be particle reactive and may be taken up for instance by Mn phases. Such a scenario seems very plausible as in Figures 26 and 27 the concentrations of As and Mn as well as Fe of the analysed foraminifera definitely show a pattern that is not common for low redox environments. There, As, Mn, and Fe should be released under reduced conditions from the sediments and thus be higher concentrated in the water (e.g. Thomson et al., 1986). This way they should be available for the foraminifera so that the concentrations found in the tests should be higher than those found in the oxic part of the core. But it is the other way around, whereas the sediments (Figures 20 – 22) correctly show that these three elements are depleted in the anoxic part, but are enriched in the oxic part of the core. Thus, the measured concentrations of these elements in the foraminiferal tests are not of primary nature and the first main cluster indicates the result of a secondary process such as sorption. This assumption is confirmed by the fact that this cluster is linked to the other two clusters last (i.e. with the longest distance).

The second main cluster consists of a set of chalcophile elements, which are immobile at low Eh values and should trace redox changes in the sea water. The elements of this cluster are in line with the results of the performed factor analyses of the sediments of the core and reflect the geochemical environments. A very similar element association representing redox-sensitivity also has been found in zooplankton in the Gulf of California (Rentería-Cano et al., 2011). In the present study, this “redox-sensitive” element assemblage is divided into three sub-clusters:

- Cu-Ni ($r = 0.6$);
- U-Cr ($r = 0.31$);
- Mo-Zn(-Cd(-Pb)) ($r = 0.21$ for Mo-Zn).

The aforementioned correlation coefficients are statistically significant for the $p = 0.05$ level.

The third cluster consists of the major substitutes of Ca (Sr and Ba, complemented by Mg) (e.g. Lea and Boyle, 1991; Lea et al., 1999). It is directly linked to the chalcophile, redox-sensitive cluster. This may attribute for the ability of the elements of the second cluster to incorporate into the calcareous tests. The accomplished distribution coefficients from the performed culture experiments of this study emphasise this assumption.

Interestingly, the cluster of the "secondary process elements" shows a critical (i.e. toxic – e.g. Riley et al., 2003) element association that is predominantly identical with the Batch II culturing experiment performed within this study. The whole dendrogram is shown in Figure 38.

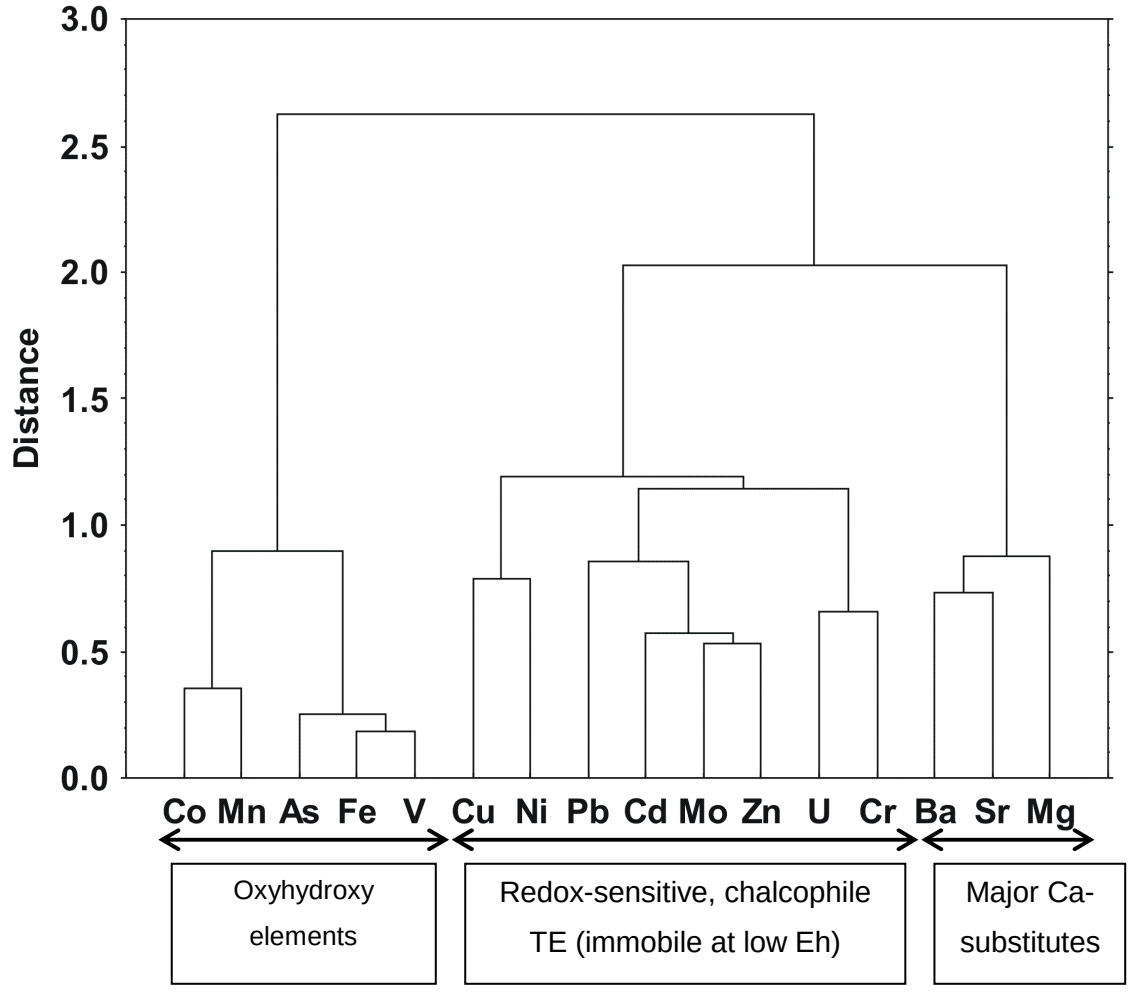

Figure 38 – Dendrogram of analysed Ca-normalised trace element concentrations in *Bulimina spp.* of ODP Site 1002, Hole C

5.2.2 Foraminifera from the Cretaceous-Palaeogene transition: Core Mullinax-1

For the foraminifera from core Mullinax-1, 11 geochemical parameters were considered. These could be reduced by the PCA to only two factors, which explain 80 % of the variance expressed by the initial data matrix. Factor loadings are shown in Figure 39.

The first factor, which explains 56 % of the total variance, consists of the chalcophile elements Pb, Cu, As, Ni, U, Cd, Zn, Co, and V. This group of elements is typically immobile under reducing conditions, and as mentioned in Section 5.2.1.2, this element association may be referred to as redox sensitive elements. Thus, it is very probable that this factor shows changing redox conditions in the Cretaceous ocean in the Brazos region. Recurrent high contents of Mo in the tests (Figure 29) of the Maastrichtian suggest periods of suboxic/anoxic conditions.

In factor two (24 % of the variance) only two elements are present: Manganese and Sr. These elements show an antagonistic trend. Manganese has a positive algebraic sign, while Sr is negative. This pattern of Mn and Sr is not unusual as it displays the diagenetic alteration that befell these tests. This can be explained by partial dissolution of the calcite tests by pore water. By this dissolution the whole Sr content will go in solution, but the re-crystallised calcite (from this pore water) will incorporate less Sr than originally was in the tests (e.g. Kitano et al., 1971; Veizer et al., 1971; Banner, 1995). If this process occurred in an anoxic environment, then the Mn content will be higher in the re-crystallised calcite as the Mn concentration in such pore waters is much higher than in sea water (Pomerol, 1983; Thomson et al., 1986). Typical diagenetic carbonate thus reflects low Sr and high Mn contents.

The factor loadings of the two factors are shown in Figure 39.

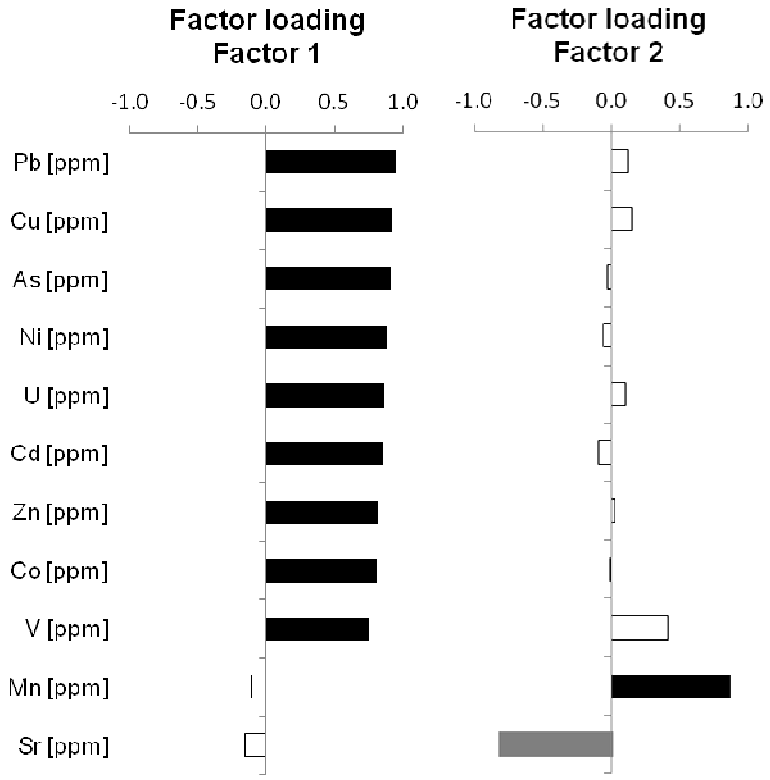

Figure 39 – Factor loadings of the two factors of the foraminiferal data from *Lenticulina spp.* from core Mullinax-1. Factor 1 (left side), Factor 2 (right side). Colours: Black = high factor loading, grey = intermediate factor loading, white = low factor loadings

5.2.3 A bridge to the past

Reconstructing past sea water chemistry (of deeper waters) is possible by applying calculated partition coefficients for benthic foraminifera. Even though the applied partition coefficients were calculated for a certain species at one specific temperature at a defined salinity and an appointed pH value, the differences between benthic species are relatively small compared to the discrepancies between planktonic and benthic foraminifera. For that reason the calculated partition coefficients for the elements V, Mn, Ni, Cu, and As were taken from the results of the present study. These were complemented by the partition coefficients for Cd, Ba, and U taken from literature (Boyle, 1988; Lea and Boyle, 1989; Russell et al., 1994, respectively) for benthic foraminifera.

5.2.3.1 Cariaco – ODP Site 1002, Hole C

Even though statistical data evaluation and the depth profiles of the foraminifera (Figures 26 and 27) showed that the tests of *Bulimina spp.* probably experienced some secondary sorption process (mentioned in Section 5.2.1.2) the data set was used for a general reconstruction of the sea water chemistry, with the exception of Mn, V, and As which were involved in that sorption process. The trace element concentrations could be reconstructed for the last 19,130 years and are shown in Figure 40.

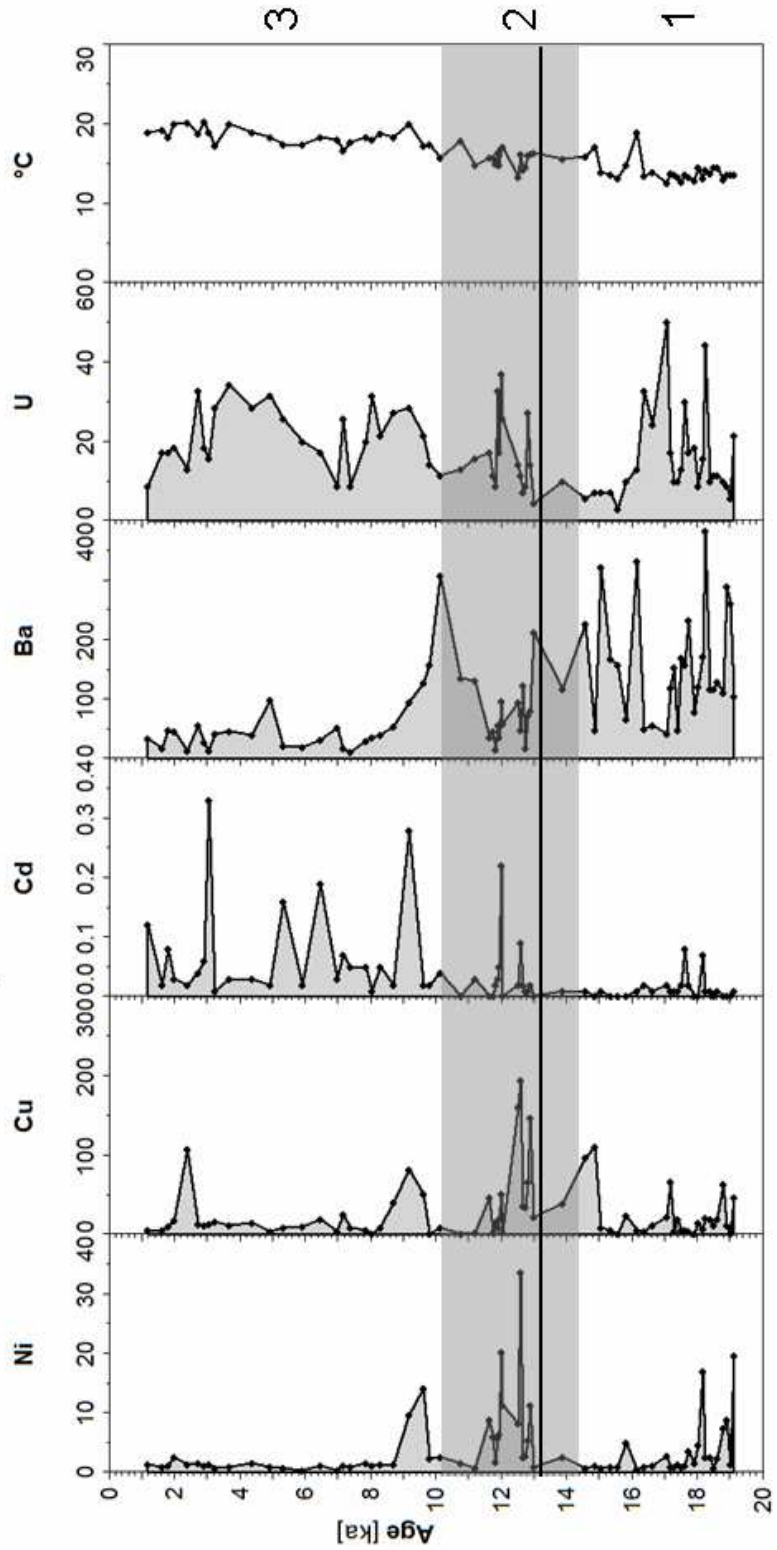

Figure 40 – Reconstruction of the sea water chemistry at ODP Site 1002 C for the last 19.13 ka. All concentrations are in µmol/mol Ca. Temperatures [℃] were calculated from $\delta^{18}O$ values (in ‰ VPDB). Black line = turnover anoxic/oxic conditions at ~12.600 years BP. Numbers 1, 2, and 3 indicate the geochemical zones as in Figures 20 – 22

The water chemistry of the sea water at ODP Site 1002 C changed throughout the mentioned time period. It traces the turnover from oxic to anoxic conditions in deep waters at approximately 12,600 years BP – when abrupt strong upwelling (probably induced by intensified trade winds which resulted from cooler sea surface temperatures) of nutrient rich water was initiated together with a rapid rise of the sea level that accompanied the peak interval of melt water discharge of the last glacial (Peterson et al., 1991). From the point of turnover until about 10, 000 years BP the cold temperatures of ~12 ℃ are also detectable in deeper waters (Figure 40) before temperatures were gradually rising up to 8 ℃. These maximum recorded temperatures of the deeper waters cover an interval from approximately 2,500 years ago until present day with temperature fluctuations no greater than 2.5 ℃. These temperatures are in line with present day temperatures in the Cariaco Basin shown in Figure 41.

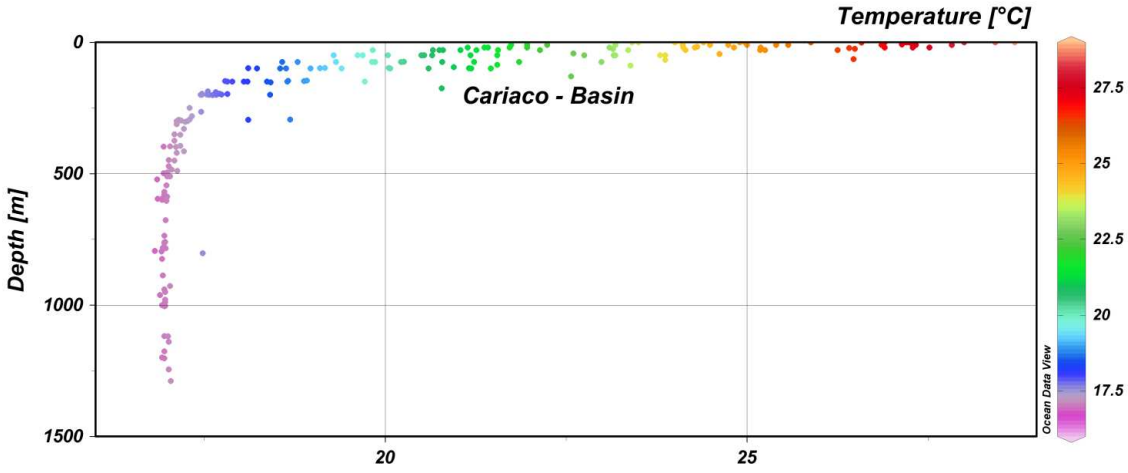

Figure 41 – Present day temperatures versus depth of the Cariaco Basin (Ocean Data View)

Interestingly, *Bulimina spp*. do not trace the warm Bølling-Ållerød interstadial (Figure 42) at the end of the Pleistocene for the deeper waters nor the following period of cold climate (Younger Dryas), although both could be proven by sediment records (Peterson and Haug, 2006; Dean, 2007) for the Cariaco Basin. Also the globally characterised “Holocene Thermal Maximum” (Renssen et al., 2012) was validated by sediment data (Peterson and Haug, 2006) for the Cariaco Basin, but cannot be

deciphered for deeper waters by the analysed *Bulimina spp.* of the present study. Planktonic foraminifera (*Globigerinoides ruber*) analysed for reference use in this study, also confirm the general warming trend for sea surface temperatures. But regarding the above mentioned periods of climate change, these foraminifera also do not reveal the appropriate temperatures. Figure 42 shows the temperature trend for the past 19,130 years.

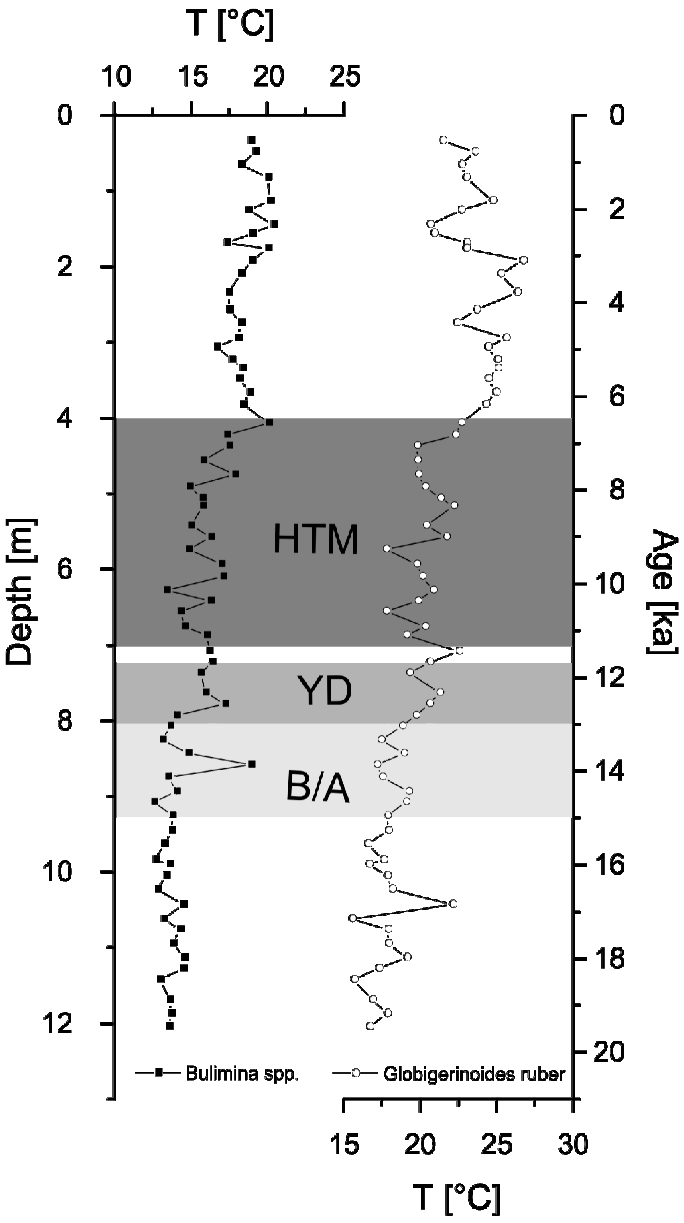

Figure 42 – Temperature trends of deeper waters (left side) and sea surface (right side) of the Cariaco Basin recorded by foraminifera for the last 19,130 years. HTM = Holocene thermal maximum, YD = Younger Dryas, B/A = Bølling-Ållerød

With the gradual warming the chemistry of the water changed. As shown in Figure 40, the element Cd especially reflects a vast change in concentration in the sea water. In the oxic part of the core Cd is only present in ultra trace amounts in the water – it demonstrates limited availability of nutrients prior to the strong upwelling and the melt water discharge around 12.6 ka BP. The lower accumulation of organic matter in the sediments of the oxic part (Figure 20) also reflects this. Despite upwelling events, Cd concentrations generally are very low in the waters of the Cariaco basin compared to sea water of other regions as displayed in Table 8.

Barium, which follows alkalinity (Lea, 1999) clearly shows that the hydrographic setting varied greatly within the analysed time period. It becomes apparent that before the anoxic turnover occurred 12,600 years ago, Ba availability was much greater than after the melting of the ice. Only during the first millennium after the melting began Ba ratios are as high as before. This may show that the anoxic water is more acidic than the oxic water. According to Table 8, Ba concentrations of the oxic part are well above average sea water concentrations, which might be explained by the association of Ba with various particulate phases in the water column (e.g. Dehairs et al., 1980).

In general, trace element concentrations in the sea water were only slightly lower during the anoxic period than in oxic times and thus suggest models which propose hardly any changes in deep water oxygen (e.g. Opdyke and Walker, 1992; Archer and Maier-Reimer, 1994). Uranium ratios support this scenario as U is a stable dimension in both parts of the core. Only during the glacial period U ratios drop severely, but this is in line with observations of Russel et al. (1996) from the Atlantic Ocean and the Caribbean Sea.

Table 8 displays average sea water concentrations (of selected elements) (Pilson, 2013 and references therein) as well as measured concentrations of North Sea water from two locations (NSW 1 and NSW 2; NSW 1 was used for the culture experiments of this study) and average trace element concentrations of the two parts of

the Cariaco core (the anoxic part and the oxic part including the transition zone – e.g. Figures 20 – 22).

Table 8 – Concentration of selected trace elements in average sea water, two North Sea waters (NSW 1 and NSW 2), and average values for the reconstructed Cariaco waters. All trace element concentrations are Ca-normalised and expressed as µmol/mol

	V	Mn	Ni	Cu	As	Cd	Ba	U
Average sea water	4.77	0.708	1.09	1.38	4.81	0.0952	14.9	1.35
NSW 1	3.48	2.90	4.64	18.8	6.09	1.09	13.7	1.06
NSW 2	4.81	3.86	2.69	15.4	4.15	0.675	11.9	1.55
Cariaco (average anoxic part)	*253**	*6.12**	4.26	26.9	*10.8**	0.0623	60.1	20.2
Cariaco (average oxic part)	*485**	*37.4**	3.56	28.8	*23.4**	0.0140	146	14.9

* = values are just for information as these elements were involved in secondary sorption processes and thus do not reflect primary signals.

5.2.3.2 Brazos (Texas) – Mullinax-1 core

As mentioned in Section 5.2.2, the tests of *Lenticulina spp.* (Brazos) unfortunately underwent diagenetic alteration (partial dissolution). Due to this, data of the reconstruction of the Cretaceous/Palaeogene transition as well as the main part of the core (latest Maastrichtian) may generally just inform about possible trace element concentrations in the sea water during the analysed time as the diagenetic signature partly overwrote the primary signal of some elements in the tests. Figure 43 shows the probable reconstructed trace element concentrations.

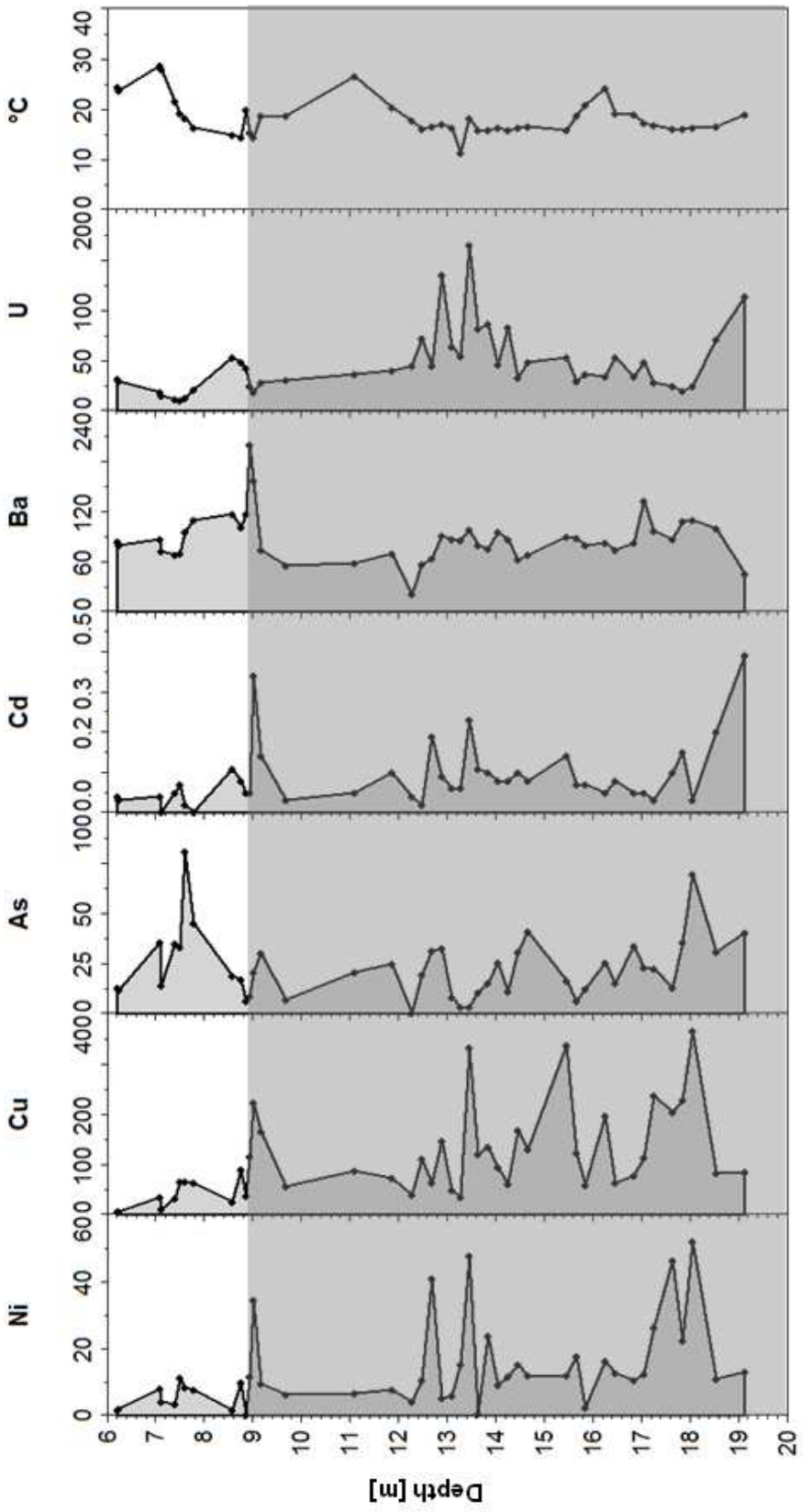

Figure 43 – Reconstructed trace element contents and temperatures of deeper sea water at Brazos. Light grey background = Cretaceous, white background = Palaeogene

Interestingly, the reconstructed temperatures are in line with published average temperatures from the Maastrichtian (e.g. Friedrich et al., 2008) meaning that the $\delta^{18}O$ values were not affected by the diagenetic process. Thus, some trace elements might reflect real trace element concentrations from the sea water.

When comparing Ca-normalised trace element ratios of the analysed tests with benthic foraminiferal test carbonate of a Cretaceous profile in Tunisia (Meudt, 2004), the analysed tests of Brazos show average trace element ratios that are within the same order of magnitude for most elements. Meudt's results show that only the Mn concentrations are lower than the ones of the present study. Additionally, he analysed hydrothermal affected tests of DSDP Site 216 and found that V, Ni, and As are slightly higher concentrated than in the Tunisian profile. Soley Mn is clearly enriched. Manganese concentrations as high as in the tests of DSDP Site 216 can also be found in the Brazos tests, revealing that the tests do not express the primary signal. Thus, Mn and probably some associated trace elements such as V may not be reconstructed correctly and the very high trace element ratios in the sea water (Table 9) are induced by secondary processes.

Table 9 reveals average sea water concentrations (Pilson, 2013 and references therein) as well as measured North Sea water (as in Table 8) and reconstructed average trace element concentrations from the Creataceous and the Palaegene at Brazos.

Table 9 – Concentration of selected trace elements in average sea water, two North Sea waters (NSW 1 and NSW 2), and average values for the reconstructed Brazos waters – Cretaceous and Palaeogene. All trace element concentrations are Ca-normalised and expressed as µmol/mol

	V	Mn	Ni	Cu	As	Cd	Ba	U
Average sea water	4.77	0.708	1.09	1.38	4.81	0.0952	14.9	1.35
NSW 1	3.48	2.90	4.64	18.8	6.09	1.09	13.7	1.06
NSW 2	4.81	3.86	2.69	15.4	4.15	0.675	11.9	1.55
Brazos (average Palaeogene)	*136**	*631**	5.78	45.9	26.5	0.04	26.5	20.4
Brazos (average Cretaceous)	*351**	*469**	16.8	156	21.9	0.11	54.2	17.5

* = values are just for information. These elements were probably involved in diagenetic processes and thus do not reflect primary signals.

The calculated trace element ratios for Cu in the sea water are well above average sea water values from Turekian (1976) and considerably above the contents of North Sea water (where anthropogenetic influences are also present – e.g. de Nooijer, 2007). Compared to studies by Boyle (1981) the Brazos Cu contents in the tests are very high, but they are in line with other Cretaceous values (e.g. Meudt, 2004).

Apart from the excluded elements Mn and V, it is surprising to see that trace element ratios do stay stable more or less throughout the whole profile. The only exception is the part between 12.0 and 14.0 m depth, where all elements but Ba are enriched – at the time when the climate was coolest and maybe a short time period of reducing conditions was present. Even around the Cretaceous/Palaeogene transition, when temperatures dropped and a major catastrophe, an impact event, took place, deep water conditions did not change dramatically. Thus, it may be predicted that the climatic turnover at the Cretacous/Palaeogene transition had no long term effect on the deep waters of Brazos.

6 Conclusions

The conditions in multi-element culture experiments better mimic natural environmental conditions than those commonly used in single element experiments. If results from single element experiments are to be applied to the natural environment, then potentially quenching effects must be taken into account, as demonstrated in Batch I experiment by the decreased uptake of both Ni and Cu when those metals are present in higher concentrations. Additionally, biological protection mechanisms ensure that potentially toxic elements are being transformed into less harmful substances (e.g. As (III) oxidation in Batch II experiment). Ignoring inter-element interference might result in artificially high toxic or subtoxic concentrations of certain elements and, thus leading to inaccurate reconstructions.

Multi-element measurements of calcareous foraminiferal tests of ODP Site 1002 clearly showed that distinct environmental conditions can be preserved in the tests. Especially in combination with multi-variate statistical methods the measurements revealed clear relationships to specific environments. In the case of the benthic foraminiferal tests of the Cretaceous-Palaeogene transition (at Brazos), no significant change induced by the catastrophe was detectable. For both localities the combination of analysing and statistical methods also pointed out that the treatment of the foraminiferal tests by the well-established leaching method may not always be a sufficient method in practise as it may not exclude secondary alteration and/or influences of the tests by oxyhyrodxides. In theory, the leaching process should remove these oxyhydroxides completetly. Thus, calcareous foraminiferal tests are only suitable up to a certain extent for palaeo reconstructions; tests definitely cannot replace sediments, but can rather complement them in palaeo climatic reconstructions.

The obtained partition coefficients of Cu, Ni, Mn, As, and V were measured successfully by means of µ-synchrotron XRF, which turned out to be a very reliable instrument to assess the concentration of trace elements in calcareous foraminiferal

tests. It showed the advantage that the sample material is not destroyed and, therefore, at the same measuring point analytical conditions may be optimised. Even though clear disadvantages of µ-synchrotron XRF are very high efforts in preparation, time, and data evaluation, this analytical method must be taken into account as an alternative method for LA-ICP-MS for future studies regarding trace element analyses of foraminiferal calcite.

7 Outlook – Prospect for future work

The culture experiments conducted in the present study reveal that there are complex interactions between trace elements considering their incorporation into calcareous foraminifera. It would certainly be important to shed light into the biochemical perspective of the effects taking place in foraminifera in regard to the elements As, V and Ni. The latter should be taken into account especially as interactions with Cu were observed in the conducted experiments. Therefore it is recommended to conduct detailed culturing studies with a main focus on Ni as well as on biological responses to the other two mentioned elements as, to date, there are no studies dealing with the effects of V and As on foraminifera.

Furthermore, a general study concerning the incorporation of Mo into calcite would be useful; in the long-run, new culturing experiments could also be conducted to use Mo/Ca ratios in addition to U/Ca ratios as a defined redox-sensitive tracer for palaeo reconstructions.

The diagenetic signal in practically all “old” foraminifera is a severe problem. In order to disentangle diagenetic calcite from primary signals an isotopic study is recommended – possibly in combination with multivariate statistics by a multi-proxy approach as proposed by Meudt (2004). Further culturing experiments with a diagenetic element mixture might also be a first step to solve this problem.

Revising to the cleaning protocol for foraminifera obvtained from core samples is an important next step in foraminiferal studies. As the present study showed, there is no guarantee that all oxyhydroxides are being removed by the leaching procedure. A detailed study regarding the foraminifera cleaning is stongly advised.

References

Adatte, T., Stinnesbeck, W. and Keller, G.: Lithostratigraphic and mineralogical correlations of near K-T boundary clastic sediments in northeastern Mexico: Implications for mega-tsunami or sea level changes? In: G. Ryder, D. Fastovstky, and S. Gartner (eds.): The Cretaceous-Tertiary event and other catastrophes in Earth history. Geol. S. Am. S., 307, 197-210, 1996.

Algeo, T.J.: Can marine anoxic events draw down the trace element inventory of seawater?, Geology, 32, 1057-1060, 2004.

Algeo, T.J. and Maynard, J.B.: Trace-element behavior and redox facies in core shales of Upper Pennsylvanian Kansas-type cyclothems, Chem. Geol., 206, 289-318, 2004.

Arenillas, I., Arz, J.A., Grajales-Nishimura, J.M., Murillo-Muneton, G., Alvarez, W., Camargo-Zanoguera, A., Molina, E. and Rosales-Dominguez, C.: Chicxulub impact event is Cretaceous/Palaeogene boundary in age: New micropaleontological evidence, Earth. Planet. Sc. Lett., 249, 241-257, 2006.

Alexandratos, V.G., Elzinga, E.J. and Reeder, R.J.: Arsenate uptake by calcite: Macroscopic and spectroscopic characterization of adsorption and incorporation mechanisms. Geochim. Cosmochim. Ac. 71, 4172-4187, 2007.

Alve, E.: Benthic foraminifera in sediment cores reflecting heavy-metal pollution in Sørfjord, western Norway, J. Foramin. Res., 21, 1-19, 1991.

Alve, E.: Benthic foraminiferal responses to estuarine pollution – a review, J. Foramin. Res., 25, 190-201, 1995.

Alve, E. and Murray, J.W.: Marginal marine environments of the Skagerrak and Kattegat: A baseline study of living (stained) benthic foraminiferal ecology, Palaeogeogr. Palaeocl. Palaeoec., 146, 171-193, 1999.

Anand, P., Elderfield, H. and Conte, M.H.: Calibration of Mg/Ca thermometry in planktonic foraminifera from a sediment trap time series, Paleoceanography, 18, 1050, 2003.

Anderson, O.R. and Lee, J.J.: Cytology an fine structure, in: Lee, J.J. and Anderson, O.R. (eds.): Biology of Foraminifera, Academic Press, 7-40, 1991.

Andreae, M.O.: Distribution and speciation of arsenic in natural waters and some marine algae. Deep-Sea Res. 25, 391-402, 1978.

Andreae, M.O.: Arsenic speciation in seawater and interstitial waters: The influence of biological-chemical interactions on the chemistry of a trace element, Limnol. Oceanogr., 24, 440-452, 1979.

Andreae, M.O and Klumpp, D.: Biosynthesis and release of organoarsenic compounds by marine algae. Environ. Sci. Technol. 13, 738-741, 1979.

Archer, D. and Maier-Reimer, E.: Effect of deep-sea sedimentary calcite preservation on atmospheric CO_2 concentrations, Nature, 367, 260-263, 1994.

Arnold, M.: Culture methods in the study of living foraminifera, J. Paleontol., 28, 404-416, 1954.

Arnon, D.T. and Wessel, G.: Vanadium as an essential element for green plants, Nature, 172, 1039-1040, 1953.

Bachmeier, K.L., Williams, A.E., Warmington, J.R. and Bang, S.S.: Urease activity in microbiologically-induced calcite precipitation, J. Biotechnol., 93, 171-181, 2002.

Banner, J.L.: Application of the trace element and isotope geochemistry of strontium to studies of carbonate diagenesis, Sedimentology, 42, 805-824, 1995.

Barras, C., Geslin, E., Duplessy, J.-C. and Jorissen, F.J.: Reproduction and growth of deep-sea benthic foraminifer *Bulimina marginata* under different laboratory conditions, J. Foramin. Res., 39, 155-165, 2009.

Barras, C., Duplessy, J.-C., Geslin, E., Michel, E. and Jorissen, F.J.: Calibration of $\delta^{18}O$ of cultured benthic foraminiferal calcite as a function of temperature, Biogeosciences, 7, 1349-1356, 2010.

Bé, A.W.H., Hemleben, C., Anderson, O.R., Spindler, M., Hacunda, J. and Tuntivate-Choy, S.: Laboratory and field observations of living planktonic foraminifera, Micropaleontology, 23, 155-179, 1977.

Bellenger, J.P., Wichard, T. and Kraepiel, A.M.L.: Vanadium requirements and uptake kinetics in the dinitrogen-fixing bacterium Azotobacter vinelandii, Appl. Environ. Microb., 74, 1478-1484, 2008.

Bemis, B.E., Spero, H.J., Bijma, J. and Lea, D.W.: Reevaluation of the oxygen isotopic composition of planktonic foraminifera: Experimental results and revised paleotemperature equations, Paleoceanography, 13, 150-160, 1998.

Bernhard, J.M., Blanks, J.K., Hintz, C.J. and Chandler, G.T.: Use of the fluorescent calcite marker calcein to label foraminiferal test, J. Foramin. Res., 34, 96-101, 2004.

Bijma, J., Faber, W.W. and Hemleben, C.: Temperature and salinity limits for growth and survival of some planktonic foraminifers in laboratory cultures, J. Foramin. Res., 20, 95-116, 1990.

Bortz, J.: Statistik für Sozialwissenschaftler, 5th Edition, Springer Verlag, Berlin, Heidelberg, New York, Barcelona Hong Kong, London, Milan, Paris, Singapore, Tokyo, 1999.

Boyle, E.A.: Cadmium, zinc, copper, and barium in foraminifera tests, Earth Planet. Sc. Lett., 53, 11-35, 1981.

Bourgeois, J., Hansen, T.A., Wiberg, P. and Kauffman, E.G.: A tsunami deposit at the Cretaceous-Tertiary boundary in Texas. Science 141: 567-570, 1988.

Boyle, E.A.: Cadmium: Chemical tracer of deep water paleoceanography, Paleoceanography, 3, 471-489, 1988.

Boyle, E.A. and Keigwin, L.D.: Deep circulation of the North Atlantic over the last 200,000 years: Geochemical evidence, Science, 218, 784-787, 1982.

Boyle, E.A. and Keigwin, L.D.: Comparison of Atlantic and Pacific paleochemical records for the last 215,000 years: Changes in deep ocean circulation and chemical inventories, Earth Planet. Sc. Lett., 76, 135-150, 1985/1986.

Bradshaw, J.S.: Preliminary laboratory experiments on ecology of foraminiferal populations, Micropaleontology, 1, 351-358, 1955.

Bradshaw, J.S.: Laboratory studies of the growth rate of the foraminifera "*Streblus beccarii* (Linné) var. *tepida* (Cushman)", J. Paleontol., 31, 1138-1147, 1957.

Broecker, W.S. and Peng, T.-H.: Tracers in the sea, Eldigio Press, Palisades, New York, 1982.

Bruland, K.W. and Lohan, M.C.: Controls of trace metals in seawater, in: The oceans and marine geochemistry, edited by Elderfield, H., Treatise on geochemistry volume 6, edited by Holland, H.D. and Turekian, K.K., Elsevier, Amsterdam, Heidelberg, 23-47, 2004.

Bruland, K.W., Donat, J.R. and Hutchins, D.A.: Interactive influences of bioactive trace metals on biological production in oceanic waters, Limnol. Oceanogr., 36, 1555-1577, 1991.

Bruland, K.W., Knauer, G.A. and Martin, J.H.: Cadmium in northeast Pacific waters, Limnol. Oceanogr., 23, 618-625, 1978.

Butler, A.: Acquisition and utilization of transition metal ions by marine organisms, Science, 281, 207-209, 1998.

Buzas-Stephens, P. and Buzas, M.A.: Population dynamics and dissolution of foraminifera in Nueces Bay, Texas, J. Foramin. Res., 35, 248-258, 2005.

Carnahan, E.A., Hoare, A.M., Hallock, P., Lidz, B.H. and Reich, C.D.: Distribution of heavy metals and foraminiferal assemblages in sediments of Biscayne Bay, Florida, USA, J. Coastal Res., 24, 159-169, 2008.

Cearreta, A., Irabien, M.J., Ulibarri, I., Yusta, I., Croudace, I.W. and Cundy, A.B.: Recent salt marsh development and natural regeneration of reclaimed areas in the Plentzia Estuary, N. Spain, Estuar. Coast. Shelf S., 54, 863-886, 2002.

Canfield, D.E.: Factors influencing organic carbon preservation in marine in marine sediments, Chem. Geol., 114, 315-329, 1994.

Calvert, S.E.: The geochemistry of deep sea sediments, in: Chemical oceanography, 2nd edition, volume VI, edited by Riley, J.P. and Chester, R., Academic Press, New York, 187-280, 1976.

Carpenter, J.H. and Manella, M.E.: Magnesium-to-chlorinity ratios in seawater, J. Geophys. Res., 78, 3621-3626, 1973.

Chang, J.S., Yoon, I.H., Lee, J.H., Kim, K.R., An, J. and Kim, K.W.: Arsenic detoxification potential of aox genes in arsenite-oxidizing bacteria isolated from natural and constructed wetlands in the Republic of Korea, Environ. Geochem. Hlth. 32, 95-105, 2010.

Cheng, L., Fenter, P., Sturchio, N.C., Zhong, Z. and Bedzyk, M.J.: X-ray standing wave study of arsenite incorporation at the calcite surface, Geochim. Cosmochim. Ac. 63, 3153-3157, 1999.

Chester, R. and Jickells, T.: Marine geochemistry, 3rd edition, John Wiley-Blackwell, Oxford, Chichester, and Hoboken, 2012.

Collier, R.W.: Particulate and dissolved vanadium in the North Pacific Ocean, Nature, 309, 441-444, 1984.

Collier, R. and Edmond, J.M.: The trace element geochemistry of marine particulate matter, Prog. Oceanogr., 13, 113-199, 1984.

Croteau, M.-N. and Luoma, S.N.: Predicting dietborne metal toxicity from metal influxes, Environ. Sci. Technol., 43, 4915-4921, 2009.

Culkin, F.: The major constituents of sea water, in: Chemical oceanography, Volume I, edited by Riley, J.P. and Skirrow, G., Academic Press, London and New York, 121-161, 1965.

Culkin, F. and Cox, R.A.: Sodium, potassium, magnesium, calcium and strontium in seawater, Deep-Sea Res., 13, 789-804, 1966.

Cullen, W.R. and Reimer, K.J.: Arsenic speciation in the environment. Chem. Rev. 89, 713-764, 1989.

de Deckker, P and Corrège, T.: A new paleothermometer: The magnesium to calcium ratio in benthic ostracod valves, Abstr. Fourth Internat. Conf. Paleoceanography (ICP IV), 92, 1992.

de Nooijer, L.J., Langer, G., Nehrke, G. and Bijma, J.: Physiological controls on seawater uptake and calcification in the benthic foraminifer *Ammonia tepida*, Biogeosciences, 6, 2669-2675, 2009.

de Nooijer, L.J., Reichart, G.J., Dueñas-Bohórquez, A., Wolthers, M., Ernst, S.R., Mason, P.R.D. and van der Zwaan, G.J.: Copper incorporation in foraminiferal calcite: Results from culturing experiments, Biogeosciences, 4, 493-504, 2007.

Dean, W.E.: Sediment geochemical records of productivity and oxygen depletion along the margin of western North America during the past 60,000 years: Teleconnections with Greenland Ice and the Cariaco Basin, Quaternary Sci. Rev., 26, 98-114, 2007.

Dehairs, F., Chesselet, R. and Jedwab, J.: Discrete suspended particles of barite and the barium cycle in the open ocean, Earth. Planet. Sc. Lett., 49, 528-550, 1980.

Delaney, M.L., Bé, A.W.H. and Boyle, E.: Li, Sr, Mg, and Na in foraminiferal calcite shells from laboratory culture, sediment traps, and sediment cores, Geochim. Cosmochim. Ac., 49, 1327-1341, 1985.

Deuser, W.G.: Cariaco Trench: Oxidation of organic matter and residence time of anoxic water, Nature, 242, 601-603, 1973.

Dieckmann, G.S., Spindler, M., Lange, M.A., Ackley, S.F. and Eicken, H.: Antarctic sea ice – a habitat for the foraminifer *Neogloboquadrina-Pachyderma*, J. Foramin. Res., 21, 182-189, 1991.

Diester-Haass, L. and Schrader, H.-J.: Neogene coastal upwelling history off northwest and southwest Africa, Mar. Geol., 29, 39-53, 1979.

Dissard, D., Nehrke, G., Reichart, G.-J., Nouet, J. and Bijma, J.: Effect of the fluorescent indicator calcein on Mg and Sr incorporation into foraminiferal calcite, Geochem. Geophy. Geosy., 10, 2009GC002417, 2009.

Dissard, D., Nehrke, G., Reichart, G.-J. and Bijma, J.: Impact of seawater pCO_2 on calcification and Mg/Ca and Sr/Ca ratios in benthic foraminifera calcite: Results from culturing experiments with *Ammonia tepida*, Biogeosciences, 7, 81-93, 2010a.

Dissard, D., Nehrke, G., Reichart, G.-J. and Bijma, J.: The impact of salinity on the Mg/Ca and Sr/Ca ratio in the benthic foraminifera *Ammonia tepida*: Results from culture experiments, Geochim. Cosmochim. Ac., 74, 928-940, 2010b.

Dueñas-Bohórquez, A., da Rocha, R.E., Kuroyanagi, A., Bijma, J. and Reichart, G.-J.: Effect of salinity and seawater calcite saturation state on Mg and Sr incorporation in cultured planktonic foraminifera, Mar. Micropaleontol., 73, 178-189, 2009.

Dyhrman, S.T. and Anderson, D.M.: Urease activity in cultures and field populations of the toxic dinoflagellate *Alexandrium*, Limnol. Oceanogr., 48, 647-655, 2003.

Egleston, E.S. and Morel, F.M.M.: Nickel limitation and zinc toxicity in a urea-grown diatom, Limnol. Oceanogr., 53, 2462-2471, 2008.

Elderfield, H. and Schultz, A.: Mid-ocean ridge hydrothermal fluxes and the chemical composition of the ocean, Annu. Rev. Earth Pl. Sc., 24, 191-224, 1996.

Elderfield, H. and Ganssen, G.: Past temperature and $\delta^{18}O$ of surface ocean waters inferred from foraminiferal Mg/Ca ratios, Nature, 405, 442-445, 2000.

Elderfield, H., Bertram, C.J. and Erez, J.: A biomineralization model for the incorporation of trace elements into foraminiferal calcium carbonate, Earth Planet. Sc. Lett., 142, 409-423, 1996.

Emerson, S.R. and Huested, S.S.: Ocean anoxia and concentrations of molybdenum and vanadium in seawater, Mar. Chem., 34, 177-196, 1991.

Emiliani, C.: Pleistocene temperatures, J. Geol., 63, 538-578, 1955.

Erez, J.: The source of ions for biomineralization in foraminifera and their implications for paleoceanographic proxies, in: Biomineralization, edited by Dove, P.M., de Yoreo, J.J. and Weiner, S., Reviews in Mineralogy and Geochemistry, volume 54, Mineralogical Society of America, Washington DC, 115-149, 2003.

Erez, J. and Luz, B.: Experimental paleotemperature equation for planktonic foraminifera, Geochim. Cosmochim. Ac., 47, 1025-1031, 1983.

Filipsson, H.L.: Culturing of benthic foraminifera for improved paleoceanographic reconstructions, PALAIOS, 23, 1-2, 2008.

Filipsson, H.L., Bernhard, J.M., Lincoln, S.A. and McCorkle, D.C.: A culture-based calibration of benthic foraminiferal paleotemperature proxies: $\delta^{18}O$ and Mg/Ca results, Biogeosciences, 7, 1335-1347, 2010.

Forchhammer, G.: On the composition of sea-water in different parts of the ocean, Philos. T. Roy. Soc. A, 155, 203-262, 1865.

Friedrich, O.: Benthic foraminifera and their role to decipher paleoenvironment during mid Cretaceous Oceanic Anoxic Events – the “anoxic benthic foraminifera” paradox, Rev. Micropal., 53, 175-192, 2010.

Friedrich, O., Erbacher, J, Moriya, K., Wilson, P.A. and Kuhnert: Warm saline intermediate waters in the Cretaceous tropical Atlantic Ocean, Nat. Geosci., 1, 2008.

Gale, A.S.: The Cretaceous-Palaeogene boundary on the Brazos River, Falls County, Texas: Is there evidence for impact-induced tsunami sedimentation? Proceedings of the Geologists Association 117: 173-185, 2006.

Gavish, E. and Friedman, G.: Progressive diagenesis in Quaternary to late Tertiary carbonate sediments: Sequence and time scale, J. Sediment. Petrol., 39, 980-1006, 1969.

Gerlach, S.A.: Oxygen conditions improve when the salinity in the Baltic Sea decreases, Mar. Pollut. Bull., 28, 413-416, 1994.

German, C.R. and von Damm, K.L.: Hydrothermal processes, in: The Oceans and Marine Geochemistry, edited by Elderfield, H., Treatise on geochemistry volume 6, edited by Holland, H.D. and Turekian, K.K., Elsevier, Amsterdam, Heidelberg, 181-222, 2004.

Gilmore, D.J., Kaaden, R. and Gimmler, H.: Vanadate inhibition of ATPases of *Dunaliella parva in vitro* an *in vivo*, J. Plant Physiol., 118, 111-126, 1985.

Goldstein, S.T.: Foraminifera: A biological overview, in: Sen Gupta, B.K. (ed.): Modern foraminifera, Kluwer Academic Publishers, 37-55, 1999.

Goldstein, S.T. and Moodley, L.: Gametogenesis and the life cycle of the foraminifer *Ammonia beccarii* (Linné) forma *tepida* (Cushman), J. Foramin. Res., 23, 213-220, 1993.

Grasshoff, K.: The hydrochemistry of landlocked basins and fjords, in: Chemical oceanography, 2nd edition, volume II, edited by Riley, J.P. and Skirrow, G., Academic Press, New York, 456-597, 1975.

Grell, K.G.: Protozoology, 3rd edition, Springer Verlag, Berlin, 1973.

Hamamura, N., Macur, R.E., Korf, S., Ackerman, G., Taylor, W.P., Kozubal, M., Reysenbach, A.L. and Inskeep, W.P.: Linking microbial oxidation of arsenic with detection and phylogenetic analysis of arsenite oxidase genes in diverse geothermal environments, Environ. Microbiol. 11, 421-431, 2009.

Handley, K.M., Héry, M. and Lloyd, J.R.: Redox cycling of arsenic by hydrothermal marine bacterium *Marinobacter santoriniensis*, Environ. Mirobiol. 11, 1601-1611, 2009.

Hart, M.B., Yancey, T.E., Leighton, A.D., Miller, B., Liu, C., Smart, C.W. and Twitchett, R.J.: The Cretaceous-Palaeogene boundary on the Brazos River, Texas: New stratigraphic sections and revised interpretations, GCAGS Journal, 1, 69-80, 2012.

Hastings, D.W., Emerson, S.R., Erez, J. and Nelson, B.K.: Vanadium in foraminiferal calcite: Evaluation of a method to determine paleo-seawater vanadium concentrations, Geochim. Cosmochim. Ac., 60, 3701-3715, 1996.

Havach, S.M., Chandler, G.T., Wilson-Finelli, A. and Shaw, T.J.: Experimental determination of trace element partition coefficients in cultured benthic foraminifera, Geochim. Cosmochim. Ac., 65, 1277-1283, 2001.

Hayward, B.W., Holzmann, M., Grenfell, H.R., Pawlowski, J. and Triggs, C.M.: Morphological distinction of molecular types in *Ammonia* – Towards a taxonomic revision of the world's most common misidentified foraminifera, Mar. Micropaleontol., 50, 237-271, 2004.

Hedberg, H.D.: Some recent and fossil brackish to freshwater foraminifera, J. Paleontol.,8, 469-476, 1934.

Heiser, U., Neumann, T., Scholten, J. and Stüben, D.: Recycling of manganese from anoxic sediments in stagnant basins by seawater inflow: A study of surface sediments from the Gotland Basin, Baltic Sea, Mar. Geol., 177, 151-166, 2001.

Hemleben, C., Spindler, M. and Anderson, O.R.: Modern planktonic foraminifera, Springer Verlag, 1989.

Hemleben, C., Bé, A.W.H., Anderson, R. and Tuntivate, S.: Test morphology, organic layers and chamber formation of the planktonic foraminifer *Globorotalia menardii* (d'Orbigny), J. Foramin. Res., 7, 1-25, 1977.

Hemming, N.G. and Hanson, G.N.: Boron isotopic composition and concentration in modern marine carbonates, Geochim. Cosmochim. Ac., 56, 537-543, 1992.

Hintz, C.J., Shaw, T.J., Chandler, G.T., Bernhard, J.M., McCorkle, D.C. and Blanks, J.K.: Trace/minor element:calcium ratios in cultured benthic foraminifera. Part I: Inter-species and inter-individual variability, Geochim. Cosmochim. Ac., 70, 1952-1963, 2006.

Hintz, C.J., Chandler, G.T., Bernhard, J.M., McCorkle, D.C., Havach, S.M., Blanks, J.K. and Shaw, T.J.: A physicochemically constrained seawater culturing system for production of benthic foraminifera, Limnol. Oceanogr.-Meth., 2, 160-170, 2004.

Hoaglin, D.C., Mosteller, F. and Tuckey, P.A. (eds.): Understanding Robust and Exploratory Data Analysis, John Wiley & Sons, New York, 1-447, 1983.

Howarth, R.J. (ed.): Statistics and data analysis in geochemical prospecting. In: Govett, G.J.S.: Handbook of Geochemical exploration, Volume 2, Elsevier, Amsterdam, 1-437, 1983.

Hunt, J.W., Anderson, B.S., Phillips, B.M., Tjeerdema, R.S., Puckett, H.M., Stephenson, M., Tucker, D.W. and Watson, D.: Acute and chronic toxicity of nickel to marine organisms: Implications for water quality criteria, Environ. Toxicol. Chem., 21, 2423-2430, 2002.

Imbrie, J., Hays, J.D., Martinson, D.G., McIntyre, A., Mix, A.C., Morley, J.J., Pisias, N.G., Prell, W.L. and Shackleton, N.J.: The orbital theory of Pleistocene climate: Support from a revised chronology of the marine $\delta^{18}O$ record, in: Berger, A., Imbrie, J., Hays, J., Kukla, G. and Saltzman, B. (eds.): Milankovitch and climate (Part 1), NATO Adv. Sci. I. C-Mat., 126, 269-305, 1984.

Jacobs, L., Emerson, S. and Huested, S.S.: Trace metal geochemistry in the Cariaco Trench, Deep-Sea Res., 34, 965-981, 1987.

Jeandel, C., Caisso, M. and Minster, J.R.: Vanadium behavior in the global ocean and in the Mediterranean Sea, Mar. Chem., 21, 51-74, 1987.

Jochum, K.P., Dingwell, D.B., Rocholl, A., Stoll, B., Hofmann, A.W., Becker, S., Besmehn, A., Bessette, D., Dietze, H.-J., Dulski, P., Erzinger, J., Hellebrand, E., Hoppe, P., Horn, I., Janssens, K., Jenner, G.A., Klein, M., McDonough, W.F., Maetz, M., Mezger, K., Münker, C., Nikogosian, I.K., Pickhardt, C., Raczek, I., Rhede, D., Seufert, H.M., Simakin, S.G., Sobolev, A.V., Spettel, B., Straub, S., Vincze, L., Wallianos, A., Weckwerth, G., Weyer, S., Wolf, D. and Zimmer, M.: The preparation and preliminary characterisation of eight geological MPI-DING reference glasses for in-site microanalysis, Geostandard Newslett., 24, 87-133, 2000.

Johnson, A. and Cronan, D.S.: Hydrothermal metalliferous sediments and waters off the Lesser Antilles. Mar. Georesour. Geotec. 16, 65-83, 2001.

Johnson, D.L. and Pilson, M.E.Q.: The oxidation of arsenite in seawater, Environ. Lett. 8, 157-171, 1975.

Jonasson, K.E., Schroderadams, C.J. and Patterson, R.T.: Benthic foraminiferal distribution at Middle Valley, Juan-de-Fuca-Ridge, a northeast Pacific hydrothermal venting site, Mar. Micropaleontol., 25, 151-167, 1995.

Jones, C.J. and Murray, J.W.: Nickel, cadmium, and copper in the northeast Pacific off the coast of Washington, Limnol. Oceanogr., 29, 711-720, 1984.

Keller, G., Stinnesbeck, W., Adatte, T. and Stüben, D.: Multiple impacts across the Cretaceous-Tertiary boundary, Earth-Sci. Rev., 62, 327-363, 2003.

Keller, G., Adatte, T., Berner, Z., Harting, M., Baum, G., Prauss, M., Tantawy, A. and Stüben, D.: Chicxulub impact predates K-T boundary: New evidence from Brazos, Texas, Earth. Planet. Sc. Lett., 255, 339-356, 2007.

Keller, G., Adatte, T., Berner, Z., Pardo, A. and Lopez-Oliva, L.: Age and biotic effects of the Chicxulub impact in Mexico, J. Geol. Soc. London, 166, 393-411, 2009.

Kitano, Y., Kanamori, N. and Oomori, T.: Measurements of distribution coefficients of strontium and barium between carbonate precipitate and solution. Abnormally high values of distribution coefficients measured at early stages of carbonate formation, Geochem. J., 4, 183-206, 1971.

Köster, R.: Wattsedimente, in: Umweltatlas Wattenmeer, Band 1, Nordfriesisches und Dithmarsches Wattenmeer, edited by Umweltbundesamt und Nationalparkverwaltungen Niedersächsisches Wattenmeer/Schleswig-Holsteinisches Wattenmeer, Eugen Ulmer Verlag, Stuttgart, 40-41, 1998/1999.

Kramar, U., Munsel, D., Berner, Z., Bijma, J. and Nehrke, G.: Determination of trace element incorporation into tests of in vitro grown foraminifera by micro-SYXRF – a basis for the development of paleoproxies, in: X-Ray Optics and Microanalysis, edited by: Denecke, M.A. and Walker, C.T., American Institute of Physics Conference Proceedings 1221, ICXOM20, New York, 154-159, 2010.

le Cadre, V. and Debenay, J.-P.: Morphological and cytological responses of *Ammonia* (foraminifera) to copper contamination: Implication for the use of foraminifera as bioindicators of pollution, Environ. Pollut., 143, 304-317, 2006.

Lea, D.W.: Trace elements in foraminiferal calcite, in: Sen Gupta, B.K. (ed.): Modern foraminifera, Kluwer Academic Publishers, 259-282, 1999.

Lea, D.W.: Elemental and isotopic proxies of past ocean temperatures, in: The oceans and marine geochemistry, edited by Elderfield, H., Treatise on geochemistry volume 6, edited by Holland, H.D. and Turekian, K.K., Elsevier, Amsterdam, Heidelberg, 365-390, 2004.

Lea, D. and Boyle, E.: Barium content of benthic foraminifera controlled by bottom-water composition, Nature, 338, 751-753, 1989.

Lea, D.W. and Boyle, E.A.: Ba in planktonic foraminifera, Geochim. Cosmochim. Ac., 55, 3321-3331, 1991.

Lea, D.W. and Spero, H.J.: Experimental determination of barium uptake in shells of planktonic foraminifera *Orbulina universa* at 22 ℃, Geochim. Cosmochim. Ac., 56, 2673-2680, 1992.

Lea, D.W. and Spero, H.J.: Assessing the reliability of paleochemical tracers: Barium uptake in the shells of planktonic foraminifera, Paleoceanography, 9, 445-452, 1994.

Lea, D.W., Mashiotta, T.A. and Spero, H.J.: Controls on magnesium and strontium uptake in planktonic foraminifera determined by live culturing, Geochim. Cosmochim. Ac., 63, 2369-2379, 1999.

Lee, J.J., Faber, Jr., W.W., Anderson, O.R. and Pawlowski, J.: Life cycle of Foraminifera, in: Lee, J.J. and Anderson, O.R. (eds.): Biology of Foraminifera, Academic Press, 285-334, 1991.

Leorri, E., Gehrels, W.R., Horton, B.P., Fatela, F. and Cearreta, A.: Distribution of foraminifera in salt marshes along the Atlantic coast of SW Europe: Tools to reconstruct past sea-level variations, Quatern. Int., 221, 104-115, 2010.

Li, L., Keller, G., Adatte, T. and Stinnesbeck, W.: Late Cretaceous sea-level changes in Tunisia: A multidisciplinary approach, J. Geol. Soc. London, 157, 447-458, 2000.

Li, Y.-H.: Distribution patterns of the elements in the oceans: A synthesis, Geochim. Cosmochim. Ac., 55, 3223-3240, 1991.

Lieutaud, A., van Lis, R., Duval, S., Capowiez, L., Muller, D., Lebrun, R., Lignon, S., Fardeau, M.-L., Lett, M.-C., Nitschke, W. and Schoepp-Cothenet, B.: Arsenite oxidase from *Ralstonia* sp. 22, J. Biol. Chem. 285, 20433-20441, 2010.

Linke, P. and Lutze, G.F.: Microhabitat preferences of benthic foraminifera – a static concept or a dynamic adaption to optimize food acquisition?, Mar. Micropaleontol., 20, 215-234, 1993.

Lipps, J.H. and Lange, M.R.: Benthic foraminifera from the meromictic Mecherchar Jellyfish Lake, Palau (western Pacific), Micropaleontology, 45, 278-284, 1999.

Loeblich, A.R. and Tappan, H.: Foraminiferal genera and their classification, van Nostand Reinhold, New York, 1988.

Lu, Y.F. and Allen, H.E.: Characterization of copper complexation with natural dissolved organic matter (DOM) – link to acidic moieties of DOM and competition by Ca and Mg, Water Res., 36, 5083-5101, 2002.

Lynch-Stieglitz, J.: Tracers of past ocean circulation, in: The Oceans and Marine Geochemistry, edited by Elderfield, H., Treatise on geochemistry volume 6, edited by Holland, H.D. and Turekian, K.K., Elsevier, Amsterdam, Heidelberg, 433-451, 2004.

Mann, E.L., Ahlgren, N., Moffett, J.W. and Chisholm, S.W.: Copper toxicity and cyanobacteria ecology in the Sargasso Sea, Limnol. Oceanogr., 47, 976-988, 2002.

Marchitto, T.M., Curry, W.B. and Oppo, D.W.: Zinc concentrations in benthic foraminifera reflect seawater chemistry, Paleoceanography, 15, 299-306, 2000.

Maréchal-Abram, N., Debenay, J.-P., Kitazato, H. and Wada, H.: Cadmium partition coefficients of cultured benthic foraminifera *Ammonia beccarii*, Geochem. J., 38, 271-283, 2004.

Martin, P.A. and Lea, D.W.: Comparison of water mass changes in the deep tropical Atlantic derived from Cd/Ca and carbon isotope records: Implications for changing Ba composition of deep Atlantic water masses, Paleoceanography, 13, 572-585, 1998.

Martin, P.A. and Lea, D.W.: A simple evaluation of cleaning procedures on fossil benthic foraminiferal Mg/Ca, Geochem. Geophys. Geosy. 3, 2001GC000280, 2002.

Martin, P.A., Lea, D.W., Rosenthal, Y., Shackleton, N.J., Sarnthein, M. and Papenfuss, T.: Quaternary deep sea temperature histories derived from benthic foraminiferal Mg/Ca, Earth Planet. Sc. Lett., 198, 193-209, 2002.

Mashiotta, T.A., Lea, D.W. and Spero, H.J.: Experimental determination of cadmium uptake in shells of planktonic foraminifera *Orbulina universa* and *Globigerina bulloides*: Implications for surface water paleoreconstructions, Geochim. Cosmochim. Ac., 61, 4053-4065, 1997.

Mashiotta, T.A., Lea, D.W. and Spero, H.J.: Glacial-interglacial changes in Subantarctic sea surface temperature and δ^{18}O-water using foraminiferal Mg, Earth Planet. Sc. Lett., 170, 417-432, 1999.

Mason, P.R.D. and Kraan, W.J.: Attenuation of spectral interferences during laser ablation inductively coupled plasma mass spectroscopy (LA-ICP-MS) using an rf only collision and reaction cell, J. Anal. Atom. Spectrom., 17, 858-867, 2002.

McManus, J., Berelson, W.M., Klinkhammer, G.P., Hammond, D.E. and Holm, C.: Authigenic uranium: Relationship to oxygen penetration depth and organic carbon rain, Geochim. Cosmochim. Ac., 69, 95-108, 2005.

Meisch, H.-U. and Becker, L.J.M.: Vanadium in photosynthesis of *Chlorella fusca* and higher plants, Biochim. Biophys. Acta, 636, 119-125, 1981.

Meisch, H.-U. and Benzschawel, H.: The role of vanadium in green plants – III. Influence on cell division of *Chlorella*, Arch. Microbiol., 116, 91-95, 1978.

Meudt, M.: Geochemie der Foraminiferenschalen: Relevanz für die Rekonstruktion von Paläoumweltbedingungen, Dissertation, Universität Karlsruhe, 1-148, 2004.

Middelburg, J.J., de Lange, G.J., van der Sloot, H.A., van Emburg, P.R. and Sophia, S.: Particulate manganese and iron framboids in Kau Bay, Halmahera (eastern Indonesia), Mar. Chem., 23, 353-364, 1988.

Millero, F.J.: Chemical oceanography, 2nd edition, CRC Press, Boca Raton, 1996.

Millero, F.J.: Redox processes in anoxic waters, in: Chemical processes in marine environments, edited by Gianguzza, A., Pelizzetti, E. and Sammartano, S., Springer-Verlag, Berlin, Heidelberg, New York, Barcelona, Hong Kong, London, Milan, Paris, Tokyo, 91-123, 2000.

Millero, F.J.: Sea water as an electrolyte, in: Chemistry of marine Waters and sediments, edited by Gianguzza, A., Pelizzetti, E. and Sammartano, S., Springer-Verlag, Berlin, Heidelberg, New York, Barcelona, Hong Kong, London, Milan, Paris, Tokyo, 3-34, 2002.

Mojtahid, M., Jorissen, F., Lansard, B. and Fontanier, C.: Microhabitat selection of benthic foraminifera in sediments off the Rhône River mouth (NW Mediterranean), J. Foramin. Res., 40, 231-246, 2010.

Moore, R.M., Webb, M., Tokarcyk, R. and Wever, R.: Bromoperoxidase and iodoperoxidase enzymes and production of halogenated methanes in marine diatom cultures, J. Geophys. Res. – Oceans, 101, 20899-20908, 1996.

Morel, F.M.M., Milligan, A.J. and Saito, M.A.: Marine bioinorganic chemistry: The role of trace metals in the oceanic cycles of major nutrients, in: The Oceans and Marine

Geochemistry, edited by Elderfield, H., Treatise on geochemistry volume 6, edited by Holland, H.D. and Turekian, K.K., Elsevier, Amsterdam, Heidelberg, 113-143, 2004.

Morford, J.L. and Emerson, S.: The geochemistry of redox sensitive trace metals in sediments, Geochim. Cosmochim. Ac., 63, 1735-1750, 1999.

Morris, A.W. and Riley, J.P.: The bromide/chlorinity and sulphate/chlorinity ratio in seawater, Deep-Sea Res., 13, 699-705, 1966.

Müller-Karger, F.E., McClain, C.R., Fisher, T.R., Esaias, W.E. and Varela, R.: Pigment distribution in the Caribbean Sea: Observations from space, Prog. Oceanogr., 23, 23-64, 1989.

Murray, J.W.: Ecology and distribution of benthic foraminifera, in: Lee, J.J. and Anderson, O.R. (eds.): Biology of Foraminifera, Academic Press, 221-253, 1991a.

Murray, J.W.: Ecology and distribution of planktonic foraminifera, in: Lee, J.J. and Anderson, O.R. (eds.): Biology of Foraminifera, Academic Press, 255-284, 1991b.

Nägler, T.F., Eisenhauer, A., Müller, A., Hemleben, C. and Kramers, J.: The δ^{44}Ca-temperature calibration on fossil and cultured *Globigerinoides sacculifer*: New tool for reconstruction of past sea surface temperatures, Geoch. Geophy. Geosy., 1, 2000GC000091, 2000.

Nalewajko, C., Lee, K and Jack, T.R.: Effects of vanadium on freshwater phytoplankton photosynthesis, Water Air Soil Poll., 81, 93-105, 1995.

Nameroff, T.J., Balistrieri, L.S. and Murray, J.W.: Suboxic trace element geochemistry in eastern tropical North Pacific, Geochim. Cosmochim. Ac., 66, 1139-1158, 2002.

Navarro, M., Sánchez, M., López, H. and López, M.C.: Arsenic contamination levels in waters, soils, and sludges in southeast Spain. Bull. Environ. Contam. Toxicol. 50, 356-362, 1993.

Nelson, A. and Donkin, P.: Processes of bioaccumulation: The importance of chemical speciation, Mar. Pollut. Bull., 16, 164-169, 1985.

Newville, M.: IFEFFIT: Interactive EXAFS analysis and FEFF fitting, J. Synchrotron Radiat., 8, 322-324, 2001.

Ni Dhubughaill, O.M. and Sadler, P.J.: The structure and reactivity of arsenic compounds, Struct. Bond. 78, 129-190, 1991.

Nozaki, Y.: A fresh look at element distribution in the North Pacific, EOS, 78, 221, 1997.

Nriago, J.: Arsenic in the environment. Part II: Human health and ecosystem effects, Wiley-Interscience Publication, New York, 1994.

Nürnberg, D. Bijma, J. and Hemleben, C.: Assessing the reliability of magnesium in foraminiferal calcite as a proxy for water mass temperatures, Geochim. Cosmochim. Ac., 60, 803-814, 1996.

Oliveira, L. and Anita, N.J.: Some observations on the urea-degrading enzyme of the diatom *Cyclotella cryptica* and the role of nickel in its production, J. Plankton Res., 8, 235-242, 1986.

Opdyke, B.N. and Walker, J.C.G.: Return of the coral reef hypothesis: Basin to shelf partitioning of $CaCO_3$ and its effect on atmospheric CO_2, Geology, 20, 733-736, 1992.

Pak, D.K., Lea, D.W. and Kennett, J.P.: Seasonal and interannual variation in Santa Barbara Basin water temperatures observed in sediment trap foraminiferal Mg/Ca, Geochem. Geophy. Geosy., 5, 2004GC000760, 2004.

Panieri, G.: The effect of shallow marine hydrothermal vent activity on benthic foraminifera (Aeolian Arc, Tyrrhenian Sea), J. Foramin. Res., 36, 3-14, 2006.

Pascual, A., Rodriguez-Lazaro, J., Weber, O. and Jouanneau, J.M.: Late Holocene pollution in the Gernika estuary (southern Bay of Biscay) evidenced by study of foraminifera and ostracoda, Hydrobiologia, 475, 477-491, 2002.

Patrick, R.: Effects of trace metals in the aquatic ecosystem, Am. Sci., 66, 185-191, 1978.

Pearce, N.J.G., Perkins, W.T., Westgate, J.A., Gorton, M.P., Jackson, S.E., Neal, C.R. and Chenery, S.P.: A compilation of new and published major and trace element data for NIST SRM 610 and NIST SRM 612 glass reference materials, Geostandard Newslett., 21, 115-144, 1997.

Pérez-Asensio, J.N. and Aguirre, J.: Benthic foraminiferal assemblages in temperate coral-bearing deposits from late Pliocene, J. Foramin. Res., 40, 61-78, 2010.

Peterson, L.C. and Haug, G.H.: Variability in the mean latitude of the Atlantic Intertropical Convergence Zone as recorded by riverine input of sediments to the Cariaco Basin (Venezuela), Palaeogeogr. Palaeocl., 234, 97-113, 2006.

Peterson, L.C., Overpeck, J.T., Kipp, N.G and Imbrie, J.: A high-resolution late Quaternary upwelling record from the anoxic Cariaco Basin, Venezuela, Paleoceanography, 6, 99-119, 1991.

Peterson, L.C., Haug, G.H., Murray, R.W., Yarincik, K.M., King, J.W., Bralower, T.J., Kameo, K., Rutherford, S.D. and Pearce, R.B.: Late Quaternary stratigraphy and sedimentation at Site 1002, Cariaco Basin (Venezuela), in: Leckie, R.M., Sigurdsson, H., Acton, G.D. and Draper, G. (eds.): Proceedings of the Ocean Drilling Program, Scientific Results, 165, 85-99, 2000.

Pilson, M.E.Q.: An introduction to the chemistry of the sea, 2nd edition, Cambridge University Press, Cambridge, New York, Melbourne, Madrid, Cape Town, Singapore, São Paulo, Delhi, Mexico City, 2013.

Piper, D.Z. and Dean, W.E.: Trace-element deposition in the Cariaco Basin under sulphate reducing conditions – a history of the local hydrography and global climate, 20 ka to the present, USGS Professional Paper 1670, 2002.

Pomerol, B.: Geochemistry of the late Cenomanian – early Turonian chalks of the Paris Basin: Manganese and carbon isotopes in carbonates as paleooceanographic indicators, Cretaceous Res., 4, 85-93, 1983.

Prasad, K.S., Subramanian, V. and Paul, J.: Purification and characterization of arsenite oxidase from *Arthrobacter* sp., Biometals 22, 711-721, 2009.

Pratte, B.S. and Thiel, T.: High-affinity vanadate transport system in the cyanobacterium *Anabaena variabilis* ATCC 29413, J. Bacteriol., 188, 464-468, 2006.

Price, R.E. and Pichler, T.: Distribution, speciation and bioavailability of arsenic in a shallow-water submarine hydrothermal system, Tutum Bay, Ambitle Island, PNG. Chem. Geol. 224, 122-135, 2005.

Ravel, B. and Newville, M.: ATHENA, ARTEMIS, HEPHAESTUS: Data analysis for X-ray absorption spectroscopy using IFEFFIT, J. Synchrotron Radiat., 12, 537-541, 2005.

Reeder, R.J., Lamble, G.M., Lee, J.F. and Staudt, W.J.: Mechanism of SeO_4^{2-} substitution in calcite – an XAFS study. Geochim. Cosmochim. Ac. 58, 5639-5646, 1994.

Reichart, G.-J., Jorissen, F., Anschutz, P. and Mason, P.R.D.: Single foraminiferal test chemistry records in the marine environment, Geology, 31, 355-358, 2003.

Renssen, H., Seppä, H., Crosta, X., Goosse, H. and Roche, D.M.: Global characterization of the Holocene Thermal Maximum, Quaternary Sci. Rev., 48, 7-19, 2012.

Rentería-Cano, M.E., Sánchez-Velasco, L., Shumilin, E., Lavín, M.F. and Gómez-Gutiérrez, J.: Major and trace elements in zooplankton from the Northern Gulf of California during summer, Biol. Trace Elem. Res., 142, 848-864, 2011.

Rickaby, R.E.M. and Elderfield, H.: Planktonic foraminiferal Cd/Ca: Paleonutrients or paleotemperature?, Paleoceanography, 14, 293-323, 1999.

Richards, F.A.: Anoxic basins and fjords, in: Chemical oceanography, Volume I, edited by Riley, J.P. and Skirrow, G., Academic Press, London and New York, 611-645, 1965.

Riley, J.P. and Tongudai, M.: The major cation/chlorinity ratios in sea water, Chem. Geol., 2, 263-269, 1967.

Riley, M.R., Boesewetter, D.E., Kim, A.M. and Sirvent, F.P.: Effects of metals Cu, Fe, Ni, V, and Zn on rat lung epithelial cells, Toxicology, 190, 171-184, 2003.

Röttger, R. and Lehmann, G.: Benthic foraminifera, in: Röttger, R., Knight, R. and Foissner, W. (eds.): A course in protozoology, Protozoological Monographs, 4, 111-123, 2009.

Rosenthal, Y., Boyle, E.D. and Slowey, N.: Temperature control on the incorporation of magnesium, strontium, fluorine and cadmium into benthic foraminiferal shells from Little Bahama Bank: Prospects for thermocline paleoceanography, Geochim. Cosmochim. Ac., 61, 3633-3643, 1997.

Russel, A.D., Emerson, S., Mix, A.C. and Peterson, L.C.: The use of foraminiferal uranium/calcium ratios as an indicator of changes in seawater uranium content, Paleoceanography, 11, 649-663, 1996.

Russell, A.D., Emerson, S., Nelson, B.K., Erez, J. and Lea, D.W.: Uranium in foraminiferal calcite as a recorder of seawater uranium concentrations, Geochim. Cosmochim. Ac., 58, 671-681, 1994.

Salami, M.B.: Biology of *Trochammina* cf. *T. Quadriloba* Högland (1947), an agglutinating foraminifer, J. Foramin. Res., 6, 142-153, 1976.

Sanyal, A. and Bijma, J.: A comparative study of the northwest Africa and eastern equatorial Pacific upwelling zones as sources of CO_2 during glacial periods based on boron isotope paleo-pH estimation, Paleoceanography, 14, 753-759, 1999.

Sanyal, A., Bijma, J., Spero, H. and Lea, D.W.: Empirical relationship between pH and the boron isotope isotopic composition of *Globigerinoides sacculifer*: Implications for the boron isotope paleo-pH proxy, Paleoceanography, 16, 515-519, 2001.

Sanyal, A., Hemming, N.G., Broecker, W.S., Lea, D.W., Spero, H.J. and Hanson, G.N.: Oceanic pH control on the boron isotopic composition of foraminifera: Evidence from culture experiments, Paleoceanography, 11, 513-517, 1996.

Sarmiento, J.L., Herbert, T.D. and Toggweiler, J.R.: Causes of anoxia in the world ocean, Global Biogeochem. Cy., 2, 115-128,1988.

Schlanger, S.O.: Strontium storage and release during deposition and diagenesis of marine carbonates release to sea-level variations, in: Lerman, A. and Meyreck, M. (eds.): Physical and chemical weathering in geochemical cycles, NATO Adv. Sci. I. C-Mat., D. Reidel Publishing Co., Dordrecht-Boston, 323-339, 1988.

Schnitker, D.: Ecotypic variation in *Ammonia beccarii* (Linné), J. Foramin. Res., 4, 217-223, 1974.

Schubert, C.: Origin of Cariaco Basin, southern Caribbean Sea, Mar. Geol., 47, 345-360, 1982.

Schulte, P., Speijer, R., Mai, H. and Kontny, A.: The Cretaceous-Palaeogene (K-P) boundary at Brazos, Texas: Sequence stratigraphy, depositional events and the Chicxulub impact, Sediment. Geol., 184, 77-109, 2006.

Schwenzer, S.P., Tommaseo, C.E., Kersten, M. and Kirnbauer, T.: Speciation and oxidation kinetics of arsenic in the thermal springs of Wiesbaden spa, Germany, Fresen. J. Anal. Chem. 371, 927-933, 2001.

Scranton, M.I., Sayles, F.L., Bacon, M.P. and Brewer, P.G.: Temporal changes in the hydrography and chemistry of the Cariaco Trench, Deep-Sea Res., 34, 945-963, 1987.

Scudlark, J.R. and Johnson, D.L.: Biological oxidation of arsenite in sea-water, Estar. Coast. Shelf S., 14, 693-706, 1982.

Sen Gupta, B.K.: Introduction to modern foraminifera, in: Sen Gupta, B.K. (ed.): Modern foraminifera, Kluwer Academic Publishers, 3-6, 1999.

Sigurdsson, H., Leckie, R.M., Acton, G.D., Abrams, L.J., Bralower, T.J., Carey, S.N., Chaisson, W.P., Cotillon, P., Cunningham, A.D., D'Hondt, S.L., Droxler, A.W., Galbrun, B., Gonzalez, J., Haug, G., Kameo, K., King, J., Lind, I.L., Louvel, V., Lyons, T.W., Murray, R.W., Mutti, M., Myers, G., Pearce, R.B., Pearson, D.G., Peterson, L.C. and Röhl, U.: Proceedings of the Ocean Drilling Program, Initial Reports, 165, 359-373, 1997.

Silver, S. and Phung, L.T.: Genes and enzymes involved in bacterial oxidation and reduction of inorganic arsenic, Appl. Environ. Microb. 71, 599-608, 2005.

Skulan, J., de Paolo, D.J. and Owens, T.L.: Biological control of calcium isotopic abundances in the global carbon cycle, Geochim. Cosmochim. Ac., 61, 2505-2510, 1997.

Smit, J., Montanari, A., Swinburne, N.H.M., Alvarez, W., Hildebrand, A.R., Margolis, S.V., Claeys, P., Lowrie, W. and Asaro, F.: Tektite-bearing, deep-water clastic unit at the Cretaceous-Tertiary Boundary in northeastern Mexico. Geology 20: 99-103, 1992.

Solé, V.A., Papillon, E., Cotte, M., Walter, P. and Susini, J.: A multiplatform code for the analysis of energy-dispersive X-ray fluorescence spectra, Spectrochim. Acta B, 62, 63-68, 2007.

Spero, H.J. and Lea, D.W.: Intraspecific stable-isotope variability in the planktic foraminifera *Globigerinoides-sacculifer* – results from laboratory experiments, Mar. Micropaleontol., 22, 221-234, 1993.

Spero, H.J., Bijma, J., Lea, D.W. and Bemis, B.E.: Effect of seawater carbonate concentration on foraminiferal carbon and oxygen isotopes, Nature, 390, 497-500, 1997.

Stoll, H.M. and Schrag, D.P.: Evidence for glacial control of rapid sea level changes in early Cretaceous, Science, 272, 1771-1774, 1996.

Stolz, J.E., Basu, P., Santini, J.M. and Oremland, R.S.: Arsenic and selenium in microbial metabolism, Annu. Rev. Microbiol. 60, 107-130, 2006.

Stouff, V., Lesourd, M. and Debenay, J.-P.: Laboratory observations on asexual reproduction (schizogony) and ontogeny of *Ammonia tepida* with comments on the life cycle, J. Foramin. Res., 29, 75-84, 1999.

Stoyan, D., Stoyan, H. and Jansen, U.: Umweltstatistik – Statistische Verarbeitung und Analyse von Umweltdaten, Teubner Verlag, Stuttgart, Leipzig, 1997.

Sunda, W.G.: Trace metal interactions with marine phytoplankton, Biol. Oceanogr., 6, 411-442, 1988-1989.

Sunda, W.G. and Huntsman, S.A.: Effect of competitive interactions between manganese and copper on cellular manganese and growth in estuarine and oceanic species of the diatom *Thalassiosira*, Limnol. Oceanogr., 28, 924-934, 1983.

Sunda, W.G. and Huntsman, S.A.: Antagonisms between cadmium and zinc toxicity and manganese limitation in a coastal diatom, Limnol. Oceanogr., 41, 373-387, 1996.

Sunda, W.G. and Huntsman, S.A.: Processes regulating cellular metal accumulation and physiological effects: Phytoplankton as model systems, Sci. Total Environ., 219, 165-181, 1998a.

Sunda, W.G. and Huntsman, S.A.: Interactions among Cu^{2+}, Zn^{2+}, an Mn^{2+} in controlling cellular Mn, Zn, and growth rate in the coastal alga *Chlamydomonas*, Limnol. Oceanogr., 43, 1055-1064, 1998b.

Syrett, P.J. and Peplinska, A.M.: The effect of nickel and nitrogen deprivation on the metabolism of urea by the diatom *Phaedactylum tricornutum*, Eur. J. Phycol., 23, 387-390, 1988.

ten Brink, H.B., Schoemaker, H.E. and Wever, R.: Sulfoxidation mechanism of vanadium from Ascophyllum nodosum, Eur. J. Biochem., 268, 132-138, 2001.

Thomson, J., Higgs, N.C., Jarvis, I., Hydes, D.J., Colley, S. and Wilson, T.R.S.: The behaviour of manganese in Atlantic carbonate sediments, Geochim. Cosmochim. Ac., 50, 1807-1818, 1986.

Toyofuku, T., Kitazato, H., Kawahata, H., Tsuchiya, M. and Nohara, M.: Evaluation of Mg/Ca thermometry in foraminifera: Comparison of experimental results and measurements in nature, Paleoceanography, 15, 456-464, 2000.

Toyofuku, T. and Kitazato, H.: Micromapping of Mg/Ca values in cultured specimens of the high-magnesium benthic foraminifera, Geochem. Geophy. Geosy., 6, Q11P05, 2005.

Trefry, J.H. and Metz, S.: Role of hydrothermal precipitates in geochemical cycling of vanadium, Nature, 342, 531-533, 1989.

Trefry, J.H., Butterfield, D.B., Metz, S., Massoth, G.J., Trocine, R.P. and Feely, R.A.: Trace-metals in hydrothermal solutions from Cleft segment on the southern Juan de Fuca Ridge, J. Geophys. Res.-Sol. Ea., 99, 4925-4935, 1994.

Tribovillard, N., Algeo, T.J., Lyons, T. and Riboulleau, A.: Trace metals as paleoredox and paleoproductivity proxies: An update, Chem. Geol., 232, 12-32, 2006.

Turekian, K.K.: Oceans, 2nd edition, Prentice-Hall, Englewood Cliffs, New Jersey, 1976.

Uppström, L.R.: The boron/chlorinity ratio of deep-sea water from the Pacific Ocean, Deep-Sea Res., 21, 161-162, 1974.

Urey, H.C.: The thermodynamic properties of isotopic substances, J. Chem. Soc., 562-581, 1947.

Valenzuela, C., Campos, V.L., Yañez, J., Zaror, C.A. and Mondaca, M.A.: Isolation of arsenite-oxidizing bacteria from arsenic-enriched sediments from Camarones River, Northern Chile, B. Environ. Contam. Tox. 82, 593-596, 2009.

Varnavas, S.P. and Cronan, D.S.: Arsenic, antimony and bismuth in sediments and waters from the Santorini hydrothermal field, Greece. Chem. Geol. 67, 295-305, 1988.

Veizer, J., Demovic, R. and Turan, J.: Possible use of strontium in sedimentary carbonate rocks as a paleoenvironmental indicator, Sediment. Geol., 5, 5-22, 1971.

Vilela, C.G., Batista, D.S., Baptista-Neto, J.A., Crapez, M. and McAllister, J.J.: Benthic foraminifera distribution in high polluted sediments from Niterói Harbor (Guanabara Bay), Rio de Janeiro, Brazil, An. Acad. Bras. Ciênc., 76, 161-171, 2004.

van der Zwaan, G.J., Duijnstee, I.A.P., den Dulk, M, Ernst, S.R., Jannink, N.T. and Kouwenhoven, T.J.: Benthic foraminifera: Proxies or problems? A review of paleoecological concepts, Earth Sci. Rev., 46, 213-236, 1999.

von Damm, K.L., Edmond, J.M., Grant, B., Measures, C.I., Walden, B. and Weiss, R.F.: Chemistry of submarine hydrothermal solutions at 21°N, East Pacific Rise, Geochim. Cosmochim. Ac., 49, 2197-2220, 1985.

von Damm, K.L.: Seafloor hydrothermal activity: Black smoker chemistry and chimneys. Ann. Rev. Earth Planet. Sci. 18, 173-204, 1990.

von Damm, K.L.: Chemistry of hydrothermal vent fluids from 9°-10°N, East Pacific Rise: "Time zero," the immediate posteruptive period, J. Geophys. Res.-Sol. Ea., 105, 11203-11222, 2000.

Ward, J.H.: Hierarchical grouping to optimize an objective function, J. Am. Stat. Assoc., 58, 236-244, 1963.

Wefer, G., Berger, W.H., Bijma, J. and Fischer, G.: Clues to ocean history: A brief overview of proxies, in: Use of proxies in paleoceanography, edited by Fischer, G. and Wefer, G., Springer, Berlin, Heidelberg, New York, Barcelona, Hong Kong, London, Milan, Paris, Singapore, Tokyo, 1-68, 1999.

Wilhelm, C. and Wild, A.: The variability of the photosynthetic unit in *Chlorella* – I. The effect of vanadium on photosynthesis, productivity, P-700 and Cytochrome f in undiluted and homocontinuous cultures of *Chlorella*, J. Plant. Physiol., 115, 115-124, 1984.

Wilson, T.R.S.: Salinity and the major elements of sea water, in: Chemical oceanography 2nd edition, volume 1, edited by Riley, J.P. and G. Skirrow, Academic Press, New York, 365-413, 1975.

Wilson-Finelli, A., Chandler, G.T., and Spero, H.J.: Stable isotope behaviour in paleoceanographically important benthic foraminifera: Results from microcosm culture experiments, J. Foramin. Res., 28, 312-320, 1998.

Yancey, T. E.: Stratigraphy and depositional environment of the Cretaceous-Tertiary boundary complex and basal Paleocene section, Brazos River, Texas,

Transactions of the Gulf Coast Association of Geological Societies, 64, 433-442, 1996.

Yanko, V., Ahmad, M. and Kaminski, M.: Morphological deformities of benthic foraminiferal tests in response to pollution by heavy metals: Implications for pollution monitoring, J. Foramin. Res., 28, 177-200, 1998.

Yu, J., Elderfield, H. and Hönisch, B.: B/Ca in planktonic foraminifera as a proxy for surface seawater pH, Paleoceanography, 22, PA2202, 2007.

Zahn, R. and Mix, A.C.: Benthic foraminiferal $\delta^{18}O$ in the ocean's temperature-salinity-density field: Constraints on ice age thermohaline circulation, Paleoceanography, 6, 1-20, 1991.

Zhang, J.-Z. and Millero, F.J.: The chemistry of the anoxic waters of the Cariaco Trench, Deep-Sea Res. Pt. I, 40, 1023-1041, 1993.

Zhou, D.: Robust statistics and geochemical data analysis, Math. Geol., 19, 207-218, 1987.

Zhu, P. and MacDougall, J.D.: Calcium isotopes in the marine environment and the oceanic calcium cycle, Geochim. Cosmochim. Ac., 62, 1691-1698, 1998.

Appendix

Appendix A: Culture solutions data

Table A1: Culture solution chemistry from the reference tank

Day	Ca [mg/L]	V [µg/L]	Cr [µg/L]	Mn [µg/L]	Co [µg/L]	Ni [µg/L]	Cu [µg/L]	As [µg/L]	Mo [µg/L]
1	414	2.18	0.38	2.34	1.00	2.26	13.9	15.0	12.9
8	412	2.15	0.66	4.20	0.95	4.90	17.9	7.15	8.94
14	424	1.62	0.49	6.77	0.79	4.83	13.6	5.90	5.15
21	410	1.75	0.45	7.58	0.84	3.77	12.4	6.44	9.37
28	409	1.62	0.35	1.44	0.68	2.98	12.7	4.53	8.35
34	412	1.83	0.58	1.90	0.85	5.46	14.0	5.21	10.5
41	417	1.64	0.90	1.93	0.79	3.28	11.4	3.55	9.07
48	413	1.64	0.66	2.12	0.74	3.08	11.5	3.53	8.03
54	415	1.90	0.68	2.10	0.74	11.2	12.3	4.52	9.22
61	418	1.78	0.72	2.64	0.72	3.84	18.6	3.62	8.22
68	409	1.78	0.72	1.68	0.74	4.56	15.5	4.26	8.66
74	417	1.84	0.54	1.30	0.66	9.12	13.3	3.30	8.20
82	414	1.84	0.86	2.08	0.72	3.44	12.7	3.74	8.64

Table A2: Culture solution chemistry from the tank with the 5-fold concentration of Batch I experiment

Day	Ca [mg/L]	V [µg/L]	Cr [µg/L]	Mn [µg/L]	Co [µg/L]	Ni [µg/L]	Cu [µg/L]	As [µg/L]	Mo [µg/L]
1	413	2.12	0.38	4.16	3.82	8.16	54.1	8.14	11.4
8	418	2.03	0.73	6.16	3.97	11.7	59.0	7.87	7.74
14	425	1.64	0.45	7.93	3.43	9.77	48.6	5.04	6.84
21	425	1.77	0.39	8.22	3.50	15.1	52.1	4.89	9.14
28	408	1.64	0.50	4.42	3.88	25.8	109	4.17	8.07
34	420	1.72	0.75	4.62	4.31	13.8	66.6	4.64	10.2
41	416	1.58	0.64	4.62	4.20	13.0	61.5	3.15	8.57
48	412	1.57	0.63	3.96	4.06	11.7	68.5	3.41	7.98
54	415	1.94	0.96	2.72	4.14	14.1	63.5	3.98	9.68
61	423	1.84	1.00	5.08	4.44	14.0	67.1	3.64	8.52
68	419	1.96	0.58	3.24	4.22	13.3	63.9	4.32	8.24
74	419	1.82	0.56	1.76	3.86	12.7	59.5	3.46	8.40
82	414	1.96	1.00	4.56	3.90	13.4	61.9	4.32	8.64

Table A3: Culture solution chemistry from the tank with the 10-fold concentration of Batch I experiment

Day	Ca [mg/L]	V [µg/L]	Cr [µg/L]	Mn [µg/L]	Co [µg/L]	Ni [µg/L]	Cu [µg/L]	As [µg/L]	Mo [µg/L]
1	412	1.98	0.28	6.64	6.94	15.6	104	10.3	9.96
8	411	1.82	0.53	8.42	6.48	19.2	99.9	6.49	7.49
14	411	1.67	0.49	9.98	6.58	18.6	94.3	4.98	7.25
21	402	1.74	0.50	7.27	6.75	18.7	89.0	4.65	9.55
28	414	1.71	0.55	7.52	7.63	23.8	114	6.45	8.45
34	407	1.75	0.97	6.92	7.92	23.3	113	4.18	9.74
41	409	1.76	0.74	6.24	7.65	22.0	111	3.38	8.53
48	413	1.64	0.61	4.24	7.86	21.7	107	3.49	8.19
54	416	2.06	0.62	2.36	6.84	21.5	102	4.10	10.3
61	414	1.70	0.58	9.42	7.94	23.4	123	3.62	8.54
68	417	1.80	0.94	4.84	7.96	27.3	121	4.12	8.40
74	416	1.84	0.64	2.12	6.84	23.5	110	3.36	8.22
82	415	2.04	1.16	4.78	6.52	24.1	109	3.88	8.70

Table A4: Culture solution chemistry from the tank with the 20-fold concentration of Batch I experiment

Day	Ca [mg/L]	V [µg/L]	Cr [µg/L]	Mn [µg/L]	Co [µg/L]	Ni [µg/L]	Cu [µg/L]	As [µg/L]	Mo [µg/L]
1	410	1.84	0.28	11.9	12.8	29.8	193	8.62	8.26
8	419	1.84	0.38	12.7	12.8	29.2	199	5.73	7.09
14	416	1.92	0.45	13.6	12.5	30.1	190	4.18	7.28
21	414	1.76	0.37	11.4	11.7	28.6	171	4.79	9.24
28	417	1.73	0.61	14.4	14.7	43.2	221	3.87	8.35
34	415	1.75	0.69	12.1	14.6	39.8	221	4.27	9.00
41	412	1.68	0.95	11.6	14.6	41.4	220	2.79	8.32
48	410	1.83	0.74	7.88	15.0	39.8	208	3.44	8.83
54	414	2.08	0.62	5.22	13.6	41.6	218	4.48	9.36
61	419	1.90	0.54	16.8	15.7	42.7	232	3.58	8.42
68	405	1.94	0.60	13.5	15.1	43.0	221	3.70	8.34
74	423	1.92	0.72	10.2	14.7	43.1	212	3.94	8.44
82	415	1.96	0.76	8.14	14.4	43.1	211	3.84	8.48

Table A5: Culture solution chemistry from the tank with the 5-fold concentration of Batch II experiment

Day	Ca [mg/L]	V [µg/L]	Cr [µg/L]	Mn [µg/L]	Co [µg/L]	Ni [µg/L]	Cu [µg/L]	As [µg/L]	Mo [µg/L]
1	416	17.8	0.64	0.24	0.78	1.54	10.3	37.6	106
8	412	18.5	1.00	2.42	0.78	2.84	16.1	20.6	70.0
14	419	16.7	1.32	3.18	0.76	2.50	14.0	20.0	68.9
21	417	16.8	0.86	1.36	0.78	2.62	12.8	18.2	70.1
28	410	17.3	2.28	1.14	0.74	2.64	13.8	20.5	67.3
34	412	16.7	1.32	2.09	0.83	3.76	12.7	22.4	70.6
41	413	16.3	1.78	1.99	0.75	4.46	12.6	19.7	76.1
48	414	15.8	1.18	2.05	0.73	4.22	11.1	20.9	72.0
54	415	16.0	0.90	1.50	0.68	2.26	9.80	21.0	74.6
61	413	16.1	1.82	1.36	0.64	2.04	12.9	23.2	70.2
68	414	17.9	1.50	1.50	0.74	2.52	12.6	23.1	75.1
74	410	17.4	1.28	1.28	0.70	2.42	11.4	20.3	74.2
82	410	16.2	1.16	1.10	0.56	2.97	11.0	20.4	69.4

Table A6: Culture solution chemistry from the tank with the 10-fold concentration of Batch II experiment

Day	Ca [mg/L]	V [µg/L]	Cr [µg/L]	Mn [µg/L]	Co [µg/L]	Ni [µg/L]	Cu [µg/L]	As [µg/L]	Mo [µg/L]
1	414	33.9	1.30	0.42	0.74	1.46	10.5	50.0	205
8	413	32.6	1.18	2.56	0.74	3.26	13.7	34.2	126
14	415	30.5	1.25	3.45	0.75	2.80	12.9	34.4	130
21	418	29.2	1.16	1.76	0.66	3.04	11.5	33.2	133.4
28	414	32.9	3.32	1.18	0.73	2.89	10.9	36.6	127
34	423	30.5	1.51	1.45	0.76	3.08	11.2	36.4	134
41	420	30.2	1.71	1.39	0.72	11.9	31.3	36.8	138
48	412	30.8	1.61	1.94	0.70	21.9	17.2	38.0	145
54	411	31.8	1.40	1.42	0.76	2.16	10.5	38.5	141
61	417	34.2	3.12	1.74	0.68	2.20	13.9	41.9	141
68	407	31.7	1.82	1.86	0.68	2.16	11.5	40.8	135
74	416	30.5	1.86	1.62	0.66	2.42	11.3	38.6	141
82	415	30.2	2.04	1.66	0.62	2.14	10.1	39.2	135

Table A7: Culture solution chemistry from the tank with the 20-fold concentration of Batch II experiment

Day	Ca [mg/L]	V [µg/L]	Cr [µg/L]	Mn [µg/L]	Co [µg/L]	Ni [µg/L]	Cu [µg/L]	As [µg/L]	Mo [µg/L]
1	412	61.9	1.98	0.34	0.70	1.50	9.42	83.5	380
8	408	58.5	1.51	2.95	0.71	2.40	12.1	63.8	240
14	417	58.1	1.52	5.42	0.76	6.13	12.9	60.1	244
21	411	57.4	1.43	5.91	0.72	3.46	11.2	61.1	256
28	416	61.9	2.15	1.60	0.70	6.38	15.0	72.3	265
34	421	60.2	2.14	1.59	0.70	17.4	14.9	70.8	262
41	414	61.5	2.16	1.96	0.70	22.1	14.7	68.0	272
48	413	60.7	2.81	7.67	1.01	9.56	13.2	70.0	277
54	420	59.0	1.78	2.20	0.74	5.76	10.7	70.7	249
61	417	63.1	4.30	1.88	0.64	8.72	13.5	76.2	257
68	419	61.9	2.92	2.50	0.70	2.02	10.6	75.6	259
74	412	63.1	2.76	1.50	0.68	2.56	10.7	76.1	260
82	414	60.4	2.62	1.66	0.64	2.20	10.1	79.0	250

Table A8: pH and salinity of the culture solution from the reference tank

	Salinity			Salinity			Salinity	
Day	[psu]	pH	Day	[psu]	pH	Day	[psu]	pH
1	23.9	8.03	23	24.0	8.08	54	24.0	7.80
2	23.9	8.04	26	24.0	8.10	56	24.0	8.04
5	23.9	7.94	28	24.1	8.11	58	23.9	8.04
6	23.9	7.94	29	24.1	8.04	61	23.9	8.00
7	24.0	7.98	30	23.8	8.09	63	23.9	8.04
8	23.9	8.00	33	23.8	8.03	65	23.9	8.02
9	24.0	8.02	35	23.9	8.00	68	23.9	8.03
12	23.9	8.00	37	23.9	7.99	70	23.9	8.02
13	24.0	8.04	40	23.9	7.97	72	24.0	8.01
14	24.0	8.01	42	23.9	7.96	75	24.0	8.04
15	24.0	8.01	44	24.0	7.99	77	24.1	8.06
16	24.0	8.01	47	23.9	7.94	79	24.1	8.00
19	24.0	8.07	49	24.0	7.90	82	24.1	8.05
21	24.0	8.10	51	24.0	7.86			

Table A9: pH and salinity of the culture solution from the tank with the 5-fold sea water concentration of Batch I experiment

	Salinity			Salinity			Salinity	
Day	[psu]	pH	Day	[psu]	pH	Day	[psu]	pH
1	23.9	8.16	23	24.0	8.05	54	24.0	7.95
2	23.9	8.17	26	24.0	8.08	56	23.9	8.07
5	23.9	8.06	28	24.0	8.09	58	24.0	8.02
6	23.9	8.00	29	24.1	8.02	61	24.0	7.96
7	24.0	7.98	30	23.9	8.09	63	24.0	7.98
8	24.0	8.05	33	23.9	8.05	65	24.0	7.95
9	24.0	8.04	35	24.0	8.06	68	24.0	7.89
12	24.0	8.03	37	24.0	8.06	70	24.0	7.87
13	24.0	8.04	40	24.0	8.04	72	24.0	7.84
14	24.0	8.03	42	24.0	8.04	75	24.0	7.88
15	24.0	8.00	44	24.0	8.05	77	24.0	7.88
16	24.0	8.01	47	24.0	8.02	79	24.0	7.87
19	24.0	8.04	49	24.0	8.01	82	24.0	7.86
21	24.0	8.06	51	24.0	7.96			

Table A10: pH and salinity of the culture solution from the tank with the 10-fold sea water concentration of Batch I experiment

	Salinity			Salinity			Salinity	
Day	[psu]	pH	Day	[psu]	pH	Day	[psu]	pH
1	23.9	8.17	23	24.0	8.08	54	24.0	7.75
2	23.9	8.16	26	24.1	8.08	56	24.0	8.07
5	23.9	8.06	28	24.0	8.10	58	24.0	8.05
6	23.9	8.01	29	24.1	8.02	61	23.9	8.02
7	24.0	7.99	30	23.9	8.07	63	23.9	8.01
8	24.0	8.04	33	24.0	8.01	65	23.9	7.98
9	24.0	8.03	35	24.0	7.93	68	23.9	7.95
12	23.9	8.02	37	24.0	7.88	70	24.0	7.95
13	24.0	8.04	40	24.0	7.93	72	24.0	7.99
14	24.0	8.04	42	24.0	7.92	75	24.0	8.05
15	24.0	8.04	44	24.0	7.92	77	24.0	8.03
16	24.1	8.03	47	24.0	7.84	79	24.0	7.96
19	24.0	8.05	49	24.0	7.80	82	24.0	8.00
21	24.0	8.07	51	24.0	7.77			

Table A11: pH and salinity of the culture solution from the tank with the 20-fold sea water concentration of Batch I experiment

	Salinity			Salinity			Salinity	
Day	[psu]	pH	Day	[psu]	pH	Day	[psu]	pH
1	23.9	8.18	23	24.1	8.06	54	24.0	7.99
2	23.9	8.14	26	24.1	8.08	56	24.0	8.09
5	24.0	8.05	28	24.1	8.09	58	23.9	8.05
6	24.0	8.01	29	24.1	8.03	61	24.0	8.01
7	24.0	7.99	30	23.9	8.10	63	24.0	8.02
8	24.0	8.05	33	23.9	8.04	65	24.0	7.99
9	24.0	8.05	35	23.9	7.99	68	24.0	8.00
12	24.0	8.05	37	24.0	7.99	70	24.0	7.97
13	24.0	8.07	40	24.0	7.96	72	24.1	8.03
14	24.0	8.05	42	24.0	7.96	75	24.0	7.98
15	24.0	8.04	44	24.0	7.99	77	24.1	7.98
16	24.1	8.08	47	24.0	7.97	79	24.1	7.96
19	24.0	8.05	49	24.0	7.93	82	24.0	8.00
21	24.0	8.07	51	24.0	7.85			

Table A12: pH and salinity of the culture solution from the tank with the 5-fold sea water concentration of Batch II experiment

	Salinity			Salinity			Salinity	
Day	[psu]	pH	Day	[psu]	pH	Day	[psu]	pH
1	23.9	8.05	23	24.0	7.97	54	24.1	7.94
2	23.9	8.03	26	24.0	8.04	56	24.0	8.05
5	23.9	7.89	28	24.0	8.10	58	23.9	7.96
6	24.0	7.81	29	24.1	8.01	61	23.9	7.88
7	24.0	7.83	30	23.9	8.09	63	23.9	7.85
8	23.9	7.87	33	24.0	8.04	65	24.0	7.79
9	23.9	7.88	35	24.0	8.03	68	24.0	7.72
12	24.0	7.94	37	24.0	8.02	70	24.0	7.70
13	24.0	7.98	40	24.0	8.02	72	24.0	7.84
14	24.0	7.99	42	24.0	7.99	75	24.2	8.09
15	24.0	7.99	44	24.0	7.96	77	24.2	8.07
16	24.0	7.99	47	24.1	7.92	79	24.1	8.05
19	24.0	7.97	49	24.1	7.88	82	24.0	8.05
21	24.0	7.96	51	24.0	7.89			

Table A13: pH and salinity of the culture solution from the tank with the 10-fold sea water concentration of Batch II experiment

	Salinity			Salinity			Salinity	
Day	**[psu]**	**pH**	**Day**	**[psu]**	**pH**	**Day**	**[psu]**	**pH**
1	23.9	8.12	23	24.1	8.09	54	24.1	8.03
2	23.9	8.10	26	24.1	8.08	56	24.0	8.11
5	24.0	7.99	28	24.1	8.11	58	24.0	8.07
6	24.0	7.90	29	24.1	8.03	61	24.0	8.02
7	24.0	7.90	30	24.0	8.11	63	24.0	8.01
8	24.0	7.96	33	24.0	8.03	65	24.0	7.94
9	24.0	7.97	35	24.0	8.02	68	24.0	7.84
12	24.0	8.01	37	24.0	8.04	70	24.0	7.80
13	24.0	8.03	40	24.0	8.05	72	24.0	7.87
14	24.0	8.03	42	24.0	8.03	75	24.0	7.98
15	24.0	8.04	44	24.0	8.05	77	24.1	7.98
16	24.1	8.06	47	24.1	8.05	79	24.1	7.96
19	24.0	8.05	49	24.0	8.02	82	24.0	8.00
21	24.1	8.08	51	24.0	8.01			

Table A14: pH and salinity of the culture solution from the tank with the 20-fold sea water concentration of Batch II experiment

	Salinity			Salinity			Salinity	
Day	**[psu]**	**pH**	**Day**	**[psu]**	**pH**	**Day**	**[psu]**	**pH**
1	23.9	8.14	23	24.1	8.07	54	24.2	7.75
2	23.9	8.15	26	24.1	8.09	56	24.0	8.11
5	24.0	8.05	28	24.1	8.10	58	24.0	8.05
6	24.0	7.96	29	24.2	8.05	61	24.0	*8.12*
7	24.0	7.96	30	24.1	8.14	63	24.0	8.01
8	24.0	7.99	33	24.1	8.04	65	24.0	8.01
9	24.0	7.99	35	24.1	8.01	68	24.0	7.97
12	24.0	7.99	37	24.1	8.00	70	24.0	8.01
13	24.0	7.98	40	24.1	8.03	72	24.1	8.00
14	24.0	7.98	42	24.1	8.00	75	24.0	8.04
15	24.0	8.00	44	24.2	7.97	77	24.0	8.02
16	24.1	8.02	47	24.2	7.93	79	24.1	7.98
19	24.1	8.04	49	24.2	7.85	82	24.1	7.99
21	24.1	8.06	51	24.2	7.80			

Appendix B: Measurements of foramineral calcite of *Ammonia tepida*

Table B1: Selected Ca-normalised trace element data of newly formed chambers from *Ammonia tepida* (reference tank) measured by means of µ-synchrotron XRF expressed as µmol/mol

Sample	Ni	Cu	Mn	V	As
A1 0	1.13	4.90	23.6	1.15	0.47
A1 1	3.14	6.83	21.8	1.24	0.23
A1 2	0.16	4.15	25.2	0.74	0.72
A1 3	0.95	3.81	11.0	0.78	0.49
A7 0	2.68	1.34	14.9	0.57	0.43
A7 1	3.30	5.45	32.4	0.37	1.82
A7 2	3.50	3.78	109	0.36	0.45
A7 3	1.55	2.85	219	0.56	0.63
A14 0	0.06	1.94	556	0.52	0.38
A14 1	2.12	1.56	237	0.72	0.06
A14 2	0.04	1.87	370	0.85	0.13
A14 3	0.35	1.53	195	0.54	0.36
A14 4	3.14	6.92	239	0.56	0.42
A20 0	0.28	2.37	31.2	0.57	0.14
A20 1	4.26	4.77	50.7	0.54	0.77
A20 2	0.23	0.68	19.5	0.58	0.19
A20 3	1.45	4.80	72.8	1.30	0.30
A20 4	4.45	2.60	106	0.36	0.71
A26 0	8.02	2.94	55.1	0.38	0.35
A26 1	5.19	5.37	17.2	0.55	0.17
A26 2	0.12	7.13	17.6	0.38	0.90
A26 3	0.62	2.03	62.8	0.93	0.00
A26 4	1.86	0.03	61.2	0.59	0.11

Table B2: Ca-normalised trace element data of newly formed chambers from *Ammonia tepida* (5-fold concentration tank; Batch I experiment) measured by means of µ-synchrotron XRF expressed as µmol/mol

Sample	Ni	Cu	Mn
B2-0	37.6	6.94	22.5
B2-1	9.53	2.28	13.7
B2-2	29.0	8.09	24.0
B9-0	9.10	8.10	7.84
B9-1	11.2	12.0	29.8
B9-2	11.3	19.9	11.6
B9-3	7.28	18.6	15.6
B9-4	10.3	20.5	25.4
B9-5	7.24	18.9	17.3
B18-0	0.10	4.26	143
B18-1	1.69	4.22	143
B18-2	3.17	5.54	53.6
B18-3	13.2	11.9	28.7
B18-4	6.29	6.79	72.4
B18-5	6.41	9.78	37.1
B27-0	50.4	9.55	22.7
B27-1	56.6	10.8	22.8
B27-2	119	18.7	26.8
B27-3	74.9	15.6	17.0
B27-4	98.0	18.4	27.2
B27-5	83.7	8.85	27.8
B35-0	18.9	5.01	6.65
B35-1	21.3	8.53	19.4
B35-2	20.2	3.17	16.9
B35-3	31.8	7.15	12.6
B35-4	29.0	5.68	11.6
B35-5	12.6	3.77	5.83

Table B3: Ca-normalised trace element data of newly formed chambers from *Ammonia tepida* (10-fold concentration tank; Batch I experiment) measured by means of µ-synchrotron XRF expressed as µmol/mol

Sample	Ni	Cu	Mn
C6-0	64.4	16.8	250
C6-1	62.8	20.2	229
C6-2	114	41.7	53.4
C6-3	122	45.1	31.7
C9-0	22.8	13.7	128
C9-1	53.7	26.5	65.7
C9-2	208	171	194
C11-0	47.1	31.9	123
C11-1	71.4	56.6	146
C11-2	45.8	36.8	120
C11-3	57.3	46.6	133
C11-4	48.7	46.9	71.8
C11-5	44.0	35.7	70.6
C12-0	277	164	21.5
C12-1	267	171	23.1
C12-2	143	98.9	22.8
C17-0	165	42.1	24.9
C17-1	108	27.4	22.5
C17-2	153	44.1	26.7

Table B4: Ca-normalised trace element data of newly formed chambers from *Ammonia tepida* (20-fold concentration tank; Batch I experiment) measured by means of µ-synchrotron XRF expressed as µmol/mol

Sample	Ni	Cu	Mn
D1-0	3.07	25.2	1281
D1-1	0.43	24.4	1072
D1-2	9.53	84.5	587
D2-0	59.9	59.8	22.7
D2-1	25.8	23.5	24.9
D2-2	26.6	26.0	25.1
D13-0	23.6	50.1	61.8
D13-1	11.0	47.9	55.7
D13-2	12.1	40.3	37.1
D19-0	25.0	37.0	59.0
D19-1	64.5	102	62.7
D19-2	93.9	152	66.4
D25-0	13.2	34.1	266
D25-1	2.48	15.5	306
D25-2	3.90	17.2	240
D25-3	15.1	43.8	242

Table B5: Ca-normalised trace element data of newly formed chambers from *Ammonia tepida* (5-fold concentration tank; Batch II experiment) measured by means of µ-synchrotron XRF expressed as µmol/mol

Sample	V	As
E1-0	0.42	0.10
E1-1	0.83	0.87
E1-2	0.90	0.71
E5-0	1.84	2.62
E5-1	0.35	6.38
E5-2	0.64	1.58
E8-0	1.04	0.45
E8-1	0.80	1.37
E8-2	0.73	0.27
E8-3	0.41	0.75
E8-4	0.40	1.07
E8-5	0.94	0.73
E36-0	0.43	0.07
E36-1	0.41	0.36
E36-2	0.52	1.39
E36-3	0.37	0.73
E36-4	0.76	0.89
E36-5	1.63	3.16
E38-0	0.39	1.08
E38-1	0.38	1.17
E38-2	1.52	1.04
E38-3	0.64	1.21
E38-4	0.58	0.72
E38-5	0.43	0.79

Table B6: Ca-normalised trace element data of newly formed chambers from *Ammonia tepida* (10-fold concentration tank; Batch II experiment) measured by means of µ-synchrotron XRF expressed as µmol/mol

Sample	V	As
F3-0	1.36	3.13
F3-1	0.83	9.13
F3-2	3.11	5.73
F3-3	0.38	5.21
F3-4	0.61	8.64
F3-5	0.58	10.9
F10-0	0.58	1.00
F10-1	4.08	0.64
F10-2	0.38	3.43
F16-0	0.55	0.15
F16-1	0.19	2.41
F16-2	0.95	1.55
F19-0	0.55	4.32
F19-1	1.15	2.14
F19-2	1.77	1.97
F19-3	1.49	1.77
F19-4	1.21	2.27
F19-5	0.98	1.23
F24-0	0.71	0.13
F24-1	0.17	0.22
F24-2	0.28	0.29

Table B7: Ca-normalised trace element data of newly formed chambers from *Ammonia tepida* (20-fold concentration tank; Batch II experiment) measured by means of µ-synchrotron XRF expressed as µmol/mol

Sample	V	As
G3K-0	2.37	34.7
G3K-1	0.90	23.4
G3K-2	0.18	21.1
G4-0	0.84	5.84
G4-1	2.23	6.99
G4-2	0.46	8.02
G4-3	2.09	6.66
G4-4	0.84	3.62
G4-5	0.34	2.26
G15-0	1.36	7.30
G15-1	2.04	4.85
G15-2	1.26	4.64
G15-3	0.35	5.63
G15-4	0.35	4.34
G15-5	2.95	3.23
G18-0	0.93	27.2
G18-1	1.32	21.2
G18-3	0.43	12.9
G18-2	0.47	8.37
G18-4	0.98	6.66
G18-5	1.30	7.43
G18-6	2.79	7.16
G20-0	2.98	3.50
G20-1	0.94	3.82
G20-2	0.98	18.3
G20-3	1.53	8.80
G20-4	1.76	6.30
G20-5	2.75	7.80
G20-6	2.59	5.01
G20-7	1.75	5.55
G20-8	0.99	6.00

Table B8: Selected Ca-normalised trace element data of newly formed chambers from *Ammonia tepida* (reference tank) measured by means of LA-ICP-MS expressed as µmol/mol

Sample	Ni	Cu	Mn
A1 1	20.7	11.6	3.84
A1 2	17.3	9.74	8.70
A1 3	19.7	10.5	11.8
A7 1	23.4	36.8	16.0
A7 2	18.0	18.3	6.88
A7 3	23.8	12.7	13.3
A7 4	16.7	9.96	13.9
A14 1	34.0	33.4	22.9
A14 2	75.4	130	21.2
A14 3	13.5	23.3	790
A14 4	14.9	17.2	43.9
A14 5	16.7	38.2	16.3
A20 1	17.4	34.2	7.54
A20 2	31.3	26.9	15.4
A20 3	15.8	7.54	500
A20 4	25.9	13.3	15.0
A30 1	11.5	5.87	54.2
A30 2	12.3	3.38	34.6
A30 3	23.2	4.26	114
A38 1	52.9	2.14	23.2
A38 2	13.7	6.40	43.0
A38 3	22.9	4.58	28.3

Table B9: Selected Ca-normalised trace element data of newly formed chambers from *Ammonia tepida* (5-fold concentration tank – Batch I experiment) measured by means of LA-ICP-MS expressed as µmol/mol

Sample	Ni	Cu	Mn
B9 1	13.8	1.72	8.90
B9 2	8.68	16.9	5.11
B9 3	7.25	21.9	8.98
B17 1	36.9	2.99	13.8
B17 2	15.7	2.39	94.8
B17 3	35.5	1.46	34.0
B18 1	9.36	16.7	27.3
B18 2	11.8	22.8	30.6
B18 3	14.3	16.8	22.8
B18 4	9.58	7.76	210
B27 1	134	55.2	33.7
B27 2	47.4	20.3	13.6
B27 3	39.0	20.0	16.2
B25 1	11.5	6.49	39.4
B25 2	13.2	3.27	268
B25 3	12.6	12.9	174
B25 4	21.6	8.13	35.5
B34 1	38.9	2.83	12.1
B34 2	12.9	1.42	11.3
B34 3	16.5	2.23	17.7

Table B10: Selected Ca-normalised trace element data of newly formed chambers from *Ammonia tepida* (10-fold concentration tank – Batch I experiment) measured by means of LA-ICP-MS expressed as µmol/mol

Sample	Ni	Cu	Mn
C6 1	60.6	78.6	14.2
C6 2	143	98.9	2320
C6 3	10.8	13.3	1076
C9 1	20.5	20.0	17.3
C9 2	25.9	11.7	18.0
C9 3	32.6	46.5	308
C12 1	91.7	55.2	14.6
C12 2	82.6	66.0	16.4
C12 3	38.4	25.5	16.2
C17 1	102	36.2	17.8
C17 2	61.7	15.3	43.8
C17 3	64.9	10.3	28.4
C30 1	95.9	23.4	30.6
C30 2	25.1	4.10	7.30

Table B11: Selected Ca-normalised trace element data of newly formed chambers from *Ammonia tepida* (20-fold concentration tank – Batch I experiment) measured by means of LA-ICP-MS expressed as µmol/mol

Sample	Ni	Cu	Mn
D1 1	15.4	12.2	93.5
D1 2	14.3	21.3	13.8
D13 1	7.25	19.8	24.4
D13 2	17.0	16.8	17.3
D13 3	18.6	31.0	19.9
D19 1	6.20	26.3	19.9
D19 2	7.72	27.6	45.2
D19 3	6.67	31.4	79.2
D25 1	33.5	200	48.5
D25 2	16.8	28.6	809
D25 3	7.72	34.9	359
D25 4	23.2	40.6	1884

Appendix C: Major, minor, and trace element contents of the sediments of the core from ODP Site 1002, Hole C, Cariaco

Table C1: Major element concentrations (part 1) of the sediments of the core from ODP Site 1002, Hole C

Depth [m]	SiO_2 [%]	TiO_2 [%]	Al_2O_3 [%]	Fe_2O_{3t} [%]	MnO [%]	MgO [%]
0.34	26.1	0.39	10.1	4.08	0.022	1.96
0.48	28.4	0.42	11.0	4.50	0.025	2.08
0.65	27.8	0.42	10.7	4.35	0.022	1.96
0.82	28.0	0.42	10.9	4.33	0.030	2.01
1.13	27.4	0.42	10.7	4.19	0.024	1.99
1.25	28.4	0.43	11.1	4.42	0.028	2.02
1.44	28.5	0.43	11.2	4.41	0.028	2.12
1.56	29.2	0.44	11.3	4.44	0.030	2.05
1.69	28.1	0.43	11.1	4.52	0.031	2.06
1.76	28.4	0.43	11.2	4.79	0.031	2.00
1.92	30.7	0.46	11.9	4.82	0.031	2.11
2.09	29.9	0.45	11.7	4.63	0.029	2.00
2.34	27.4	0.42	10.7	4.44	0.030	1.96
2.57	30.2	0.46	11.8	4.79	0.030	2.02
2.74	29.8	0.46	11.5	4.59	0.030	1.96
2.94	31.6	0.49	12.4	4.83	0.032	2.09
3.06	29.3	0.45	11.3	4.64	0.028	2.03
3.23	27.6	0.44	10.7	4.47	0.024	2.06
3.34	31.8	0.49	12.3	4.92	0.023	1.90
3.48	30.1	0.46	11.4	4.61	0.022	1.95
3.66	31.1	0.47	11.6	4.58	0.023	1.98
3.82	32.5	0.44	10.8	4.31	0.021	1.92
4.07	36.0	0.36	8.44	3.30	0.017	1.78
4.23	34.7	0.38	8.63	3.59	0.021	1.92
4.37	37.0	0.33	7.63	3.05	0.017	2.04
4.56	37.3	0.31	7.17	2.91	0.018	1.95
4.75	37.9	0.28	6.68	2.69	0.016	1.83
4.91	37.7	0.32	7.59	3.07	0.019	1.89
5.06	34.6	0.35	7.96	3.19	0.019	2.18
5.16	32.3	0.42	9.67	3.93	0.030	2.24
5.42	32.8	0.43	10.5	4.32	0.024	2.07
5.57	35.9	0.42	9.91	4.20	0.022	1.75
5.73	33.7	0.39	9.23	3.96	0.026	1.86
5.93	40.4	0.40	9.67	3.93	0.027	1.81
6.09	34.3	0.37	8.66	3.83	0.036	1.60

Table C1 continued

Depth [m]	SiO_2 [%]	TiO_2 [%]	Al_2O_3 [%]	Fe_2O_{3t} [%]	MnO [%]	MgO [%]
6.27	32.2	0.48	11.9	5.01	0.046	1.75
6.41	38.8	0.61	14.2	6.20	0.049	1.83
6.55	36.8	0.56	13.4	5.25	0.099	2.23
6.75	36.9	0.56	12.8	5.17	0.054	2.59
6.86	48.8	0.73	16.0	6.10	0.049	2.05
7.08	52.7	0.73	15.5	6.08	0.047	1.82
7.23	51.0	0.81	18.2	6.40	0.053	2.19
7.37	51.9	0.85	18.9	6.69	0.053	2.11
7.63	49.8	0.79	17.5	6.52	0.042	2.17
7.78	46.4	0.56	11.5	4.58	0.055	1.99
7.93	48.5	0.64	12.7	4.79	0.040	2.09
8.07	37.5	0.55	12.9	4.86	0.061	2.46
8.25	39.5	0.60	13.9	5.06	0.062	2.50
8.43	37.9	0.56	13.5	5.19	0.058	2.37
8.58	29.4	0.43	9.92	4.58	0.090	5.71
8.74	41.3	0.68	14.9	6.42	0.044	2.54
8.93	45.7	0.68	14.7	6.00	0.045	2.52
9.07	24.8	0.38	8.84	4.34	0.068	3.83
9.25	40.9	0.65	14.4	6.39	0.048	2.39
9.45	66.8	0.50	8.47	4.29	0.026	1.17
9.63	51.2	0.68	14.0	5.98	0.036	1.91
9.84	38.6	0.62	13.9	6.37	0.054	2.49
9.90	51.6	0.53	8.82	5.28	0.036	1.71
10.05	43.8	0.68	14.8	5.89	0.048	2.46
10.23	40.1	0.62	13.9	5.85	0.058	2.73
10.43	42.0	0.66	15.0	6.32	0.058	2.57
10.62	41.9	0.67	15.2	6.46	0.051	2.34
10.76	44.5	0.56	11.9	5.02	0.049	2.30
10.95	52.3	0.67	13.4	5.87	0.041	1.96
11.13	42.3	0.67	14.9	6.08	0.057	2.45
11.27	38.0	0.60	13.8	6.34	0.077	2.45
11.42	43.0	0.67	14.6	6.02	0.076	2.47
11.69	42.4	0.65	14.4	6.26	0.054	2.37
11.87	43.5	0.68	15.2	6.21	0.080	2.50
12.04	39.9	0.64	14.7	6.87	0.064	2.43

Table C2: Major element concentrations (part 2) of the sediments of the core from ODP Site 1002, Hole C

Depth [m]	CaO [%]	Na_2O [%]	K_2O [%]	P_2O_5 [%]	S [%]	C_{org} [%]
0.34	17.5	2.99	0.91	0.17	1.50	4.16
0.48	17.5	2.95	0.83	0.19	1.27	3.86
0.65	19.2	2.55	0.88	0.18	1.92	3.59
0.82	18.8	2.55	0.82	0.17	1.73	3.79
1.13	17.5	2.91	0.97	0.17	1.58	3.72
1.25	19.0	2.46	0.88	0.18	1.30	3.33
1.44	18.7	2.61	0.91	0.18	1.77	3.18
1.56	19.4	2.29	0.93	0.17	1.34	2.80
1.69	19.6	2.34	0.96	0.18	2.13	2.92
1.76	19.7	2.28	0.95	0.17	2.94	2.86
1.92	17.5	2.33	1.06	0.19	1.89	3.31
2.09	18.9	2.03	0.84	0.20	1.56	3.39
2.34	20.2	2.25	0.93	0.20	2.09	3.01
2.57	18.3	2.37	1.07	0.19	2.01	2.80
2.74	16.3	2.48	1.41	0.19	2.65	2.85
2.94	14.9	2.39	1.39	0.16	1.83	2.60
3.06	15.7	2.77	1.18	0.18	1.79	3.46
3.23	16.0	3.21	1.24	0.16	2.48	3.17
3.34	13.7	2.47	1.53	0.17	2.10	3.27
3.48	13.7	2.96	1.30	0.21	1.11	4.08
3.66	14.2	2.93	1.26	0.19	1.37	3.73
3.82	12.6	3.00	1.30	0.19	1.42	4.47
4.07	14.0	2.91	1.36	0.24	1.26	3.63
4.23	15.5	2.63	1.16	0.18	1.73	3.72
4.37	16.9	2.47	1.03	0.16	1.35	2.40
4.56	15.7	3.08	1.18	0.13	1.50	2.37
4.75	16.0	2.38	1.25	0.13	1.06	2.16
4.91	16.5	2.39	1.04	0.12	0.88	2.20
5.06	17.4	2.90	0.98	0.14	1.13	1.99
5.16	18.4	2.03	0.85	0.17	1.39	2.37
5.42	16.2	2.42	1.22	0.15	1.96	2.28
5.57	13.1	2.69	1.46	0.18	2.87	2.93
5.73	14.9	2.63	1.30	0.15	2.29	3.44
5.93	9.21	3.50	1.57	0.15	1.46	3.49
6.09	13.7	2.91	1.41	0.11	1.83	3.76

Table C2 continued

Depth [m]	CaO [%]	Na_2O [%]	K_2O [%]	P_2O_5 [%]	S [%]	C_{org} [%]
6.27	13.5	2.43	1.58	0.12	2.00	3.38
6.41	9.10	2.31	1.82	0.23	1.00	1.88
6.55	13.9	2.23	1.55	0.11	2.49	0.98
6.75	14.6	1.88	1.43	0.13	2.21	1.00
6.86	5.35	2.00	2.05	0.07	2.73	0.39
7.08	3.90	1.80	1.90	0.07	2.30	0.30
7.23	3.25	2.14	2.24	0.12	0.32	0.33
7.37	2.63	1.95	2.27	0.11	0.26	0.28
7.63	4.79	1.88	2.17	0.11	0.61	0.40
7.78	12.2	1.70	1.42	0.09	0.92	1.09
7.93	9.56	1.81	1.69	0.10	1.14	0.81
8.07	15.0	1.94	1.21	0.11	0.85	1.20
8.25	12.5	2.42	1.50	0.10	0.87	1.08
8.43	13.1	2.34	1.61	0.12	2.15	0.99
8.58	18.5	1.42	0.72	0.15	0.81	1.48
8.74	9.03	2.07	1.80	0.11	2.36	1.13
8.93	7.91	2.15	1.77	0.09	1.66	1.02
9.07	17.9	1.58	0.69	0.15	1.30	1.89
9.25	10.4	2.02	1.65	0.10	2.00	1.36
9.45	5.61	1.51	0.99	0.06	1.73	0.69
9.63	5.53	2.08	1.67	0.08	1.85	0.86
9.84	11.4	1.96	1.58	0.11	2.26	1.29
9.90	11.1	1.76	0.95	0.09	1.85	1.06
10.05	9.17	1.93	1.77	0.11	1.38	1.14
10.23	10.7	2.38	1.61	0.11	1.58	1.46
10.43	8.99	2.44	1.74	0.11	1.34	1.11
10.62	9.14	2.07	1.72	0.11	1.58	1.35
10.76	12.0	2.10	1.25	0.10	0.55	1.18
10.95	6.60	1.87	1.65	0.09	1.66	0.91
11.13	9.19	2.14	1.71	0.10	1.82	1.13
11.27	12.1	1.87	1.56	0.12	2.35	1.26
11.42	9.51	1.94	1.75	0.09	1.40	1.08
11.69	9.61	2.01	1.70	0.10	1.96	1.21
11.87	8.71	1.94	1.85	0.10	1.52	1.13
12.04	9.40	2.27	1.77	0.09	0.97	1.06

Table C3: Trace element concentrations (part 1) of the sediments of the core from ODP Site 1002, Hole C

Depth [m]	Sc [ppm]	V [ppm]	Cr [ppm]	Ni [ppm]	Cu [ppm]	Zn [ppm]	Ga [ppm]	As [ppm]	Rb [ppm]	Sr [ppm]
0.34	24	221	79	62	31	106	19	17	118	829
0.48	28	216	78	103	32	117	18	15	113	769
0.65	31	212	81	81	31	108	20	15	108	842
0.82	22	183	85	94	30	110	19	13	106	811
1.13	35	209	88	64	32	110	20	12	114	801
1.25	32	186	87	80	29	109	20	18	107	831
1.44	33	183	85	84	28	107	20	16	106	810
1.56	34	175	84	155	28	111	20	14	106	864
1.69	26	164	82	96	29	112	20	18	104	858
1.76	31	185	82	182	29	108	22	22	106	857
1.92	20	185	88	136	31	116	22	17	105	816
2.09	38	199	82	116	32	115	20	17	102	884
2.34	26	166	86	297	29	108	21	15	100	865
2.57	33	176	87	162	29	117	21	14	108	806
2.74	21	172	96	64	28	110	21	14	102	728
2.94	27	158	117	76	27	118	24	17	111	718
3.06	30	183	92	77	32	122	20	11	112	748
3.23	27	173	81	72	30	115	21	10	113	748
3.34	18	193	95	79	34	134	24	12	116	663
3.48	27	198	90	87	32	126	22	11	114	657
3.66	22	190	88	80	34	128	22	11	119	660
3.82	19	210	87	86	34	128	21	10	117	660
4.07	28	145	66	48	28	100	19	7	84	653
4.23	28	148	69	67	29	102	19	7	86	808
4.37	35	117	62	46	24	87	18	6	69	850
4.56	22	105	55	40	23	84	17	6	68	790
4.75	32	102	62	38	24	80	17	5	62	826
4.91	32	109	62	37	23	87	17	7	70	893
5.06	30	102	66	38	26	85	17	6	73	965
5.16	34	126	72	45	24	100	20	8	84	1070
5.42	28	139	76	51	28	105	20	7	97	867
5.57	21	149	79	61	31	110	19	7	93	704
5.73	26	163	74	64	27	99	19	7	93	810
5.93	14	207	76	62	34	109	19	8	92	565
6.09	19	194	81	75	33	105	19	9	87	656

Table C3 continued

Depth [m]	Sc [ppm]	V [ppm]	Cr [ppm]	Ni [ppm]	Cu [ppm]	Zn [ppm]	Ga [ppm]	As [ppm]	Rb [ppm]	Sr [ppm]
6.27	19	190	90	86	40	135	23	15	103	735
6.41	13	170	89	73	39	145	23	22	109	529
6.55	18	132	75	44	33	134	24	5	97	717
6.75	19	131	79	50	34	126	23	3	91	738
6.86	5	143	81	48	36	148	26	3	112	331
7.08	7	134	87	38	39	147	26	5	107	228
7.23	6	169	90	43	42	161	27	8	124	252
7.37	7	177	96	45	42	161	27	7	125	218
7.63	8	160	95	52	44	163	29	7	124	301
7.78	16	96	73	42	28	109	20	6	94	609
7.93	14	117	71	33	31	121	22	5	97	557
8.07	18	135	74	39	33	131	23	3	99	773
8.25	18	144	79	48	37	153	23	3	102	674
8.43	15	129	74	52	33	148	24	4	98	700
8.58	30	118	71	42	32	323	20	3	74	853
8.74	13	180	91	58	42	146	24	19	104	465
8.93	10	159	89	52	44	146	24	8	104	438
9.07	35	148	71	48	33	116	20	20	82	1075
9.25	10	173	90	47	44	140	23	11	101	525
9.45	8	81	58	21	26	86	17	8	52	298
9.63	8	145	90	40	41	134	23	14	94	305
9.84	14	172	88	58	42	145	24	14	104	568
9.90	16	102	79	27	30	95	17	9	61	672
10.05	15	163	92	46	42	147	24	10	105	522
10.23	13	153	85	44	40	142	23	7	107	606
10.43	15	169	85	44	40	147	24	9	109	520
10.62	9	172	93	48	44	152	24	9	107	512
10.76	16	127	82	42	35	123	21	8	85	699
10.95	8	138	83	44	36	120	22	10	82	360
11.13	14	161	88	46	40	143	24	7	107	555
11.27	16	165	86	52	41	136	23	11	103	686
11.42	13	157	87	55	41	143	24	7	106	560
11.69	13	161	88	52	40	143	23	10	104	543
11.87	12	162	86	49	43	154	25	8	110	542
12.04	12	169	121	74	39	145	22	11	107	552

Table C4: Trace element concentrations (part 2) of the sediments of the core from ODP Site 1002, Hole C

Depth [m]	Y [ppm]	Zr [ppm]	Nb [ppm]	Mo [ppm]	Cd [ppm]	Ba [ppm]	La [ppm]	Ce [ppm]	Pb [ppm]	U [ppm]
0.34	10	69	9	112	5	183	19	35	8	19
0.48	11	76	10	119	5	196	19	37	8	19
0.65	13	73	9	102	4	195	21	38	7	23
0.82	11	73	8	71	5	187	20	36	10	20
1.13	11	73	9	83	6	189	20	36	8	19
1.25	12	71	8	72	4	178	17	33	13	17
1.44	14	71	9	63	4	186	22	33	9	21
1.56	12	78	9	51	4	215	22	42	10	13
1.69	13	72	7	51	3	198	23	40	8	18
1.76	14	73	7	52	4	197	21	39	9	15
1.92	15	77	8	81	4	217	20	37	13	17
2.09	15	78	9	77	4	242	20	37	11	19
2.34	13	70	9	69	5	225	20	35	13	17
2.57	16	77	8	78	4	248	21	39	11	23
2.74	16	80	9	59	3	251	25	41	13	14
2.94	17	85	10	41	3	237	25	47	15	15
3.06	14	81	10	97	8	278	24	43	13	22
3.23	14	77	9	97	6	247	23	41	10	19
3.34	17	87	11	122	10	270	25	46	12	22
3.48	15	82	11	166	10	275	23	38	10	24
3.66	14	86	10	143	9	283	22	42	0	28
3.82	14	82	9	169	16	328	20	38	8	44
4.07	13	63	8	135	12	183	20	32	0	19
4.23	14	72	8	128	13	185	19	34	8	25
4.37	11	64	7	88	5	211	17	28	6	18
4.56	12	64	7	74	6	208	18	28	0	14
4.75	10	54	5	60	6	200	16	27	7	14
4.91	13	64	6	71	6	179	17	30	8	16
5.06	14	73	7	71	4	179	18	29	7	16
5.16	18	96	9	63	4	208	22	40	10	18
5.42	16	79	8	105	3	228	21	35	11	21
5.57	15	75	8	156	10	239	21	36	10	28
5.73	11	66	7	136	7	206	21	35	9	23
5.93	12	65	8	147	10	237	20	32	11	24
6.09	12	60	7	112	12	227	19	29	9	23

Table C4 continued

Depth [m]	Y [ppm]	Zr [ppm]	Nb [ppm]	Mo [ppm]	Cd [ppm]	Ba [ppm]	La [ppm]	Ce [ppm]	Pb [ppm]	U [ppm]
6.27	17	82	9	179	9	327	24	43	14	22
6.41	25	102	10	152	7	306	27	51	14	12
6.55	22	97	11	9	2	256	27	53	16	9
6.75	23	105	10	4	2	242	25	48	13	12
6.86	27	146	13	4	1	313	34	66	17	4
7.08	31	219	12	4	2	331	33	64	17	0
7.23	30	139	15	3	2	338	34	68	18	0
7.37	30	136	15	2	2	330	34	67	20	0
7.63	30	147	13	2	2	339	35	69	21	0
7.78	25	203	11	3	2	224	27	53	14	10
7.93	27	237	12	2	2	252	29	57	15	7
8.07	22	109	10	2	2	227	26	48	13	13
8.25	23	108	10	2	1	255	28	51	17	10
8.43	22	101	10	5	2	241	26	52	20	11
8.58	17	93	7	5	2	194	19	35	40	16
8.74	24	113	11	13	3	271	27	51	17	11
8.93	26	133	11	5	2	264	27	52	15	8
9.07	20	83	7	10	4	202	21	37	14	33
9.25	24	110	11	6	1	266	26	53	19	11
9.45	19	246	8	4	1	178	20	36	11	6
9.63	24	154	10	10	1	263	27	50	15	4
9.84	22	107	10	10	2	255	26	50	14	8
9.90	26	267	9	8	2	183	22	41	11	9
10.05	27	122	11	4	2	266	28	53	16	10
10.23	23	111	10	5	2	264	29	52	14	12
10.43	25	114	10	4	2	271	27	53	16	7
10.62	26	115	11	4	2	279	27	52	21	9
10.76	25	195	9	5	1	229	25	46	12	14
0.95	25	199	11	12	2	256	26	49	13	6
11.13	24	117	11	8	1	276	28	53	15	11
11.27	22	106	11	14	3	260	27	51	13	12
11.42	25	159	11	6	2	271	29	55	16	11
11.69	24	125	11	8	1	267	27	51	14	7
11.87	25	119	12	5	2	290	30	58	15	7
12.04	23	109	11	11	3	276	26	49	17	10

Appendix D: Measurements of foraminiferal calcite of *Bulimina spp.* (ODP Site 1002, Hole C, Cariaco)

Table D1: Ca-normalised trace element data (part 1) of *Bulimina spp.* (Cariaco Trench) expressed as µmol/mol

Depth [m]	Mg	P	S	V	Cr	Mn	Fe	Co	Ni	Cu
0.34	3105	184	8624	1.29	0.80	10.6	236	0.03	1.46	0.82
0.48	2754	149	2149	2.17	0.83	8.41	271	0.07	1.07	0.74
0.65	3440	207	2808	2.24	0.90	10.9	269	0.02	1.23	1.46
0.82	3163	214	2414	12.09	1.59	18.3	1284	0.16	2.66	2.54
1.13	2484	154	1930	4.63	0.92	10.4	503	0.11	1.54	15.1
1.25	2902	282	2056	10.75	2.09	19.8	982	0.11	1.54	1.90
1.44	3169	160	2103	6.18	0.96	13.2	697	0.13	1.19	1.51
1.56	2957	174	3691	6.73	1.01	19.1	695	0.12	1.36	1.79
1.69	3205	188	3311	8.80	4.02	33.8	2183	0.26	1.37	2.17
1.76	3261	205	3432	7.59	1.15	24.7	2077	0.13	0.18	1.64
1.92	3666	226	2379	6.69	1.70	16.3	978	0.26	1.82	2.01
2.09	2699	177	1835	1.13	0.49	9.96	67.9	0.02	1.03	0.53
2.34	2860	166	1724	3.87	1.00	9.57	522	0.06	0.76	1.19
2.57	2675	240	1796	1.39	0.53	10.5	216	0.02	0.51	1.33
2.74	2462	170	2130	9.58	1.69	14.2	945	0.17	1.17	2.71
2.94	2692	168	1887	1.27	0.61	19.1	251	0.03	0.44	0.50
3.06	2659	174	1855	6.63	1.28	10.9	787	0.10	1.51	3.51
3.23	2569	148	1956	1.12	0.85	8.00	239	0.20	2.00	1.18
3.34	2735	187	1858	2.20	1.14	10.9	395	0.21	1.69	0.85
3.48	3138	178	1407	1.17	0.61	15.6	202	0.04	0.81	0.17
3.66	2483	174	1828	0.97	0.28	6.86	111	0.04	0.25	1.22
3.82	2981	224	1814	0.99	1.12	9.51	149	0.04	2.60	5.56
4.07	4297	735	2922	3.27	4.94	14.5	386	0.28	10.2	11.3
4.23	2693	215	2646	0.71	1.64	13.7	194	0.23	49.8	7.05
4.37	3279	328	1848	0.52	0.74	14.8	120	0.04	2.98	0.15
4.56	3327	207	2594	0.16	0.92	12.8	65.8	0.06	0.39	1.13
4.75	3437	191	1729	0.42	0.67	6.19	68.8	0.05	0.28	0.19
4.91	3559	228	2018	0.69	0.76	14.5	82.4	0.03	0.18	0.29
5.06	2855	154	1912	0.79	2.31	11.8	280	0.09	10.1	6.44
5.16	3061	200	2041	0.29	0.41	13.5	200	0.05	7.54	0.22
5.42	2427	164	2192	0.20	0.89	20.0	70	0.13	0.73	1.92
5.57	3087	531	2662	0.40	0.37	13.4	155	0.05	6.86	1.11
5.73	2677	198	2140	0.60	0.66	15.2	192	0.04	7.71	2.57
5.93	3132	246	1505	3.55	16.5	24.6	630	0.25	21.0	7.04
6.09	2168	202	1241	0.91	0.08	14.2	154	0.06	13.4	0.25

Table D1 continued

Depth [m]	Mg	P	S	V	Cr	Mn	Fe	Co	Ni	Cu
6.27	2442	216	1326	0.21	0.35	15.4	90.9	0.04	9.33	22.5
6.41	2486	164	1186	0.15	0.34	28.4	54.1	0.05	35.4	27.1
6.55	8180	206	3536	2.16	0.32	119	1253	0.13	3.15	4.98
6.75	8411	192	3983	1.69	0.43	103	1120	0.31	3.08	4.73
6.86	3124	315	5615	5.06	0.31	76.8	2806	0.94	6.24	9.36
7.08	3039	234	7929	11.9	1.52	246	6284	3.72	12.0	20.5
7.23	3319	113	2025	0.63	0.28	146	318	0.04	2.03	3.14
7.37	3362	154	1867	1.60	0.71	108	446	0.16	2.87	5.48
7.63	3398	166	2015	2.03	0.23	65.0	1084	0.19	0.59	13.5
7.78	3144	131	1973	1.37	0.21	50.0	931	0.11	1.70	15.5
7.93	3669	244	2557	3.03	0.53	49.0	1089	0.09	1.68	1.27
8.07	3122	165	2031	2.83	0.27	46.6	1225	0.04	0.22	0.76
8.25	3545	152	2079	0.83	0.32	59.5	338	0.04	0.26	0.17
8.43	3343	247	5566	8.39	1.28	61.6	3577	0.77	5.43	3.38
8.58	4474	227	2550	3.42	0.47	69.8	1289	0.12	0.95	0.73
8.74	3171	219	1800	5.52	0.89	84.1	1210	0.11	1.51	0.50
8.93	3509	247	2107	7.09	0.54	93.3	1542	0.12	0.66	1.71
9.07	3891	275	2524	13.7	1.19	115	3191	0.30	3.16	3.02
9.25	3125	162	4320	21.8	0.63	42.4	4601	0.54	1.49	9.35
9.45	2843	144	1756	4.24	0.21	40.8	1114	0.16	0.46	0.53
9.63	2031	269	3592	9.75	0.14	35.4	3063	0.62	1.90	2.69
9.84	3450	177	2136	3.86	0.35	77.6	1001	0.15	1.01	0.69
9.90	3485	367	2018	2.85	0.67	117	690	0.04	1.47	0.72
10.05	2862	855	1889	5.92	0.68	84.3	1408	0.05	4.51	0.61
10.23	3535	172	2003	2.75	0.26	149	777	0.04	3.75	0.17
10.43	2952	185	1762	6.01	0.97	58.6	1785	0.23	5.13	2.12
10.62	3455	163	2229	4.68	0.28	60.2	1144	0.05	7.56	0.96
10.76	3836	265	1999	6.48	3.55	225	1824	0.24	3.23	2.79
10.95	3365	152	2699	9.09	2.16	39.1	2671	0.35	3.15	2.60
11.13	3012	155	2486	5.75	0.14	45.5	1840	0.20	1.05	1.52
11.27	2164	143	1344	5.83	1.86	44.6	2244	0.21	2.95	2.76
11.42	2581	168	2034	8.09	2.75	48.9	2898	0.18	8.46	8.80
11.69	1964	128	1118	6.82	2.87	65.4	1701	0.06	10.1	1.70
11.87	3040	136	1277	4.78	1.88	156	1583	0.17	2.96	0.17
12.04	2633	165	1406	12.1	2.99	80.7	3877	0.40	11.0	6.40

Table D2: Ca-normalised trace element data (part 2) of *Bulimina spp.* (Cariaco Trench) expressed as µmol/mol, isotopic measurements as ‰ VPDB

Depth [m]	Zn	As	Rb	Sr	Mo	Cd	Ba	Pb	U	$\delta^{13}C$	$\delta^{18}O$
0.34	24.6	1.29	0.09	1423	1.42	0.36	12.7	0.01	0.06	2.06	0.08
0.48	12.4	0.65	0.08	1313	1.34	0.06	6.34	0.03	0.12	1.99	0.01
0.65	32.4	0.83	0.21	1456	0.88	0.22	17.7	0.07	0.12	2.19	0.22
0.82	16.5	1.15	0.17	1493	1.86	0.10	16.7	0.46	0.13	2.26	-0.17
1.13	18.1	0.51	0.02	1361	1.11	0.07	4.58	0.31	0.09	1.52	-0.20
1.25	14.8	1.44	0.26	1452	1.04	0.12	20.9	0.19	0.23	1.94	0.11
1.44	12.6	0.80	0.08	1401	1.17	0.18	10.1	0.18	0.13	2.05	-0.25
1.56	26.3	0.79	0.13	1047	1.21	0.95	5.12	0.14	0.11	2.97	0.05
1.69	10.0	2.35	0.14	1317	1.86	0.04	15.7	0.02	0.21	1.79	0.43
1.76	20.8	3.11	0.02	1299	2.86	0.12	17.2	0.01	0.24	1.81	-0.17
1.92	21.3	0.79	0.09	1312	1.11	0.08	14.4	0.02	0.20	2.56	0.06
2.09	46.4	0.23	0.12	1255	0.38	0.07	36.1	0.01	0.22	2.01	0.22
2.34	8.98	0.50	0.11	1261	0.51	0.45	7.84	0.01	0.18	1.51	0.40
2.57	3.78	0.33	0.02	1280	0.33	0.05	7.48	0.03	0.14	1.81	0.38
2.74	9.44	1.01	0.37	1410	1.26	0.55	11.3	0.23	0.12	1.02	0.22
2.94	3.34	0.34	0.02	1500	4.37	0.11	19.3	0.11	0.06	1.71	0.26
3.06	10.4	0.63	0.22	1352	1.11	0.21	6.02	0.10	0.18	1.47	0.57
3.23	18.9	0.69	0.04	1448	1.09	0.14	4.32	0.02	0.06	1.47	0.35
3.34	12.0	0.53	0.14	1429	1.31	0.15	10.8	2.77	0.14	1.55	0.20
3.48	0.74	0.02	0.03	1408	0.36	0.04	12.9	0.02	0.22	1.51	0.25
3.66	7.82	0.02	0.03	1418	0.06	0.15	15.0	0.46	0.15	1.54	0.10
3.82	3.93	0.09	0.03	1413	0.05	0.05	19.8	0.02	0.19	0.83	0.19
4.07	99.8	0.49	0.69	1359	4.79	0.80	34.7	2.02	0.21	0.84	-0.18
4.23	76.0	0.23	0.11	1415	0.36	0.07	47.0	0.59	0.15	0.42	0.43
4.37	18.8	0.06	0.03	1459	0.15	0.06	58.0	0.38	0.12	0.85	0.40
4.56	1.15	0.38	0.05	1552	0.09	0.13	114	1.01	0.08	0.81	0.77
4.75	0.83	0.02	0.04	1540	0.13	0.01	49.8	0.09	0.09	0.22	0.31
4.91	0.52	0.34	0.07	1423	0.76	0.10	48.2	0.33	0.11	0.72	0.97
5.06	0.88	0.02	0.06	1482	1.08	0.01	13.2	0.02	0.12	0.41	0.79
5.16	0.99	0.02	0.04	1431	0.07	0.01	16.6	0.03	0.08	0.58	0.78
5.42	5.43	0.13	0.07	1430	0.05	0.05	5.55	0.28	0.06	0.99	0.95
5.57	0.93	0.02	0.04	1430	0.07	0.08	20.4	0.73	0.23	0.74	0.66
5.73	0.78	0.08	0.11	1580	0.14	0.14	13.0	0.76	0.12	1.15	0.98
5.93	0.69	0.02	0.36	1309	0.88	0.65	35.9	0.02	0.26	0.64	0.51
6.09	1.08	0.03	0.05	1413	0.08	0.01	21.5	0.03	0.18	0.88	0.48

Table D2 continued

Depth [m]	Zn	As	Rb	Sr	Mo	Cd	Ba	Pb	U	$\delta^{13}C$	$\delta^{18}O$
6.27	0.71	0.02	0.03	1400	0.05	0.05	35.1	0.02	0.11	0.68	1.30
6.41	70.9	0.02	0.09	1476	0.06	0.27	17.5	0.02	0.08	0.42	0.67
6.55	11.6	0.54	0.04	1580	0.19	0.07	45.6	0.17	0.05	0.63	1.10
6.75	0.59	0.17	0.03	1451	0.04	0.04	6.23	0.13	0.06	0.31	1.04
6.86	2.08	0.23	0.04	1373	1.29	0.02	26.9	0.03	0.19	0.63	0.72
7.08	18.1	3.85	0.59	1352	0.78	0.07	30.0	0.78	0.10	0.34	0.68
7.23	0.79	0.95	0.03	1436	0.06	0.01	78.3	0.02	0.03	0.84	0.64
7.37	0.51	0.43	0.38	1384	0.04	0.02	43.5	0.03	0.07	0.31	0.81
7.63	10.3	2.42	0.03	1414	0.06	0.02	84.0	0.67	0.04	0.86	0.74
7.78	16.8	0.38	0.04	1454	0.07	0.01	17.5	0.28	0.05	0.77	0.46
7.93	85.6	0.97	0.23	1359	0.51	0.02	119	0.52	0.05	0.33	1.16
8.07	0.65	0.53	0.03	1470	0.05	0.01	61.9	0.47	0.05	0.59	1.25
8.25	0.76	0.12	0.03	1470	0.06	0.01	58.0	0.02	0.02	0.28	1.36
8.43	0.65	1.31	0.13	1377	0.05	0.01	24.5	0.67	0.07	0.77	0.99
8.58	0.58	1.36	0.03	1426	0.04	0.03	123	1.19	0.09	0.57	0.08
8.74	17.4	1.42	0.03	1367	0.13	0.07	18.1	0.07	0.23	1.10	1.28
8.93	3.61	0.96	0.03	1410	0.06	0.04	20.9	0.22	0.17	1.29	1.16
9.07	3.51	2.89	0.04	1381	0.31	0.06	15.7	0.72	0.35	0.97	1.49
9.25	3.64	2.35	0.03	1388	0.20	0.04	44.2	1.07	0.12	1.18	1.21
9.45	0.65	0.81	0.03	1428	0.05	0.04	56.4	0.02	0.07	0.91	1.22
9.63	17.0	1.48	0.03	1415	0.16	0.02	17.7	0.27	0.07	1.15	1.33
9.84	0.65	0.97	0.03	1465	0.05	0.06	62.8	0.02	0.09	0.98	1.46
9.90	0.72	0.51	0.03	1631	0.05	0.24	58.0	0.02	0.21	0.94	1.25
10.05	0.97	1.57	0.04	1438	0.07	0.06	86.2	0.03	0.12	1.01	1.30
10.23	0.75	0.32	0.03	1505	0.06	0.01	28.7	0.02	0.13	1.26	1.43
10.43	1.86	1.12	0.25	1430	0.04	0.01	44.5	0.21	0.06	1.37	1.05
10.62	0.89	0.69	0.04	1381	0.07	0.21	63.8	0.02	0.11	0.79	1.34
10.76	0.66	1.43	0.03	1453	0.05	0.02	141	0.05	0.31	1.28	1.10
10.95	7.02	2.09	0.03	1479	0.32	0.04	43.1	0.17	0.07	1.26	1.20
11.13	0.63	0.71	0.03	1406	0.12	0.01	43.2	0.21	0.08	1.66	1.04
11.27	0.55	0.78	0.04	1425	0.20	0.02	47.4	0.01	0.08	1.72	1.05
11.42	22.6	1.82	0.03	1482	0.21	0.01	41.0	0.31	0.07	1.34	1.39
11.69	0.74	0.79	0.03	1420	0.06	0.01	107	0.02	0.06	1.34	1.25
11.87	0.76	0.62	0.03	1454	0.06	0.01	96.8	0.02	0.04	1.83	1.23
12.04	2.74	2.01	0.03	1419	0.25	0.02	38.9	0.46	0.15	1.64	1.26

Appendix E: Measurements of foraminiferal calcite of *Lenticulina spp.* (Mullinax-1 core, Brazos, USA)

Table E1: Ca-normalised trace element data (part 1) of *Lenticulina spp.* (Brazos) expressed as µmol/mol

Depth [m]	Mg	V	Cr	Mn	Co	Ni	Cu	Zn
6.22	5588	2.96	2.70	2328	0.20	1.69	0.78	11.2
6.25	5724	2.42	1.98	2185	0.17	1.88	0.88	8.89
7.08	6612	2.17	1.21	1991	0.82	8.18	4.82	10.1
7.13	8974	2.38	0.68	2740	0.52	4.06	1.59	8.04
7.41	5248	1.31	1.44	2416	0.55	3.47	4.39	7.35
7.50	4425	1.18	4.63	825	1.34	11.3	9.11	95.0
7.60	4606	0.97	2.39	418	0.95	8.22	9.13	10.1
7.79	4125	1.03	3.59	504	1.77	7.55	8.98	39.7
8.58	4040	1.26	0.91	251	0.41	1.63	3.49	27.3
8.77	3478	0.68	1.12	250	0.73	9.86	12.5	33.6
8.86	3319	1.01	3.65	285	0.55	0.03	5.31	55.2
8.94	6058	2.26	2.24	4003	0.16	11.5	16.3	23.7
9.01	5294	1.19	8.19	264	1.11	34.6	31.1	155.3
9.18	4683	2.65	3.75	1953	0.44	9.56	23.3	84.3
9.68	5558	3.24	4.55	2170	0.49	6.42	7.93	33.4
11.10	5594	3.71	3.97	2376	1.31	6.44	12.1	21.4
11.88	6083	5.16	5.45	1941	0.79	7.63	10.1	69.9
12.29	7213	0.41	2.42	61.4	0.09	4.16	5.38	27.7
12.49	4753	3.83	27.2	1594	0.41	10.4	155	201
12.69	8102	2.98	30.2	233	1.66	40.8	89.5	401
12.89	6427	6.57	5.39	420	1.65	5.29	20.6	222
13.09	3361	1.82	0.85	344	0.78	5.96	6.73	46.8
13.29	5384	1.43	1.03	441	1.02	15.3	4.78	35.7

Table E1 continued

Depth [m]	Mg	V	Cr	Mn	Co	Ni	Cu	Zn
13.45	1579	6.76	5.05	256	2.51	47.8	46.6	111
13.65	4124	2.64	0.84	363	0.61	0.45	17.0	70.6
13.85	5251	2.09	7.47	362	1.06	23.9	18.8	71.2
14.06	4533	2.65	3.52	325	2.01	9.23	13.3	92.6
14.26	4133	4.84	3.41	449	1.26	11.7	8.59	53.5
14.46	4779	2.40	3.22	299	2.68	15.0	23.3	87.9
14.66	4967	5.45	6.18	1844	2.09	12.1	18.2	90.5
15.46	3958	3.52	2.25	518	1.52	11.9	47.3	75.7
15.66	3901	7.45	4.41	733	2.55	17.5	17.3	98.4
15.86	4893	6.18	3.12	1148	1.21	2.42	8.16	46.0
16.26	8383	6.42	3.99	3371	1.67	16.3	27.6	81.0
16.46	6952	4.62	5.89	2895	1.61	12.8	8.87	77.9
16.86	4510	5.64	3.64	1996	2.48	10.6	10.7	37.9
17.06	6620	5.82	10.2	2655	1.44	12.3	15.9	25.2
17.26	4570	6.17	10.6	600	2.64	26.3	33.0	683
17.66	3833	2.47	4.11	680	4.76	46.2	28.4	220
17.86	4216	3.25	5.12	565	4.53	22.2	32.0	29.6
18.06	5226	2.97	9.26	668	4.49	51.8	51.3	28.7
18.55	7106	11.3	7.13	2768	1.81	10.8	11.4	35.7
19.15	7682	5.22	10.2	629	0.64	12.9	11.9	164
19.75	6124	2.71	1.12	725	1.80	18.1	16.0	136
20.15	5547	2.03	1.43	809	1.75	13.2	66.3	395

Table E2: Ca-normalised trace element data (part 2) of *Lenticulina spp.* (Brazos) expressed as µmol/mol, isotopic measurements as ‰ VPDB

Depth [m]	As	Sr	Mo	Cd	Ba	Pb	U	$\delta^{13}C$	$\delta^{18}O$
6.22	0.65	1509	0.31	0.11	30.9	0.40	0.22	-1.49	-3.37
6.25	0.59	1507	0.30	0.09	29.5	0.41	0.21	-1.13	-3.20
7.08	1.77	1668	1.18	0.12	32.0	1.49	0.13	-1.49	-4.26
7.13	0.72	1576	0.59	0.01	26.6	0.51	0.11	-1.89	-4.10
7.41	1.75	1760	0.52	0.14	25.3	1.31	0.08	-0.71	-2.70
7.50	1.66	1935	1.71	0.21	25.8	2.35	0.07	-0.68	-2.17
7.60	4.02	2335	2.42	0.07	35.2	2.41	0.09	-0.69	-1.94
7.79	2.24	2027	1.02	0.05	40.6	1.81	0.15	-0.55	-1.58
8.58	0.93	1782	0.53	0.31	43.2	1.03	0.37	0.12	-1.25
8.77	0.84	2282	3.27	0.22	37.4	2.28	0.34	0.01	-1.16
8.86	0.30	1871	0.49	0.16	43.0	1.10	0.29	-0.6	-2.36
8.94	0.44	1451	0.23	0.15	111	1.53	0.17	0.33	-1.36
9.01	1.03	1939	0.89	0.98	58.0	4.69	0.13	0.26	-1.11
9.18	1.49	1616	1.61	0.39	27.4	4.25	0.22	-0.43	-2.08
9.68	0.35	1468	0.33	0.10	20.6	1.27	0.21	-0.41	-2.06
11.10	1.03	1399	0.52	0.14	21.5	1.84	0.26	-1.59	-3.80
11.88	1.25	1305	0.45	0.30	25.6	3.67	0.28	-0.53	-2.43
12.29	0.02	2070	0.57	0.11	7.82	0.22	0.32	-0.17	-1.85
12.49	0.98	1433	1.02	0.04	20.9	7.18	0.51	0.02	-1.50
12.69	1.58	1133	0.62	0.55	23.6	0.98	0.31	0.05	-1.58
12.89	1.63	1487	1.27	0.27	33.5	5.08	0.95	0.24	-1.69
13.09	0.41	1644	0.69	0.17	31.8	1.61	0.45	0.17	-1.53
13.29	0.16	1634	0.36	0.19	31.5	1.07	0.38	0.01	-0.47

Table E2 continued

Depth [m]	As	Sr	Mo	Cd	Ba	Pb	U	$\delta^{13}C$	$\delta^{18}O$
13.45	5.76	1909	0.92	6.57	36.2	5.94	1.15	-0.21	-1.95
13.65	0.51	1597	0.27	0.31	29.2	4.24	0.57	0.19	-1.42
13.85	0.75	1453	0.46	0.28	27.6	2.27	0.61	0.13	-1.44
14.06	1.28	1560	1.54	0.23	35.2	2.84	0.32	0.31	-1.52
14.26	0.54	1551	0.41	0.23	32.2	2.91	0.58	0.27	-1.46
14.46	1.55	1384	5.13	0.29	23.2	3.68	0.23	0.21	-1.55
14.66	2.05	1522	1.81	0.24	25.3	2.29	0.34	0.35	-1.58
15.46	0.83	1734	2.84	0.42	33.2	4.94	0.37	0.13	-1.47
15.66	0.32	1377	1.90	0.21	32.4	6.37	0.21	-0.13	-2.10
15.86	0.62	1494	0.22	0.19	29.4	2.52	0.25	-0.84	-2.57
16.26	1.27	1383	0.38	0.14	30.2	4.82	0.24	-1.71	-3.28
16.46	0.76	1153	1.26	0.23	27.4	2.09	0.37	-0.24	-2.17
16.86	1.68	1377	0.97	0.15	30.6	2.90	0.24	-0.16	-2.13
17.06	1.15	1736	0.82	0.14	49.1	3.34	0.34	0.11	-1.74
17.26	1.11	1965	2.76	0.11	35.8	6.56	0.19	0.19	-1.65
17.66	0.65	1930	1.51	0.30	32.2	5.71	0.17	0.18	-1.51
17.86	1.78	2285	2.58	0.44	39.9	6.76	0.14	0.03	-1.49
18.06	3.47	2293	5.41	0.08	40.4	5.54	0.17	0.02	-1.54
18.55	1.52	1606	0.42	0.57	36.8	1.81	0.51	-0.05	-1.59
19.15	2.02	1604	1.97	1.12	16.5	6.94	0.80	-0.12	-2.14
19.75	1.61	1423	0.43	1.48	25.8	5.64	0.17	n.e.m.	n.e.m.
20.15	1.24	1138	0.31	1.19	33.9	7.85	0.25	n.e.m.	n.e.m.

n.e.m. = not enough material for reliable analysis